THE ROLE OF DYNAMIC CDK1 PHOSPHORYLATION IN CHROMOSOME SEGREGATION IN SCHIZOSACCHAROMYCES POMBE

A Dissertation Presented

By

SUNG HUGH CHOI

Submitted to Faculty of the

University of Massachusetts Graduate School of Biomedical Science, Worcester

In partial fulfillment of the requirement for the degree of

DOCTOR OF PHILOSOPHY

FEBRUARY 15, 2010

MOLECULAR GENETICS AND MICROBIOLOGY

Interdisciplinary Graduate Program

COPYRIGHT INFORMATION

THE ROLE OF DYNAMIC CDK1 PHOSPHORYLATION IN CHROMOSOME SEGREGATION IN *SCHIZOSACCHAROMYCES POMBE*

A Dissertation Presented By

Sung Hugh Choi

The signatures of the Dissertation Defense Committee signifies completion and approval as to style and content of the Dissertation

Dannel McCollum. Ph.D., Thesis Advisor

Stephen Doxsey, Ph.D., Member of Committee

Peter Pryciak, Ph.D., Member of Committee

William Theurkauf, Ph.D., Member of Committee

Jennifer Tirnauer, Ph.D., Member of Committee

The signature of the Chair of the Committee signifies that the written dissertation meets the requirements of the Dissertation Committee

Kirsten Hagstrom, Ph.D., Chair of Committee

The signature of the Dean of the Graduate School of Biomedical Sciences signifies that the student has met all graduation requirements of the School.

Anthony Carruthers, Ph.D.
Dean of the Graduate School of Biomedical Sciences

Interdisciplinary Graduate Program

February 15, 2010

To Jiyoun, my family in Korea
for their love, patience and support
&
For my kids, Ian and Olivia

Acknowledgements

I have enjoyed the great academic atmosphere since I joined the laboratory of Dr. Dannel McCollum. He is a great mentor both scientifically and personally. I really appreciate all his advice, encouragement and patience to keep me on right track of my doctoral study. This thesis could not have been done without him.

Special thanks should go to current and former members of the McCollum lab for making this place warm and fun every day. I especially appreciate Quanwen, Youngsam, and Sussane to teach and guide me to yeast genetics and Samriddha, Chun-Ti, Paramasivam, and Hanhui for fruitful discussion and suggestions. To Sabastian and Sneha, I wish you enjoy the time at Biotech IV and gook luck. Juan Carlos! Chat with you in all kinds of topic was really helpful to pass through long journey of my Ph.D. study.

I would like to acknowledge to the members of my thesis committee, Dr. William Theurkauf, Dr. Stephen Doxsey, Dr. Peter Pryciak and Dr. Kirsten Hagstrom for their supportive idea to complete my thesis research. Special thanks also go to our collaborators Dr. Viesturs Simanis and his lab member, Marie-Pierre Peli-Gulli for sharing data and helpful discussion prior to publication, to Dr. John R Yates III and his lab members, Ian McLeod and Ali Sarkeshik for mass spectrometry analysis, as well as to Dr. Kathleen Gould, Dr. Fred Chang and Dr. Phong Tran for generously sharing yeast strains.

I also thank to people in Biotech IV and to UMass Korean society for their support to make my doctoral life fun and warm. With them, my family and I have never been lonely in life in a foreign country.

Finally and most of all, I dedicate my deepest gratitude to my wife Jiyoun, and my family in Korea for their endless patience, love and support and also to my kids, Ian and Hain (Olivia). Love from my family is the most powerful source for me to pass through the obstacles I have met during my doctoral study.

Abstract

The proper transmission of genetic materials into progeny cells is crucial for maintenance of genetic integrity in eukaryotes and fundamental for reproduction of organisms. To achieve this goal, chromosomes must be attached to microtubules emanating from opposite poles in a bi-oriented manner at metaphase, and then should be separated equally through proper spindle elongation in anaphase. Failure to do so leads to aneuploidy, which is often associated with cancer. Despite the presence of a safety device called the spindle assembly checkpoint (SAC) to monitor chromosome bi-orientation, mammalian cells frequently possess merotelic kinetochore orientation, in which a single kinetochore binds microtubules emanating from both poles. Merotelically attached kinetochores escape from the surveillance mechanism of the SAC and when cells proceed to anaphase cause lagging chromosomes, which are a leading cause of aneuploidy in mammalian tissue cultured cells. The fission yeast monopolin complex functions in prevention of mal-orientation of kinetochores including merotelic attachments during mitosis. Despite the known importance of Cdk1 activity during mitosis, it has been unclear how oscillations in Cdk1 activity drive the dramatic changes in chromosome behavior and spindle dynamics that occur at the metaphase/anaphase transition. In two separate studies, we show how dynamic Cdk1 phosphorylation regulates chromosome segregation. First, we demonstrate that sequential phosphorylation and dephosphorylation of monopolin by Cdk1 and Cdc14 phosphatase respectively helps ensure the orderly execution of two discrete steps in mitosis, namely sister kinetochore bi-orientation at metaphase and spindle elongation in anaphase

(chapter II) . Second, we show that elevated Cdk1 activity is crucial for correction of merotelic kinetochores produced in monopolin and heterochromatin mutants (Chapter III).

TABLE OF CONTENTS

LIST OF FIGURES

CHAPTER I

General Introduction

To maintain correct numbers of chromosomes, eukaryotic cells must segregate duplicated chromosomes equally into two daughter cells during mitosis, since failure to do so leads to aneuploidy which is often associated with tumor progression and miscarriage (reviewed in Cimini and Degrassi, 2005; Draviam et al., 2004; Hassold and Hunt, 2001). Upon onset of mitosis, the centrosomes (the spindle pole bodies in yeasts), the major microtubule organizing center (MTOC)s in mitosis, start to form the mitotic spindle and separate themselves to opposite sides of the nucleus (Crasta et al., 2008). For equal segregation of chromosomes, sister kinetochores must capture microtubules emanating from opposite poles at metaphase in a bi-oriented fashion (Figure 1-1).

Once cells establish chromosome bi-orientation at metaphase, cells progress to anaphase: chromosomes are segregated by cohesion breakage between sister chromatids (Figure 1-1). The segregated chromosomes are further separated toward opposite cell cortexes by spindle elongation during anaphase and divided equally into two daughter cells after cytokinesis. Since this metaphase/anaphase transition is irreversible, eukaryotic cells very carefully examine chromosome bi-orientation by monitoring whether all the microtubule binding sites at sister kinetochores are occupied by microtubules coming from opposite poles and that the paired sister kinetochores are under tension generated by pulling forces from opposite poles. Unless chromosome bi-orientation is established, cells halt cell

Figure 1-1: Chromosome Segregation in metaphase/anaphase transition

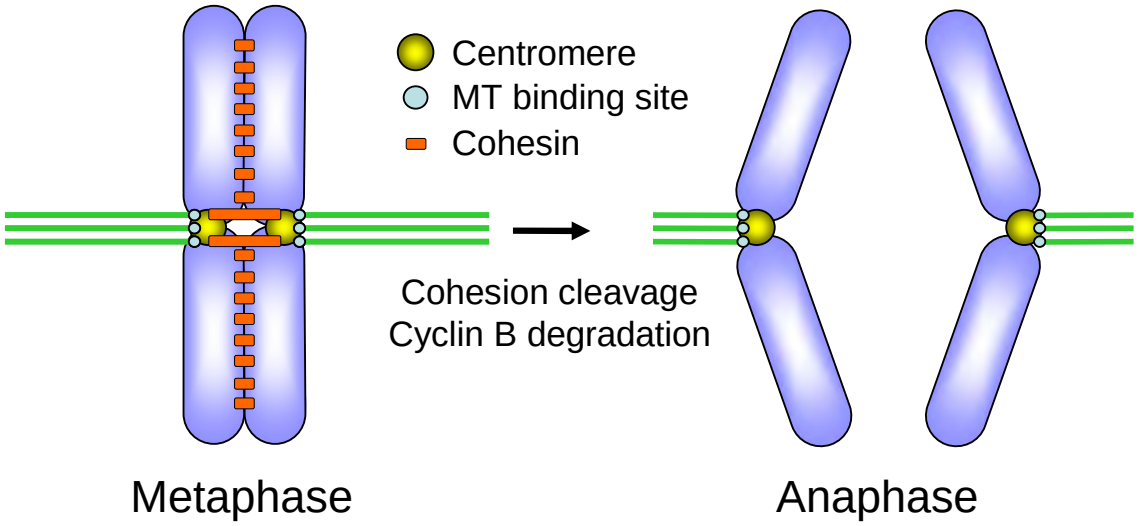

Figure 1-1: Chromosome Segregation in metaphase/anaphase transition

Upon entry onto mitosis, chromosomes become condensed and attach to microtubules emanating from duplicated centrosomes. At metaphase, paired sister chromatids bind to microtubules emanating from opposite poles and align at the metaphase plate. After anaphase onset, sister chromatids are segregated by cleavage of the cohesin complex which glues the two centromeres together and cyclin degradation drops Cdk1 activity and drives spindle elongation during anaphase for complete delivery of chromosomes to two daughter cells.

cycle progression to anaphase in order to provide enough time to correct misattached kinetochore-microtubules.

This cell cycle machinery is highly conserved from unicellular yeast to human. This along with the ease of genetics, gene manipulation, biochemistry and cell biology in yeast make it an ideal model system to study basic cell cycle regulatory mechanisms. The fission yeast, *Schizosaccharomyces pombe*, which was used in this study, is a great miniature system to explore the mechanisms required for chromosome bi-orientation. Its centromeres closely resemble those in animal cells in that they are large (~35 to 100kb) and contain multiple inverted repeat units, which are important for establishing centromeric cohesion (Pidoux and Allshire, 2004) and each kinetochore is bound to 2-4 microtubules compared to 20-30 in mammalian cells (Ding et al., 1993). Furthermore, *S. pombe* harbors only three chromosomes, so it is a very attractive model system to visualize kinetochore dynamics and chromosome behavior during mitosis.

The Centromere and Kinetochore

The centromere is a chromosome locus where many proteins bind to form a large protein complex called the kinetochore, which functions to attach the chromosomes to spindle microtubules. Although the components of kinetochores are highly conserved, the size of centromeres varies widely (reviewed in Cleveland et al., 2003; Pidoux and Allshire, 2004). Budding yeast centromeres are the simplest and most dissected ones, spanning only ~125bp of DNA, with three distinct elements, CDE I, CDE II, CDE III (Figure 1-2). The fission yeast centromeres span 35-110 kb and consist of a central core region of non-repetitive

DNA (*cnt*), flanked by inverted repeat regions, called the inner most repeats (*imr*) and outer repeats (*otr*) (Figure 1-2). The kinetochore is assembled in the central core region of the *cnt* and *imr* sequences and silent chromatin forms in the heterochromatic outer repeat domain. Human centromeres span 0.3-10 Mb and are composed of tandemly repeated array (1500 to 30000 copies) of a 171 bp sequence element termed α-satellite (α-I and α-II satellite) DNA flanked by heterochromatin (Figure 1-2).

The major difference between the central core chromatin of centromere and the rest of the genome is the presence of the histone H3 variant CENP-A, which replaces histone H3 in centromere regions (Stoler et al., 1995; Takahashi et al., 2000; Vafa and Sullivan, 1997). All eukaryotes have a conserved hierarchy of building kinetochores on CENP-A nucleosomes: CENP-A recruit CENP-C, then the KMN network (KNL-1/Mis12 complex/Ndc80 complex)(Przewloka and Glover, 2009). In budding yeast, the unconserved central DNA element CDE II interacts with Cse4, the homolog of CENP-A and Mif2, the homolog of CENP-C. With the help of Cbf1 and the CBF3 protein complex which bind CDE I and CDE III respectively, the Cse4/CENP-A nucleosome recruits other protein complexes such as Spc105 (KNL-1 homolog), the Ctf19 complex (Mis12 complex homolog), the Ndc80 complex, the chromosome passenger complex and the DASH complex to form stable kinetochores (reviewed in Cleveland et al., 2003; Przewloka and Glover, 2009). In fission yeast, both central core and innermost repeat sequences recruit CENP-A homolog Cnp1, CENP-C homolog Cnp3, and the KMN network components, Spc7 (KNL-1), the MIND complex (Mis12), and the Ndc80 complex to build microtubule binding sites (Goshima et al., 1999; Przewloka and Glover, 2009; Takahashi et al., 2000).

Figure 1-2: Organization of Eukaryotic centromeres

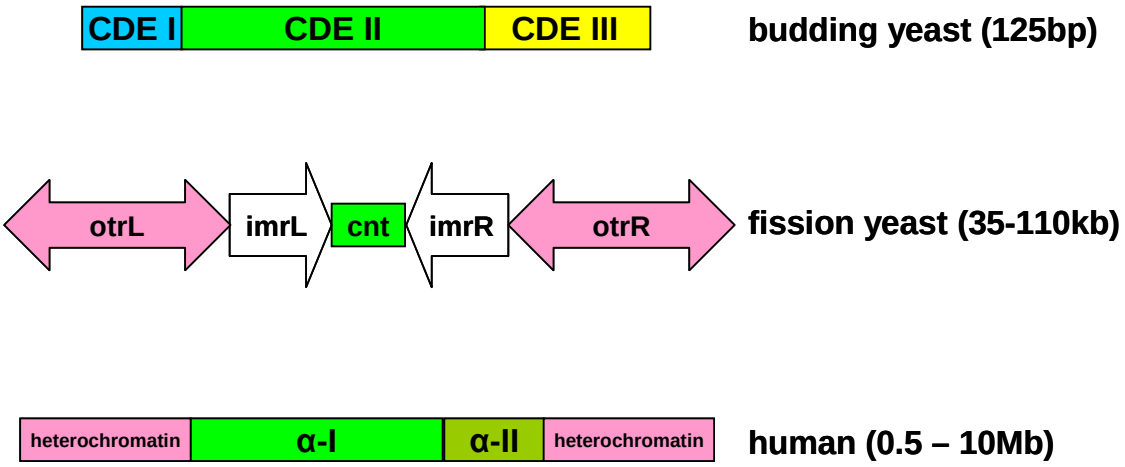

Figure 1-2: Organization of Eukaryotic centromeres

Schematic representation of eukaryotic centromeres. (Top) Budding yeast centromeres are comprised of three sequence domains (blue: CDE I, green: CDE II, yellow: CDE III). (Middle) Fission yeast centromeres consist of a central core (cnt , green box) of nonconserved and non-repetitive sequences flanked by innermost repeats (imr, white arrows) and outer repeats (otr, pink arrows), which together forms an inverted repeat around the central core. (Bottom) Human centromeres are composed of α-I satellite DNA (green) and a more divergent α-II satellite (dark green), flanked by heterochromatin (pink). (modified from the spatial separation model from Cleveland et al., 2003; Pidoux and Allshire, 2004)

Unlike budding yeast, outer repeat sequences recruit Swi6, the homolog of HP1, and are modified as heterochromatin, which is required for the incorporation of the fission yeast cohesin, Rad21 (Bernard et al., 2001; Lachner et al., 2001).

In vertebrates, CENP-A nucleosomes are bound to central core DNA in multiple spots in a single centromere with random distribution. These multiple spots occupied by CENP-A nucleosomes are assembled together to establish the inner kinetochore to form multiple microtubule binding sites through the interaction with at least 18 other proteins known as the constitutive centromere-associated network (CCAN) (Cheeseman and Desai, 2008; Przewloka and Glover, 2009). Flanking regions around the centromere core are modified as heterochromatin and are enriched in proteins involved in chromatid cohesion. CENP-A and the CCAN proteins constitutively localize at the inner kinetochore throughout the cell cycle, but outer kinetochore proteins are assembled only during mitosis. Three highly conserved protein complexes called the KMN network have been identified at the outer kinetochores. The KMN network is composed of KNL1, the Mis12 complex of four proteins (hMis12, hDsn1$^{Q9H410/Mis13}$, hNnf1^{PMF1}, and hNsl1$^{DC31/Mis14}$) and the Ndc80 complex of four proteins (Hec1/hNdc80, Nuf2, Spc24, and Spc25) and they assemble within the outer kinetochore to form microtubule binding sites (Cheeseman et al., 2006; Cheeseman and Desai, 2008; DeLuca et al., 2006; Desai et al., 2003). Many other proteins are transiently recruited to kinetochores after entry into mitosis including the spindle assembly checkpoint components, microtubule motor proteins, the chromosome passenger complex proteins, MCAK, large coiled coil proteins CENP-E, CENP-F, and microtubule binding proteins that regulate end-on attachment dynamics (Musacchio and Salmon, 2007)

Spindle Assembly Checkpoint

Eukaryotes have a ubiquitous safety device called the spindle assembly checkpoint (SAC) that monitors kinetochore-microtubule attachment and tension between paired sister kinetochores to ensure the fidelity of chromosome segregation in mitosis (Musacchio and Salmon, 2007). During early mitosis, the SAC is activated at unattached or tensionless kinetochores to allow time for improperly attached kinetochores to be properly attached prior to loss of sister chromatid cohesion and chromosome separation at the metaphase/anaphase transition. Therefore, the SAC can be activated by various perturbations affecting kinetochore microtubule attachments, such as mutations in centromeric DNA, impairment of kinetochore assembly, and interference with microtubule dynamics (Pangilinan and Spencer, 1996; Rieder and Maiato, 2004; Spencer and Hieter, 1992).

Screens in *Saccharomyces cerevisiae* identified various genes including *Mad1* (mitotic arrest deficient), *Mad2*, *Mad3* (*BUBR1* in human), *Bub1* (budding uninhibited by benzimidazole), *Bub3*, which are required for the checkpoint function (Hoyt et al., 1991; Li and Murray, 1991). Mutations in those genes bypass the mitotic arrest induced by drugs that interfere with spindle assembly. These genes are highly conserved and they constitute the core of the SAC, which is active in prometaphase to prevent the premature separation of sister chromatids.

The SAC proteins are accumulated at unattached kinetochores in prometaphase (Cleveland et al., 2003; Howell et al., 2000; Howell et al., 2004; Kallio et al., 2002a) and negatively regulate the function of Cdc20, a co-factor of the E3 ubiquitin ligase known as

the anaphase promoting complex/cyclosome (APC/C) (Buschhorn and Peters, 2006; Pesin and Orr-Weaver, 2008; Yu, 2002). At the metaphase/anaphase transition, the APC/C ubiquitinates two key substrates, securin and cyclin B, to target them for subsequent degradation by the 26S proteasome (Musacchio and Salmon, 2007). Securin is an inhibitor of a protease called separase, and the degradation of securin leads to activation of separase, which cleaves the cohesin complex ring that glues duplicated sister chromatids, resulting in separation of sister chromatids. On the other hand, cyclin B degradation demolishes the kinase activity of Cdk1 to promote mitotic exit. Cells frequently possess monotelic attachment in which only one sister kinetochore binds to microtubules from one pole (Figure 1-3). It is the most common mis-attachment in prometaphase (Musacchio and Salmon, 2007). The SAC prevents progression into anaphase of cells with these types of attachments by inhibiting Cdc20 function to prolong prometaphase until all the chromosomes are bi-oriented.

In addition to microtubule attachment, the SAC also monitors tension between sister kinetochores generated by intra- and inter-kinetochore stretching of bi-oriented chromosomes (Nicklas et al., 1995; Nicklas et al., 2001; Pinsky and Biggins, 2005). Cells can also possess syntelic attachments, in which both sister kinetochores bind to microtubules from the same pole during early mitosis (Figure 1-3). A syntelic attachment is recognized by the SAC since it does not provide enough tension between a paired sister kinetochores. This mis-attachment is destabilized and corrected by Aurora-B/Ipl1 kinase (Hauf et al., 2003; Lampson et al., 2004; Tanaka et al., 2002). The most problematic mis-attachment in vertebrates is a merotelic attachment, in which a single kinetochore binds to

Figure 1-3: The spindle assembly checkpoint

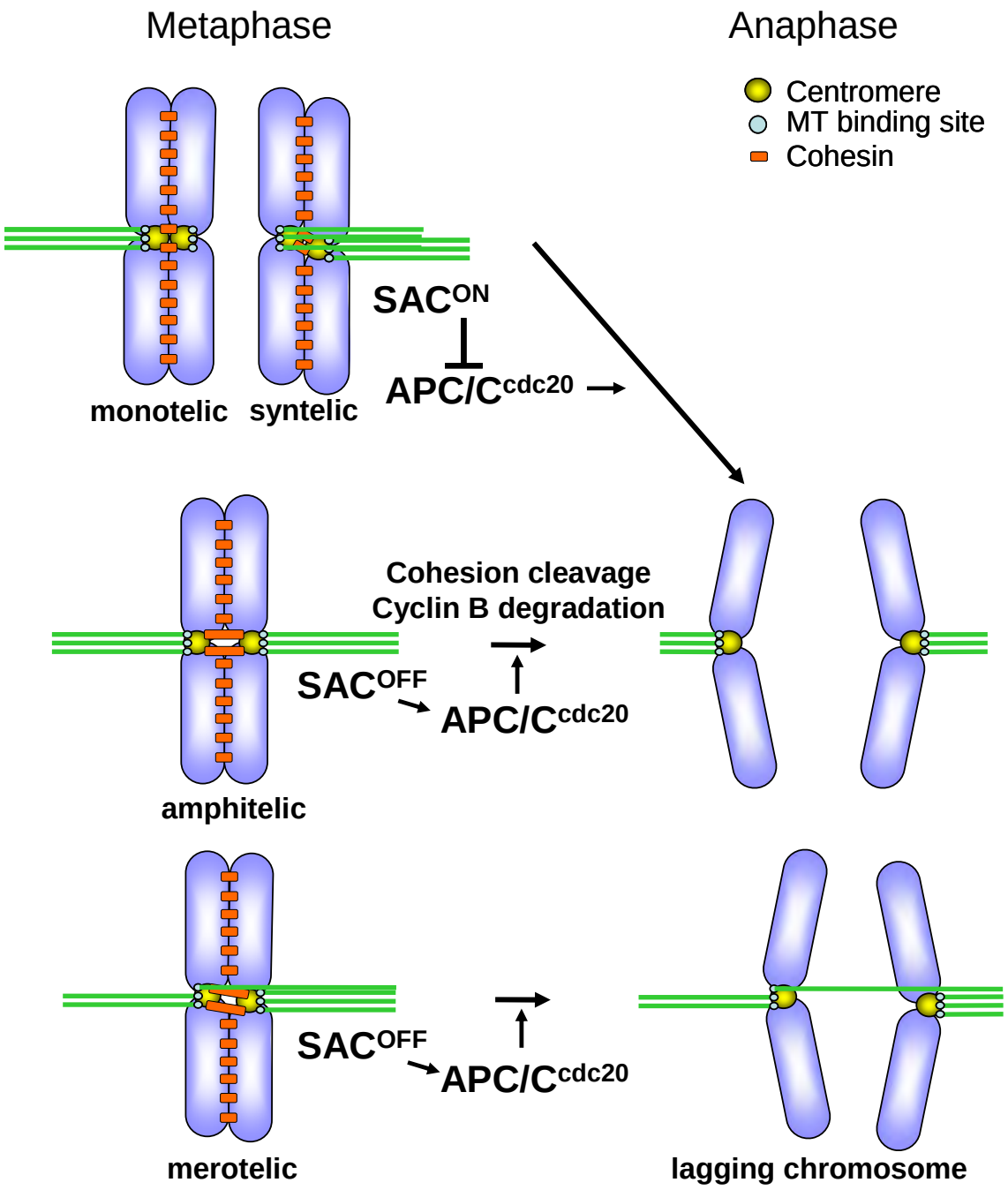

Figure 1-3: The spindle assembly checkpoint delays anaphase onset until chromosome bi-orientation is established

The spindle assembly checkpoint (SAC) monitors both kinetochore-microtubule attachment and tension between paired sister kinetochores. Cells frequently possess monotelically and syntelically attached kinetochores during early mitosis (top) and trigger the SAC to halt cell cycle progression into anaphase by inhibiting the APC/C^{cdc20} complex function to block degradation of cohesin and cyclin B. Once chromosome bi-orientation is accomplished by amphitelic attachment (middle), cells turn off the SAC and progress into anaphase. Merotelically attached kinetochores (bottom) are not detected by the SAC since they satisfy the requirement for both attachment and tension at paired sister kinetochores, and cells with these defects progress into anaphase with lagging chromosomes.

microtubules from both poles (Figure 1-3). These types of attachments are not thought to be sensed by the SAC since the requirements for both attachment and tension are satisfied (Cimini et al., 2004; Cimini et al., 2003). As a result, merotelically attached sister chromatids can be separated after anaphase onset, but move slowly toward either pole or stay in the middle of cell, depending on the ratio of microtubules bound at kinetochores from both poles and are observed as lagging chromosomes in anaphase. Lagging chromosomes are a leading cause of aneuploidy in animal tissue cultured cells (Cimini et al., 2001). Nevertheless, many merotelic attachments are corrected before anaphase onset by Aurora B kinase (Cimini et al., 2003; Cimini et al., 2006) or during anaphase by anaphase spindle mechanics (Cimini et al., 2004). Detailed molecular mechanisms involved in the correction of merotelic attachment are still not well worked out.

The Chromosome Passenger Complex

The chromosome passenger complex (CPC) is comprised of Aurora B kinase, and three non-enzymatic components, INCENP, Survivin, and Borealin/Dasra-B. The non-enzymatic subunits of the complex are essential to promote activation, targeting, and stability of Aurora B kinase (reviewed in Vader et al., 2006). These proteins are well conserved among species except Borealin, which was only recently identified in budding and fission yeasts (Bohnert et al., 2009; Nakajima et al., 2009). The CPC proteins show a very dynamic localization during mitosis. They localize to chromatin in the beginning of mitosis, move to inner centromeres between paired sister kinetochores at prometaphase, and transfer to the spindle midzone at anaphase. This complex localization pattern allows them to orchestrate

chromosome condensation, alignment, chromosome-microtubule interactions, and cytokinesis (Adams et al., 2001; Ruchaud et al., 2007; Vader et al., 2006).

The CPC functions at kinetochores at metaphase to promote proper kinetochore attachment to microtubules. Studies in various organisms revealed that Aurora B kinase is required to both detect tension between paired kinetochores and correct aberrant kinetochore microtubule attachments (Vader et al., 2006). It has been thought that Aurora B breaks the connections between misattached chromosomes and spindle microtubules, which then triggers the spindle assembly checkpoint. (Biggins and Murray, 2001; Biggins et al., 1999; Kallio et al., 2002b; Petersen and Hagan, 2003; Tanaka et al., 2002; Vanoosthuyse and Hardwick, 2009). This role of Aurora B is mediated by its localization to inner centromeres, which lie between sister kinetochores. Aurora B kinase destabilizes microtubule attachments by phosphorylating key kinetochore components. In budding yeast, Aurora/Ipl1 disrupts kinetochore microtubule interaction by phosphorylating components of the Dam1 complex, which forms a ring-like structure around kinetochore microtubules near at their plus ends (Cheeseman et al., 2002) but mammalian homologs for the Dam1 complex have not been identified yet. Studies in vertebrate kinetochores revealed that Aurora B phosphorylates Hec1/Ndc80 to negatively regulate microtubule interaction with the KMN network (Cheeseman et al., 2006; DeLuca et al., 2006). The vertebrate KinI kinesin MCAK is another important substrate of the Aurora B complex. Unlike common kinesin, KinI family members have their motor domains in the middle of the protein and use ATP hydrolysis to depolymerize microtubule ends (Desai et al., 1999; Hunter et al., 2003). MCAK depletion results in chromosome congression and segregation defects due to

misattached kinetochores (Kline-Smith et al., 2004). MCAK localizes at inner centromeres, and its microtubule depolymerizing activity is inhibited by Aurora B phosphorylation. When the SAC is activated at poorly attached kinetochores, unphosphorylated MACK is highly accumulated at these kinetochores. While phosphorylated MCAK stays in the inner centromere, unphosphorylated MCAK moves to the outer kinetochore to depolymerize detached microtubules caused by Aurora B activity. Microtubule depolymerization by MCAK provides another chance to empty microtubule binding sites to attach newly growing microtubules (Andrews et al., 2004; Lan et al., 2004).

A key question in Aurora B kinase function is how Aurora B selectively senses mis-attached kinetochores and destabilizes improper attachments. The spatial separation model has been proposed to address this issue. (Andrews et al., 2004; Tanaka et al., 2002). In this model, the activity of Aurora B might be constant, but when sister kinetochores are bi-oriented at metaphase, tension applied to paired sister kinetochores drives both outer kinetochores including microtubule binding sites away from Aurora B, which concentrates in the core region of inter-centromeres (Figure 1-4). In contrast, outer kinetochores under a lack of tension would stay in the region of Aurora B (Figure 1-4), thereby Aurora B could phosphorylate kinetochore substrates to destabilize kinetochore-microtubules. This model was recently confirmed by a beautiful study that used FRET (fluorescence resonance energy transfer) bio-sensors as Aurora B substrates (Liu et al., 2009). The authors showed that an outer kinetochore targeted Aurora B FRET substrate is selectively phosphorylated only at tensionless sister chromatids, and forced mis-localized Aurora B at outer kinetochores phosphorylates an outer kinetochore targeted FRET substrate under tension

Figure 1-4: The spatial separation model of Aurora B kinase

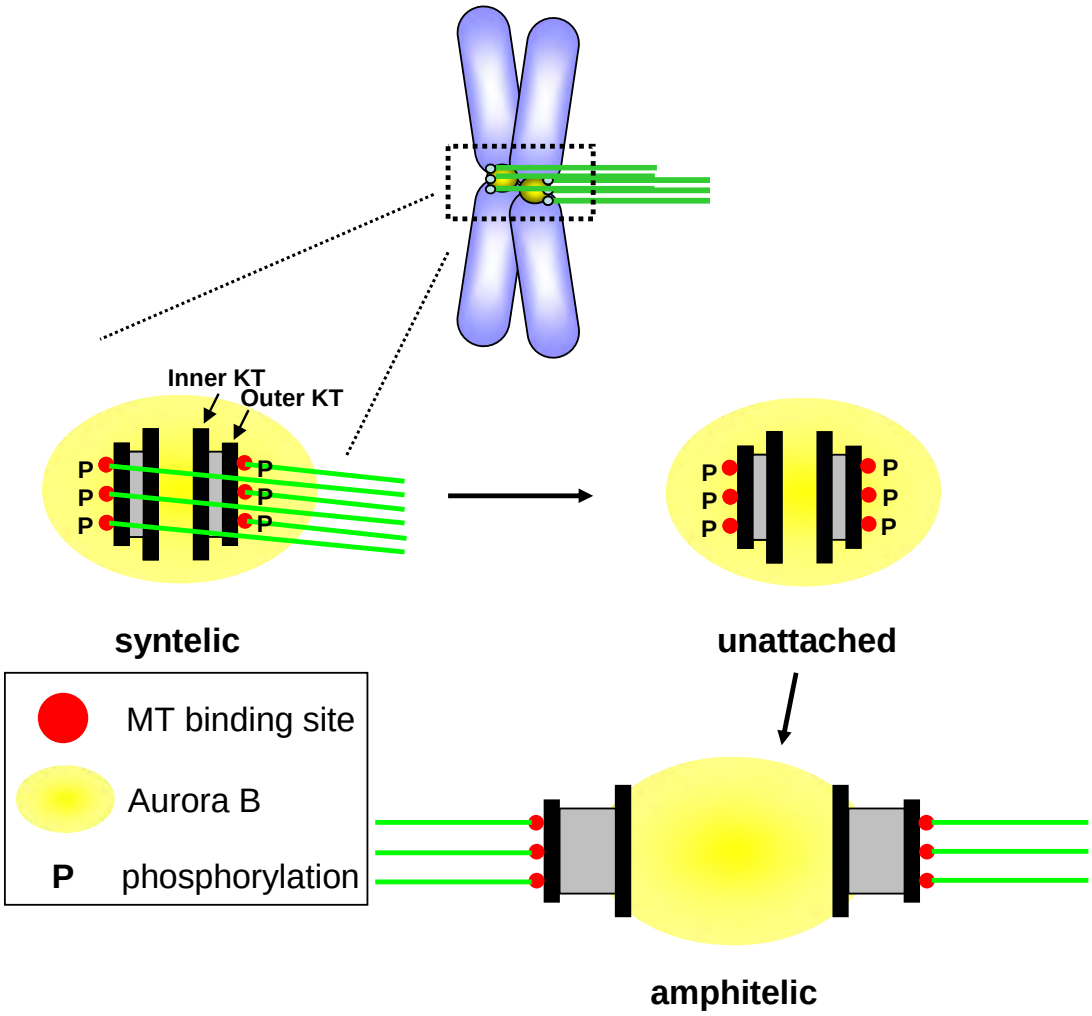

Figure 1-4: The spatial separation model can explain how Aurora B selectively senses and detaches tensionless microtubules from kinetochores

In the spatial separation model, Aurora B kinase activity is constant and concentrated at the core region of inter-centromeres in bi-oriented sister chromatids (see amphitelically attached kinetochores). Outer kinetochores in amphitelically attached sister chromatids are distanced from Aurora B and keep their kinetochore-microtubule interaction until the SAC turns off. In contrast, lack of tension between paired sister kinetochores places both outer kinetochores within range of Aurora B. Outer kinetochore proteins are phosphorylated by Aurora B and lose their interaction with kinetochore microtubules, resulting in generation of unattached kinetochores and spindle checkpoint activation. Newly growing plus ends of microtubules bind kinetochores and repeat this cycle until chromosome bi-orientation is accomplished (modified from the spatial separation model from Liu et al., 2009; Tanaka et al., 2002).

and triggers the SAC due to destabilization of bi-oriented kinetochores (Liu et al., 2009). The N-terminal region of both Ndc80 and Nuf2 in the Ndc80 complex have Calponin-homology domain that bind microtubules and Ndc80 has an additional microtubule binding motif in its N-terminal tail (Cheeseman et al., 2006; Ciferri et al., 2008; DeLuca et al., 2006). Aurora B phosphorylates Ndc80 at its N-terminal tail to destabilize kinetochore-microtubule interaction (Cheeseman et al., 2006; Ciferri et al., 2008; DeLuca et al., 2006). However, a budding yeast study showed that Survivin and INCENP in budding yeast can directly connect centromeres and microtubules, thereby might function themselves as tension sensors, suggesting that the CPC may directly sense the tension (Sandall et al., 2006).

The CPC transfers from the kinetochores to the spindle midzone after anaphase onset to function in its role in cytokinesis. In budding yeast, this translocation is negatively regulated by Cdk1/cyclin B dependent phosphorylation of INCENP. Dephosphorylation at Cdk1 sites within the coiled-coil domain of INCENP by Cdc14 phosphatase targets the CPC from kinetochores to the spindle midzone (Pereira and Schiebel, 2003). However, similar phosphorylation sites were not identified in the coiled-coil regions of human INCENP by a recent phosphoproteomics study (Nousiainen et al., 2006). The expression of a nondestructible cyclin B mutant protein prevented the transfer of Aurora B to the spindle midzone during anaphase in human cells (Murata-Hori et al., 2002), suggesting that phosphorylation dependent regulation of CPC translocation to the spindle is conserved, while phosphorylation sites of INCENP required for the translocation may vary between organisms. However, it is unclear whether Cdk1 phosphorylation on the CPC may affect its

kinetochore dynamics at metaphase. In addition to phosphorylation dependent regulation, in vertebrates, the translocation of the CPC to the central spindle also depends on spindle dynamics and a kinesin related motor protein, Mklp2. The CPC failed to localize to the central spindle after treatment of anaphase cells with the microtubule stabilizing drug taxol (Wheatley et al., 2001). INCENP and Survivin can interact directly with polymerized microtubules in vitro (Li et al., 1998; Mackay et al., 1993; Wheatley et al., 2001), but it is not clear whether this interaction is required for CPC translocation during anaphase.

The Monopolin Complex

The chromosome number must be halved during meiosis I to bring about segregation of maternal and paternal homologous chromosomes. To do so, sister kinetochores must be mono-oriented at metaphase I to attach to microtubules coming from the same spindle pole. The monopolin complex was first identified in *S. cerevisiae*, where it is required for the mono-orientation of homologous paired sister kinetochores during meiosis I (Toth et al., 2000). The monopolin complex contains the meiosis specific component Mam1, which is essential for this mono-orientation of sister kinetochores (Toth et al., 2000). The monopolin complex comprises two sub-complexes, Mam1 with the casein-kinase 1 (Hrr25), and the nucleolar proteins Csm1 and Lrs4 (Petronczki et al., 2006; Rabitsch et al., 2003). The molecular clamp model was proposed by the authors to explain the function of monopolin during meiosis I. According to this model, the monopolin complex clamps two individual microtubule binding sites on a pair of homologous sister kinetochores to facilitate binding of the paired kinetochores to microtubules emanating from same pole to accomplish the

mono-orientation (Figure 1-5A). Lack of monopolin resulted in the failure of the first meiotic nuclear division due to frequent chromosome bi-orientation instead of mono-orientation since two microtubule binding sites on the paired sister kinetochores bind to microtubules from both poles, resulting in equal segregation of paternal and maternal centromeres (Rabitsch et al., 2003).

Monopolin in *S. cerevisiae* does not seem to function in mitosis and meiosis II as a molecular clamp (Rabitsch et al., 2003; Toth et al., 2000) likely because budding yeast has only one microtubule binding site on each kinetochore and this molecular clamp would not be necessary for the establishment of chromosome bi-orientation during mitosis and meiosis II. In contrast, kinetochores in fission yeast, like those in mammalian cells, bind multiple microtubules. In fission yeast, both heterochromatin and the monopolin complex comprising Pcs1 and Mde4 (orthologs of budding yeast Csm1 and Lrs4 respectively) are required for the prevention of merotelic attachments in mitosis and meiosis II (Figure 1-5B) (Gregan et al., 2007). The monopolin complex is not required for mono-orientation of sister kinetochores at meiosis I in fission yeast (Gregan et al., 2007; Rabitsch et al., 2003). The meiosis I specific kinetochore protein Moa1 may replace the role of the budding yeast Mam1 in the fission yeast through a different mechanism (Yokobayashi and Watanabe, 2005).

Iterative PSI-BLAST searches revealed that orthologs of monopolin exist in several fungal species (Gregan et al., 2007), but mammalian orthologs have not been identified to date. Mammalian cells have many more microtubule binding sites at kinetochores than

Figure 1-5: A molecular clamp model of the monopolin complex

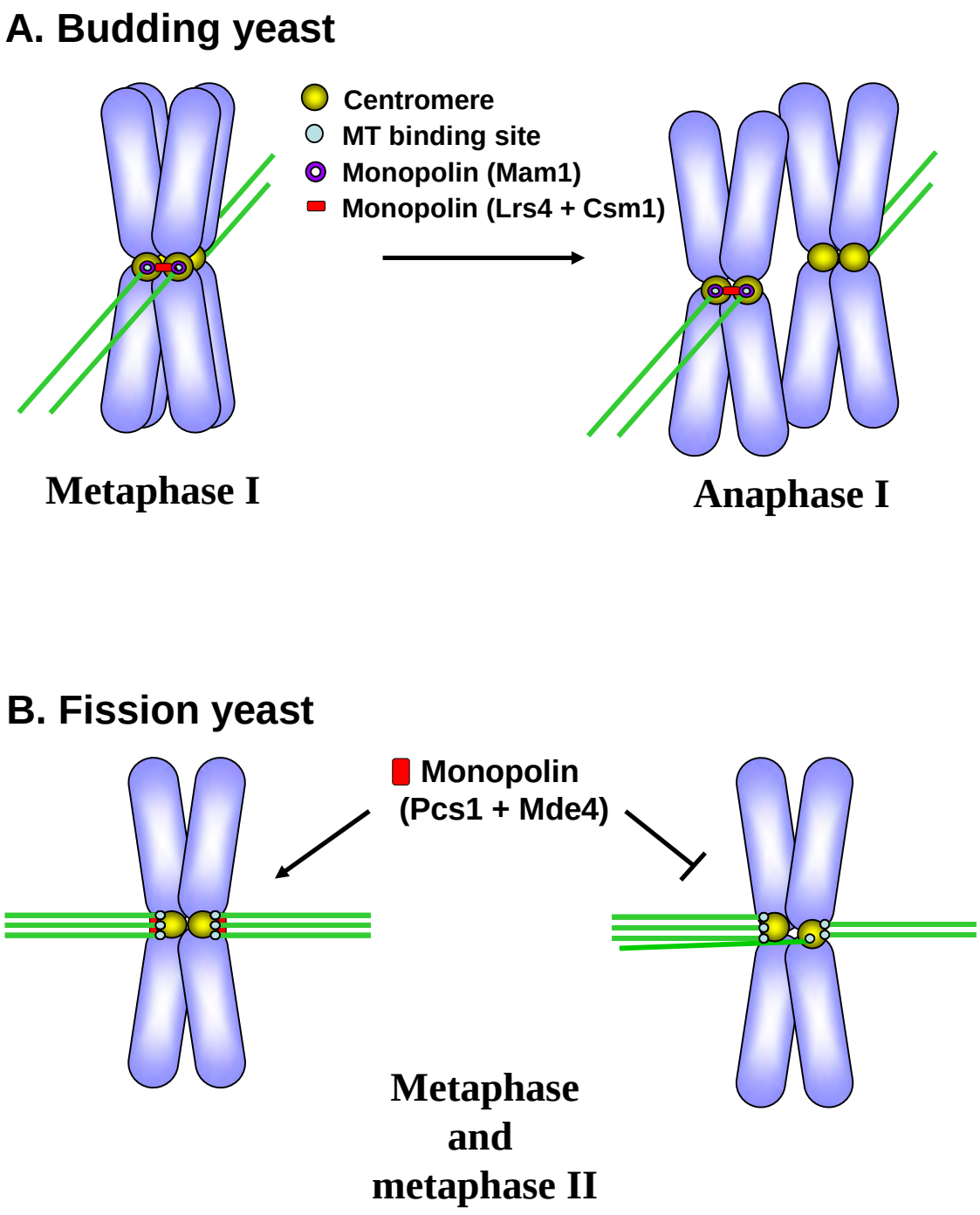

Figure 1-5: A model for how the monopolin complex clamps microtubule binding sites for proper chromosome orientation

(A) Meiosis I in *S. cerevisiae*. A pair of homologous sister chromatids must be mono-oriented at metaphase I to be co-segregated in first round of meiosis. In *S. cerevisiae*, the monopolin complex clamps or bundles two individual MT binding sites together on a pair of homologous sister kinetochores to face microtubules emanating from same pole to establish kinetochore mono-orientation at metaphase I.
(B) Mitosis and mitosis II in *S. pombe*. Duplicated sister chromatids must be bi-oriented to segregate chromosomes equally into two daughter cells. In *S. pombe*, the monopolin complex may clamp or bundle multiple MT binding sites on same kinetochore together to face microtubules emanating from the same pole. In the absence of the monopolin, MT binding sites move freely on kinetochores and MT binding sites on the same kinetochore bind microtubules from both poles, resulting in lagging chromosome production in anaphase.

fission yeast, and a monopolin-like mechanism is likely to be more important in mammalian cells to prevent merotelic attachments (Cimini et al., 2001).

In addition to its role at kinetochores, the budding yeast Csm1-Lrs4 monopolin complex was shown to interact with the RENT complex (Cdc14, Net1 and Sir2), which regulates ribosomal DNA (rDNA) silencing to suppress unequal recombination of rDNA repeats (Huang et al., 2006). A recent study revealed that the Csm1-Lrs4 complex tethers rDNA to the nuclear envelope via the interaction with two proteins of the inner nuclear membrane, Heh1 and Nur1, to keep rDNA away from the recombination foci in the nucleus (Mekhail et al., 2008).

As shown in Chapter II (Choi et al., 2009), we observed that the fission yeast monopolin Pcs1 and Mde4 also localize to the anaphase spindle, probably on parallel microtubules, to contribute to spindle elongation and integrity. Cdk1 phosphorylates Mde4 during early mitosis and keeps the Pcs1-Mde4 complex at kinetochores for monopolin's function in chromosome bi-orientation. Moreover, our study suggests that the *S. pombe* monopolin might be required to prevent not only merotelic attachments but also other misattachments including monotelic and syntelic attachments, which can be recognized by the spindle checkpoint. Mde4 is the first identified target of the *S. pombe* Cdc14-like protein (Clp1) involved in regulation of the anaphase spindle. At the metaphase/anaphase transition, Clp1 and unknown redundant phosphatases dephosphorylate Mde4 to target the Pcs1-Mde4 complex to the anaphase spindle.

The above studies suggest that the monopolin complexes in budding yeast and fission yeast function as a crosslinker to connect microtubule binding sites together at

kinetochores, to anchor rDNA repeats to nuclear membrane, or to bundle parallel spindle microtubules. Direct interaction partners of monopolin at kinetochores, rDNA and the anaphase spindle have not been identified to date and it is still a mystery how cells control the role of the monopolin in a temporal and spatial manner.

In addition, *S. pombe* monopolin or heterochromatin mutants provide a good model system to study how cells deal with merotelic attachment, since those mutants are viable but show a significant frequency of lagging chromosomes in anaphase. As shown in Chapter III, we used those mutants to explore how Cdk1 activity helps to correct merotelic kinetochore orientation before anaphase onset.

Master mitotic regulators: Cdk1 and Cdc14 phosphatase

In higher eukaryotes, the cell cycle is regulated by formation of complexes between different cyclin-dependent kinases (Cdks) and certain cyclins at each phase of the cell cycle. It has been four decades since maturation promoting factor (MPF) was discovered in frog oocytes (Masui and Markert, 1971), and MPF was characterized as a complex of cyclin B and cyclin dependent kinase 1 (Cdk1) during the late 1980s (reviewed in Lindqvist et al., 2009; O'Farrell, 2001). Mitotic entry is mediated by a network of proteins that regulate activation of the cyclin B-Cdk1 complex using two different mechanisms: first, oscillating cyclin B levels are regulated at the level of transcription, which begins in S phase and peaks in the late G2, and second at the level of proteolysis, which is mediated by the anaphase promoting complex/cyclosome (APC/C) at the metaphase/anaphase transition. The activity of Cdk1 is also regulated by phosphorylation on Cdk1 itself. The phosphorylation on the T-

loop of Cdk1 is required for full Cdk1 activity. The activation of the cyclin B-Cdk1 complex is also regulated by additional phosphorylations on T14 and Y15 of Cdk1 by the opposing activities of Wee1 and Myt1 kinase and Cdc25 phosphatases (O'Farrell, 2001). Wee1/Myt1 kinases phosphorylate T14 and Y15 of Cdk1 to inhibit the activity of Cdk1, while Cdc25 phosphatase reverses those phosphorylations to restore activity. This switch very quickly turns on mitotic entry by two positive feedback loops: Cdc25 is activated and Wee1 and Myt1 are inactivated by mitotic phosphorylation accomplished by Cdk1 and Plk1 (polo-like kinase 1). These feedback loops lead to rapid activation of the accumulated reserve of cyclin B-Cdk1 at mitotic entry (Lindqvist et al., 2009; O'Farrell, 2001).

In the fission yeast, Cdc2 is the only Cdk, and it is known to bind four different B-type cyclins, Cig1, Cig2, Puc1 and Cdc13 (reviewed in Moser and Russell, 2000). The protein level of Cdc2 does not change throughout the cell cycle, while cyclin levels oscillate. Cdc2-Cig2 mainly governs S phase, while Cdc2-Cdc13 regulates mitosis.

Cdks control the cell cycle by catalyzing the transfer of phosphate from ATP to specific protein substrates. While the regulation of Cdk activity has been vigorously explored during past decades, the role of the phosphorylation of individual Cdk substrates was defined by a limited number of studies, despite its importance in cell cycle control. Recent progress in constructing an ATP analog sensitive Cdk1 mutant (*cdk1-as*) combined with phosphopeptide enrichment and quantitative mass spectrometry makes it possible to identify more than three hundred of the in vivo Cdk1 substrates in *S .cerevisiae* (Holt et al., 2009). These authors also previously identified a couple of hundred targets of Cdk1 *in vitro* using a budding yeast proteomic library (Ubersax et al., 2003). Defined Cdk1 substrate

candidates were classified by a strong enrichment in cell cycle related categories such as DNA replication, actin and cell polarity, kinetochore, spindle and cytokinesis. Similar phosphoproteome analysis was carried out in the fission yeast using mitotically arrested cells to define 1194 in vivo substrates of the *S. pombe* mitotic kinases including Cdk1 (Wilson-Grady et al., 2008), and in human HeLa cells more than one thousand proteins showed increased phosphorylation during mitosis; the majority of those are Cdk1 substrates (Dephoure et al., 2008). These studies provide great background to cell cycle researchers to explore the detailed mechanism of Cdk1 to regulate the function of individual proteins in specific cell cycle events.

Cyclin degradation mediated by the APC/C complex causes Cdk1 activity to drop at anaphase onset. However Cdk1 down-regulation itself is not able to drive cells to exit mitosis. Cdk1 substrates phosphorylated in early mitosis must be dephosphorylated during late mitosis for proper mitotic exit. Cdc14 family phosphatases are known as major antagonizers of Cdk1, which reverse Cdk1 phosphorylation during anaphase (Stegmeier and Amon, 2004). Cdc14 phosphatase was first identified in *S. cerevisiae*. In the budding yeast, Net1/Cfi1 sequesters and keeps Cdc14 inactive in the nucleolus during G1, S phase, and early mitosis, but Cdc14 is released from the nucleolus after anaphase onset. Two regulatory protein networks, the Cdc14 early anaphase release (FEAR) network and the mitotic exit network (MEN) mediate the phosphorylation of Net1 to reduce its affinity with Cdc14, thus releasing the active phosphatase. The FEAR network promotes initial release of Cdc14 from the nucleolus during early anaphase, which is important for rDNA segregation during anaphase (D'Amours et al., 2004). In late anaphase, the MEN

accelerates Cdc14 release and maintains Cdc14 in the cytoplasm. The released fully active Cdc14 dephosphorylates relevant Cdk1 substrates to promote various events of anaphase such as stabilization of the spindle microtubules, relocalization of the chromosome passenger complex, spindle midzone assembly, spindle disassembly on completion of chromosome segregation, cytokinesis and cell abscission (reviewed in Queralt and Uhlmann, 2008). Currently known Cdc14 substrates in budding yeast include microtubule regulators Ase1, Ask1, Fin1 and INCENP Sli15 (Higuchi and Uhlmann, 2005; Khmelinskii et al., 2007; Pereira and Schiebel, 2003; Woodbury and Morgan, 2007). Cdc14 functions like it does in budding yeast in other eukaryotes. However, Cdc14 phosphatases are freed from nucleolar sequestration earlier at mitotic entry in other organisms. In *S. pombe*, Clp1 (Cdc14-like protein 1) is released from the nucleolus by an unknown mechanism at mitotic entry (Chen et al., 2006; Cueille et al., 2001; Trautmann et al., 2001). A Net1 ortholog has not been identified to date and FEAR orthologous protein components do not affect Clp1 localization and function (Chen et al., 2006; Jin et al., 2007). Clp1 is not essential for cell viability in fission yeast but functions in cytokinesis, mitotic exit, chromosome segregation and spindle elongation (Choi et al., 2009; Cueille et al., 2001; Fu et al., 2009; Trautmann et al., 2004; Trautmann et al., 2001; Wolfe and Gould, 2004; Wolfe et al., 2006). As for its role in cytokinesis, Clp1 binds Mid1, which is a scaffold protein for contractile ring assembly. Targeting of Clp1 to the contractile ring by Mid1 affects the dynamics of key contractile ring components Cdc15 and myosin II, which is important to stabilize the contractile ring complex (Clifford et al., 2008), and Clp1 also participates in cytokinesis as a positive regulator of the septation initiation network (SIN, the fission yeast MEN

homologous pathway) (Cueille et al., 2001; Trautmann et al., 2001). However, because Clp1 is not essential in *S. pombe*, it suggests that other unknown redundant phosphatases function together with Cdc14 to reverse Cdk1 phosphorylation for mitotic exit in *S. pombe*.

Known examples of potential substrates of Cdc14 in higher eukaryotes include the *C. elegans* kinesin ZEN-4 (human MKLP1) (Gruneberg et al., 2002; Mishima et al., 2004) and the human PRC1 (Ase1 ortholog) (Zhu et al., 2006). In contrast to budding yeast, and like in fission yeast, Cdc14 is not essential for organism viability in *C. elegans* (Saito et al., 2004). The vertebrate ortholog Cdc14B is not required for mitotic exit (Berdougo et al., 2008). It is possible that Cdc14A and Cdc14B have redundant functions, or other phosphatases such as PP1, PP2A, and the dual-specificity phosphatase Ptpcd1 could control mitotic exit and/or function together with Cdc14 (reviewed in Bollen et al., 2009).

In addition to the role of Cdc14 in mitotic exit, Cdc14 functions in other cell cycle stages as well. Human Cdc14B also relocalizes to the cytoplasm from the nucleolus to dephosphorylate and activate the APC activator Cdh1 and mediates APC^{cdh1}-dependent Plk1 degradation to block mitotic entry in response to DNA damage (Bassermann et al., 2008).

In *S. pombe*, Clp1 is released from the nucleolus at mitotic entry, but high Cdk1 activity phosphorylates Clp1 to suppress its activity by 40% during early mitosis (Wolfe et al., 2006). We previously found that Clp1 also localizes at kinetochores at metaphase, and it is involved in chromosome bi-orientation probably through crosstalk with Aurora kinase (Trautmann et al., 2004). The Proteomics study used in Chapter II also showed that the chromosome passenger complex (CPC) components, Pic1 (INCENP), Bir1 (Survivin), and

Nbl1 (Borealin) are the most abundant proteins interacting with Clp1 at metaphase, suggesting that enrichment of Clp1 at kinetochores may regulate the dynamics of the CPC at kinetochores at metaphase to promote chromosome bi-orientation despite the reduced phosphatase activity of Clp1. As shown in Chapter II, Cdk1 competes with Clp1 for regulation of the monopolin component Mde4 to facilitate proper microtubule attachments at kinetochores at metaphase. Our works suggest that Cdc14 might have a role in chromosome segregation during early mitotic stages as well, but the detailed mechanisms of Cdc14 regulation of other proteins involved in chromosome segregation remains to be explored.

CHAPTER II

A phosphorylation dependent switch defines discrete roles for the monopolin complex in chromosome attachment and spindle elongation

Figure 2-4B was contributed by Dr. Marie-Pierre Peli-Gulli and Dr. Viesturs Simanis.

Summary

It is not well known how oscillations in Cdk1 activity drive the dramatic change in chromosome behavior and spindle dynamics that occur at the metaphase/anaphase transition. The yeast monopolin complex has been proposed to allow normal segregation of chromosomes in anaphase by preventing merotelic attachment of individual kinetochores to microtubules from opposite poles. In addition to its function at kinetochores at prometaphase/metaphase, here we show that the *Schizosaccharomyces pombe* monopolin protein complex plays additional roles in spindle stability in anaphase, and the distinct functions of the complex in metaphase and anaphase are determined by the phosphorylation state of the Mde4 subunit. When Cdk1 activity is high in metaphase, Mde4 is hyperphosphorylated on Cdk1 phosphorylation sites and localizes to kinetochores to prevent improper microtubule attachments. A non-phosphorylatable mutant of Mde4 does not localize to kinetochores, appears prematurely on the metaphase spindle, and interferes with spindle dynamics and chromosome segregation, illustrating the importance of Cdk1 phosphorylation in regulating metaphase monopolin activity. When Cdk1 activity drops in anaphase, the *S. pombe* Cdc14 phosphatase Clp1 and unknown phosphatase(s) dephosphorylate Mde4 and trigger monopolin translocation to the mitotic spindle, where it promotes spindle elongation and its integrity especially in early anaphase, coupling the late mitotic loss of Cdk1 activity to anaphase spindle dynamics. Taken together, these findings illustrate how the sequential phosphorylation and dephosphorylation of the monopolin complex ensures the orderly execution of discrete steps in mitosis.

Introduction Chapter II

For equal segregation of chromosomes to each daughter cell, sister kinetochores must attach to microtubules emanating from opposite poles at metaphase in a bioriented fashion. Most defects in attachment of chromosomes to the spindle microtubules trigger the spindle assembly checkpoint, which stops cell cycle progression and promotes correction of attachment defects (Musacchio and Salmon, 2007). However merotelic attachment, in which a single kinetochore binds to microtubules from both poles, has been believed not to be sensed by the spindle assembly checkpoint since requirements for both attachment and tension at kinetochores are satisfied (Cimini, 2007). Thus, cells with merotelically attached chromosomes proceed into anaphase but develop lagging chromosomes, which often do not segregate properly after cytokinesis. Merotelically attached lagging chromosomes are the most common cause of aneupoloidy in cultured mammalian cells (Cimini et al., 2001).

The centromeres of the fission yeast *Schizosaccharomyces pombe* resemble those in animal cells. They are larger (~35-110kb) than those in the budding yeast and contain a central core region of non-repetitive DNA which recruits many proteins to form kinetochores. Multiple inverted repeat sequences flank core centromere sequences to form silent heterochromatin, which is important for establishing centromeric cohesion (Pidoux and Allshire, 2004). In contrast to the budding yeast kinetochores which bind only one microtubule (Winey et al., 1995), each mammalian and fission yeast kinetochore binds multiple microtubules (2-4 microtubules in the case of fission yeast) (Ding et al., 1993). Because each fission yeast kinetochore can bind multiple microtubules, merotelic

orientation can occur in early mitosis, thus mechanisms are required to prevent merotelic attachments. A recent study showed that both centromeric heterochromatin and the monopolin complex are required to prevent merotelic attachments in *S. pombe* (Gregan et al., 2007). The monopolin complex was initially identified in *S. cerevisiae* where it is required during meiosis I to orient duplicated sister kinetochores to the same pole (Petronczki et al., 2006; Rabitsch et al., 2003; Toth et al., 2000). The *S. pombe* monopolin consists of a complex between the Pcs1 and Mde4 proteins, which localizes to the central core of centromeres (Gregan et al., 2007). Monopolin is not required for mono-orientation of sister chromatids during meiosis I in fission yeast. However monopolin is required during mitosis and meiosis II to prevent lagging chromosomes caused by merotelic attachments (Gregan et al., 2007). It has been proposed that monopolin acts as a clamp to align microtubule binding sites together at kinetochores to prevent merotelic attachments which can not trigger the spindle assembly checkpoint (Gregan et al., 2007; Monje-Casas et al., 2007; Petronczki et al., 2006). However, how monopolin function is regulated during mitosis in *S. pombe* remains unclear. It also remains to be tested whether the spindle assembly checkpoint is activated in monopolin mutants, which may suggest that the monopolin complex is required to prevent not only merotelic attachment but also other kinetochore mis-orientations such as unattached, monotelic and syntelic kinetochore for chromosome bi-orientation.

The evolutionarily conserved Cdc14 phosphatase is known to dephosphorylate Cdk1 substrates. The *S. pombe* Cdc14-like-phosphatase Clp1 is sequestered in the nucleolus in interphase and released to the nucleus and cytoplasm at mitotic entry. Once

released it decorates the contractile ring and the mitotic spindle to carry out multiple cell cycle dependent functions to regulate mitotic entry, contractile ring stability, and spindle dynamics, and to coordinate mitosis with cytokinesis (Clifford et al., 2008; Cueille et al., 2001; Fu et al., 2009; Trautmann et al., 2001; Wolfe et al., 2006). We have shown previously that Clp1 also localizes at kinetochores at metaphase and plays a role in chromosome segregation (Trautmann et al., 2004); however, substrates of Clp1 at kinetochores have not been identified yet. Here we show that the monopolin subunit Mde4 is a substrate of both Cdk1 and Clp1. Phosphorylation of Mde4 on Cdk1 sites keeps monopolin on kinetochores by preventing premature localization to the mitotic spindle. Dephosphorylation of Mde4 by Clp1 and other unknown phosphatase(s) at anaphase onset allows monopolin to localize to the mitotic spindle, where it maintains spindle integrity and normal spindle elongation, especially in early anaphase. Thus, the proper regulation of both sequential phosphorylation and dephosphorylation of Mde4 is necessary for the dual roles of monopolin in kinetochore bi-orientation at metaphase and spindle dynamics at anaphase to keep the fidelity of chromosome segregation.

Results Chapter II

Identification of Clp1 substrates at early mitosis

Mitotic cyclin-Cdk1 complexes drive the striking early mitotic events such as chromosome condensation and alignment, nuclear envelope breakdown and mitotic spindle assembly (Sullivan and Morgan, 2007). Cdk1 activity drops dramatically through cyclin degradation at the metaphase/anaphase transition once all sister chromatid pairs are bi-oriented. Dephosphorylation of Cdk1 substrates during anaphase is expected to be required for proper mitotic exit. It was thought that the Cdc14 phosphatase is mainly required to reverse Cdk1 phosphorylation at anaphase for proper mitotic exit (Stegmeier and Amon, 2004). However, previous work from our lab has found that the *S. pombe* Cdc14 phosphatase Clp1 localizes to kinetochores at metaphase, and the *clp1Δ* mutant showed chromosome segregation defects, implying that Clp1 substrates regulate chromosome segregation (Trautmann et al., 2004). Despite the known important roles of Cdk1 and Cdc14 during mitosis, limited numbers of Cdk1 substrates have been identified (Brown et al., 1999; Loog and Morgan, 2005; Peeper et al., 1993), and no kinetochore protein involved in chromosome segregation has been reported as a substrate of Clp1 in fission yeast.

To identify the Cdk1 and Clp1 substrates involved in chromosome segregation, we applied a tandem affinity purification scheme (Tasto et al., 2001). Since the dephosphorylation reaction by wild type Clp1 is too transient to isolate enough protein complexes for mass spectrometry analysis, we used a substrate trapping allele of Clp1, Clp1-C286S, for the purification (Figure 2-1). In this mutant allele, Cysteine^{286} in the

Figure 2-1: Purification scheme using a substrate trapping allele Clp1

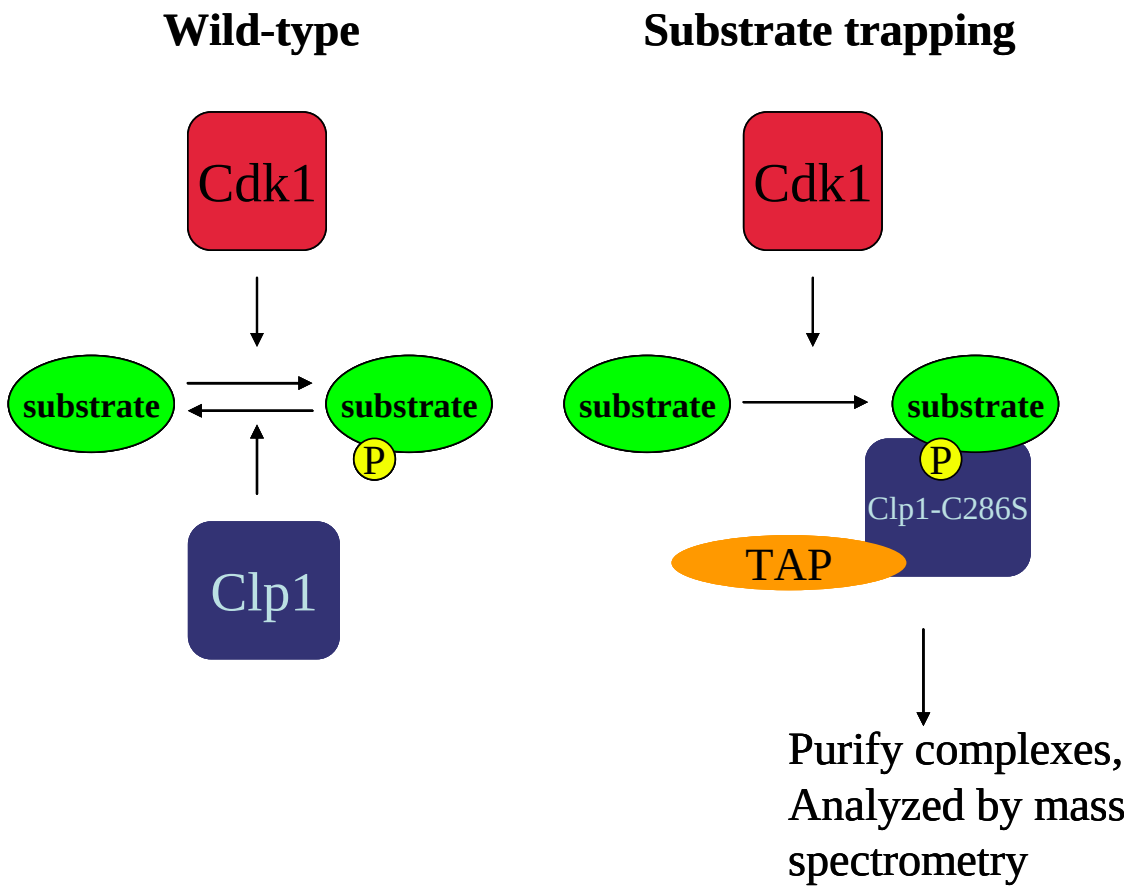

Figure 2-1: Purification scheme using a substrate trapping allele to isolate Cdk1 and Clp1 substrate

Tandem affinity purification strategy was used to identify Cdk1 and Clp1 substrates. Since dephosphorylation reaction of wildtype Clp1 is too transient to isolate enough protein complexes for mass spectrometry analysis, a substrate trapping allele of Clp1, Clp1-C286S was used for the purification. Clp1-C286S is phosphatase inactive but keeps the binding affinity for its substrates. Purified Clp1-C286S protein complexes from metaphase arrested cells were precipitated in 25% TCA, and analyzed by tandem mass spectromery (LC-MS/MS) analysis.

Figure 2-2: Candidate Cdk1 and Clp1 substrates

Cytokinesis

Cdc15
Cdc16
Cdc7 kinase
Sid2 kinase
Pak1 kinase
Rad24
Rad25
Mid2

Telophase/G1 Transcription

Sep1
Cdc10

Uncharacterized

SPBC725.12
SPBC215.06c
SPBC36B7.06c
SPCC736.12c
SPCC191.01
SPAC14C4.05c
SPAC3G9.01
SPAC29E6.09
SPAC12B10.02c

Chromosome Segregation

Aurora kinase
Survivin
INCENP
Borealin
} Chromosome Passenger Complex

Pcs1
Mde4
} Monopolin

Dis2 PP1 phosphatase
Bub1 kinase
Ase1
Klp9
Klp5
Klp6

Cell cycle

Cdc25 phosphatase
Wee1 kinase
Cdc22
Sum3/Ded1 helicase

Others

Gar1
Sap1

Figure 2-2: Candidate Cdk1 and Clp1 substrates or interacting proteins in purified Clp1 complex isolated from metaphase arrested cells.

Numerous proteins that interact with Clp1 were identified by tandem affinity purification using a substrate trapping allele of Clp1 followed by mass spectrometry analysis. A subset of the identified are listed and placed into different categories of cell cycle events. Cells were arrested at prometaphase and metaphase the using cold sensitive tubulin mutant *nda3-KM311* or temperature sensitive proteasome mutant *mts3-1* respectively. Mass spectrometry also identified phosphorylation status of individual proteins at Cdk1 sites. Proteins shown in red were identified as phosphorylated at their Cdk1 sites in vivo in this and/or other studies.

catalytic domain of Clp1 was mutated to Serine causing loss of catalytic activity, but this mutation keeps its binding affinity to the substrates (Trautmann et al., 2004; Wolfe and Gould, 2004). Clp1-C286S protein complexes were purified from prometaphase and metaphase arrested cells using tubulin mutation *nda3-KM311* and proteasome mutation *mts3-1* respectively. Final eluates were precipitated in 25% TCA (Trichloroacetic acid), and then analyzed by tandem mass spectrometry analysis. Numerous proteins that co-purified with Clp1 were identified and summarized in different categories of cell cycle events (Figure 2-2 and Appendix A).

Mde4 is phosphorylated by Cdk1 during mitosis and interacts with the Cdc14 like phosphatase Clp1

The *S. pombe* monopolin proteins Pcs1 and Mde4 were identified in the Clp1 protein complex isolated from prometaphase and metaphase arrested cells by mass spectrometry. Mde4 has twelve potential Cdk1 phosphorylation sites (SP/TP motifs), and five of them were identified as phosphorylated by mass spectrometry (Figure 2-3A). However, sequence coverage of Mde4 from the mass spectrometry analysis was only 30%, raising the possibility that the remaining seven Cdk1 sites might be phosphorylated in vivo as well. Pcs1 has one potential Cdk1 site but it was not identified as phosphorylated in vivo (data not shown). To confirm the apparent interaction between monopolin and Clp1 identified using mass spectrometry, we carried out co-immunoprecipitation and Western blotting experiments. Mde4-GFP co-immunoprecipitated with the substrate-trapping mutant, Clp1-C286S-13Myc, but not with wild-type Clp1-13Myc (Figure 2-3B), suggesting that Clp1

Figure 2-3

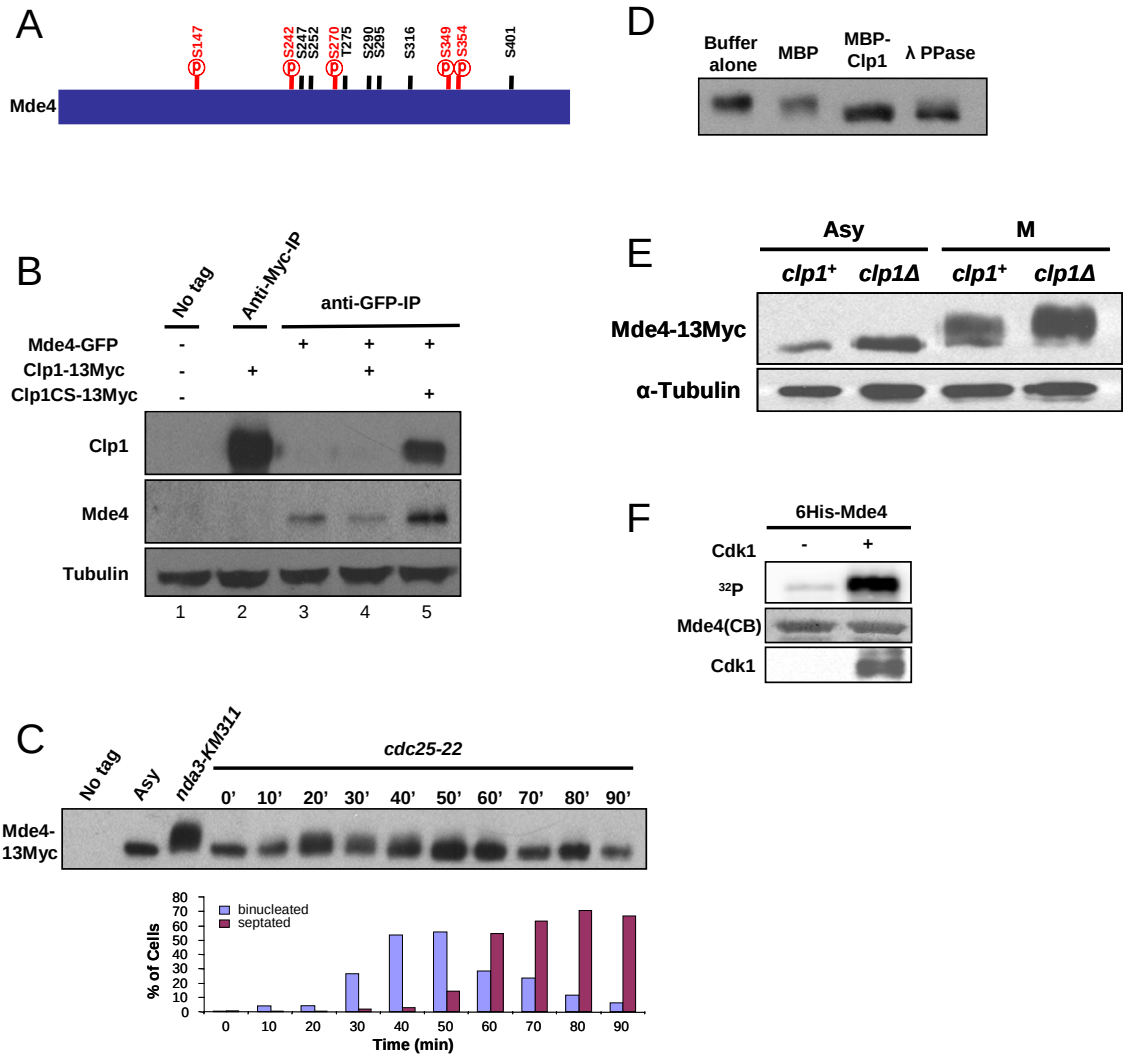
A
Mde4
S147
S242
S247
S252
S270
T275
S290
S295
S316
S349
S354
S401
B
No tag
Anti-Myc-IP
anti-GFP-IP
Mde4-GFP
Clp1-13Myc
Clp1CS-13Myc
Clp1
Mde4
Tubulin
1 2 3 4 5
C
No tag
Asy
nda3-KM311
cdc25-22
0' 10' 20' 30' 40' 50' 60' 70' 80' 90'
Mde4-13Myc
binucleated
septated
% of Cells
Time (min)
D
Buffer alone
MBP
MBP-Clp1
λ PPase
E
Asy
M
clp1+ clp1Δ clp1+ clp1Δ
Mde4-13Myc
α-Tubulin
F
6His-Mde4
Cdk1
32P
Mde4(CB)
Cdk1

Figure 2-3: Mde4 is Phosphorylated by Cdk1 during Mitosis and Interacts with Clp1

(A) Schematic representation of Mde4 depicting 12 consensus Cdk1 phosphorylation sites. Five of the twelve predicted phosphorylation sites (indicated with red "ⓟ"s) were identified by mass spectrometric analysis of Clp1-C286S-TAP purified from cells arrested at prometaphase using the *nda3-KM311* and *mts3-1* mutants and from cells 60 min after release from a *cdc25-22* arrest.
(B) Interaction between Mde4 and Clp1 was determined by immunoprecipitation followed by western blotting using cell lysates from the following asynchronous cultures: wild-type (1), *clp1-13Myc* (2), *mde4-GFP* (3), *mde4-GFP clp1-13Myc* (4), and *mde4-GFP clp1-C286S-13Myc* (5). The lower panel shows the tubulin loading control from whole cell extracts prior to immunoprecipitation.
(C) Cell cycle dependent changes in Mde4 phosphorylation were determined by analyzing the gel migration of Mde4-13Myc. *cdc25-22 mde4-13Myc* cells were arrested at the restrictive temperature of 36°C for 4 hours to synchronize them in G2 phase, and were then shifted to the permissive temperature of 25°C. Samples were taken at the indicated time points and the migration shift of Mde4-13Myc (upper panel) and cell-cycle progression (lower panel) were determined by western blot analysis and microscopy, respectively. Lysates from wild-type cells (No tag), asynchronous *mde4-13Myc* (Asy), and *mde4-13Myc* cells arrested in mitosis via the *nda3-KM311* mutation (*nda3-KM311*) are also shown.
(D) Immunoprecipitated Mde4-13Myc from *mde4-13Myc clp1Δ* cells arrested in prometaphase via the *nda3-KM311* mutation was treated with buffer alone, recombinant maltose binding protein (MBP), MBP-Clp1, or lambda phosphatase (λ PPase) and then analyzed using western blotting.
(E) Gel migration of Mde4-13Myc was analyzed by immunoprecipitation followed by western blotting of Mde4-13Myc isolated from either asynchronous (Asy) cells or cells arrested in prometaphase (M) via *nda3-KM311* mutation in either a *clp1*$^{+}$ and *clp1Δ* background. Lower panel shows the tubulin loading control.
(F) In vitro kinase assays were performed with Cdk1 immunoprecipitated via Cdc13 (*S. pombe* cyclin B) antibodies from prometaphase arrested *nda3-KM311*cells with bacterially expressed 6His-Mde4 as substrate. γ-^{32}P-labeled protein was detected with a Phosphorimager (Molecular Dynamics), and the gel was stained with Coomassie blue (CB) as a loading control. The level of Cdk1 was determined by western blotting.

interaction with Mde4 is not by domain to domain interaction but is mediated by phosphorylation on Mde4. Because Clp1 dephosphorylates sites phosphorylated by Cdk1 whose activity peaks in early mitosis, we checked whether Mde4 is phosphorylated during early mitosis. In cells released from the synchronous cultures arrested at G2 phase by *cdc25-22* mutation, slower migrating forms of Mde4-13Myc appeared during early mitosis, decreased during late mitosis, and then disappeared after mitotic exit (Figure 2-3C). To confirm that the shift was due to phosphorylation, Mde4-13Myc isolated from prometaphase-arrested cells was treated with recombinant Clp1 purified from *E. coli*. Treatment with Clp1 eliminated the migration shift of Mde4-13Myc (Figure 2-3D), confirming that Mde4 is phosphorylated in vivo, and that Clp1 can dephosphorylate Mde4 in vitro. Migration shift was enhanced in prometaphase arrested cells in the absence of $clp1^{+}$ (Figure 2-3E), suggesting that Mde4 is more highly phosphorylated in *clp1Δ* mutants. Moreover, oscillation of Mde4 migration shift resembles that of Cdk1 activity during the cell cycle. Consistent with this, Mde4 purified from *E. coli* can be phosphorylated in vitro by active Cdk1 isolated from prometaphase arrested cells using cold sensitive tubulin mutant *nda3-KM311* (Figure 2-3F). Taken together, these data show that Mde4 is phosphorylated by Cdk1 in early mitosis, and then becomes dephosphorylated by Clp1 in anaphase.

Clp1 promotes loading of monopolin onto the spindle during anaphase

To test how phosphorylation affects Mde4 function, we examined whether changes in Mde4 phosphorylation state correlates with changes in Mde4 localization. Previous results

showed that in interphase, when Mde4 is dephosphorylated, the Mde4-Pcs1 complex localizes at the nucleolus and kinetochores, which cluster at the nuclear periphery next to the spindle pole bodies (SPBs) (Gregan et al., 2007; Rabitsch et al., 2003). As cells enter into mitosis and Mde4 becomes phosphorylated, the Mde4-Pcs1 complex remains at kinetochores but leaves the nucleolus (Gregan et al., 2007; Rabitsch et al., 2003). Additionally we found that in anaphase, when Mde4 becomes dephosphorylated, Mde4 and Pcs1 localize to both ends of the anaphase spindle (Figure 2-4A and 2-4B). Because Mde4 is more highly phosphorylated in *clp1*Δ cells just prior to anaphase onset (Figure 2-3E), we examined Pcs1 and Mde4 localization in *clp1*Δ mutants as they progressed through mitosis. Pcs1-GFP localization was observed by time-lapse microscopy, using cells co-expressing the SPB marker Cdc11-GFP to monitor cell cycle progression (Figure 2-4B). In wild-type cells faint Pcs1-GFP spots, presumably corresponding to kinetochores, could be observed between the two SPBs in early mitosis. At anaphase onset Pcs1-GFP localized to the spindle (Figure 2-4B, red arrow) and then to both ends of the spindle at late anaphase. In *clp1*Δ cells, Pcs1-GFP spots at putative kinetochores were observed as in wild-type cells, however Pcs1-GFP was only observed faintly at both ends of the spindle at late anaphase (Figure 2-4B). As with Pcs1-GFP, Mde4-GFP localized faintly on the spindle in late, but not early, anaphase in *clp1*Δ cells (Figure 2-4C). The reduced spindle localization of Pcs1 and Mde4 in *clp1*Δ or *clp1-C286S* cells was not due to reduced protein levels since both proteins were present at or above wild-type levels in Clp1 mutant cells (Figure 2-3E and Figure 2-4D). In interphase, localization of Pcs1 and Mde4 to the nucleolus and kinetochores was not affected in *clp1*Δ cells (Figure 2-4C, and Figure 2-4E). These results

Figure 2-4

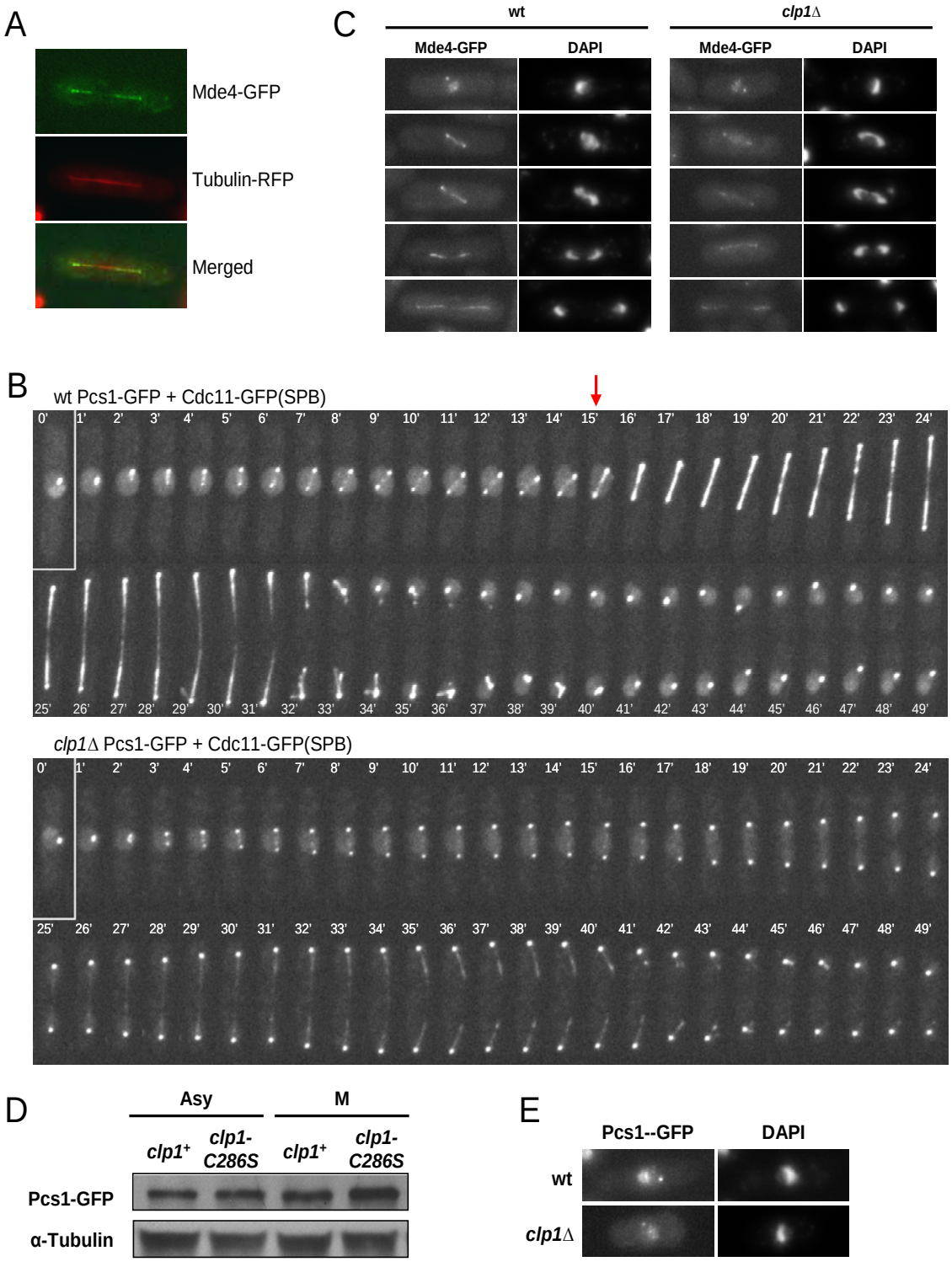
A
Mde4-GFP
Tubulin-RFP
Merged
C
wt
clp1Δ
Mde4-GFP
DAPI
Mde4-GFP
DAPI
B
wt Pcs1-GFP + Cdc11-GFP(SPB)
clp1Δ Pcs1-GFP + Cdc11-GFP(SPB)
D
Asy
M
clp1+
clp1-C286S
clp1+
clp1-C286S
Pcs1-GFP
α-Tubulin
E
Pcs1--GFP
DAPI
wt
clp1Δ

Figure 2-4: Clp1 Promotes Loading of Monopolin onto the Spindle during Anaphase

(A) *mde4-GFP* cell expressing mRFP-α-tubulin was imaged by fluorescence microscopy.
(B) *pcs1-GFP cdc11-GFP* (upper panel) and *clp1*Δ *pcs1-GFP cdc11-GFP* (lower panel) cells were analyzed using fluorescent time-lapse microscopy. Images were collected at one minute intervals, beginning immediately prior to entry into mitosis. The spindle pole body marker Cdc11-GFP was used to monitor cell-cycle progression. At time 0, both cells are in interphase just prior to mitotic entry. The arrow indicates anaphase onset, when Pcs1 begins to localize to the spindle.
(C) Mde4-GFP localization is shown in wild-type (WT, left panels) and *clp1*Δ cells (right panels). Interphase cells are shown in the top row, and cells from early to late anaphase are shown in the lower panels. Cells were grown asynchronously, fixed, stained with DAPI, and imaged by fluorescence microscopy.
(D) Protein level of Pcs1-GFP was examined by immunoprecipitation followed by western blotting of Pcs1-GFP isolated from either asynchronous (Asy) cells or cells arrested in prometaphase (M) via *nda3-KM311* mutation in either a *clp1*$^{+}$ and *clp1Δ* background. Lower panel shows the tubulin loading control.
(E) Pcs1-GFP localization in interphase is shown in wild-type (WT, top) and *clp1*Δ cells (bottom). Cells were grown asynchronously, fixed, stained with DAPI, and imaged by fluorescence microscopy.

suggest that dephosphorylation of Mde4 may be important for monopolin localization to the spindle.

Overproduction of nondestructible Cdc13 (cyclin B) inhibits the loading of Monopolin onto the spindle during Anaphase

Cdk1 activity drops after anaphase onset by the degradation of cyclin B by APC/C^{Cdc20} mediated proteolysis via the 26S proteasome (Buschhorn and Peters, 2006; Pesin and Orr-Weaver, 2008; Yu, 2002). To further confirm the effect of phosphorylation of Mde4 in the loading of monopolin onto the spindle during anaphase, we overproduced nondestructible *S. pombe* cyclin B, Cdc13ΔDB in which the destruction box of Cdc13 was deleted (Chang et al., 2001). Wild-type cells overexpressing Cdc13ΔDB displayed high levels of Cdk1 activity and accumulated in anaphase, leading to defects in mitotic exit (Chang et al., 2001; Yamano et al., 1996). The maintenance of active Cdk1 until anaphase by overproduction of Cdc13ΔDB led to a migration shift of Mde4 on SDS-PAGE, probably due to phosphorylation of Mde4 by Cdk1 in vivo (Figure 2-5A), but Mde4 was less phosphorylated than in prometaphase arrested cells using tubulin mutant, *nda3-KM311*, most likely because cells are less synchronized by overproduction of nondestructible Cdc13 than by *nda3-KM311* arrest. In cells overproducing Cdc13ΔDB, Mde4-GFP was not loaded onto the anaphase spindle, but localized diffusely throughout the nucleus (Figure 2-5B). Consistent with lack of localization of monopolin onto the early anaphase spindle in *clp1Δ* cells, these data suggest that phosphorylation of Mde4 by Cdk1 inhibits the loading of monopolin onto the spindle.

Figure 2-5

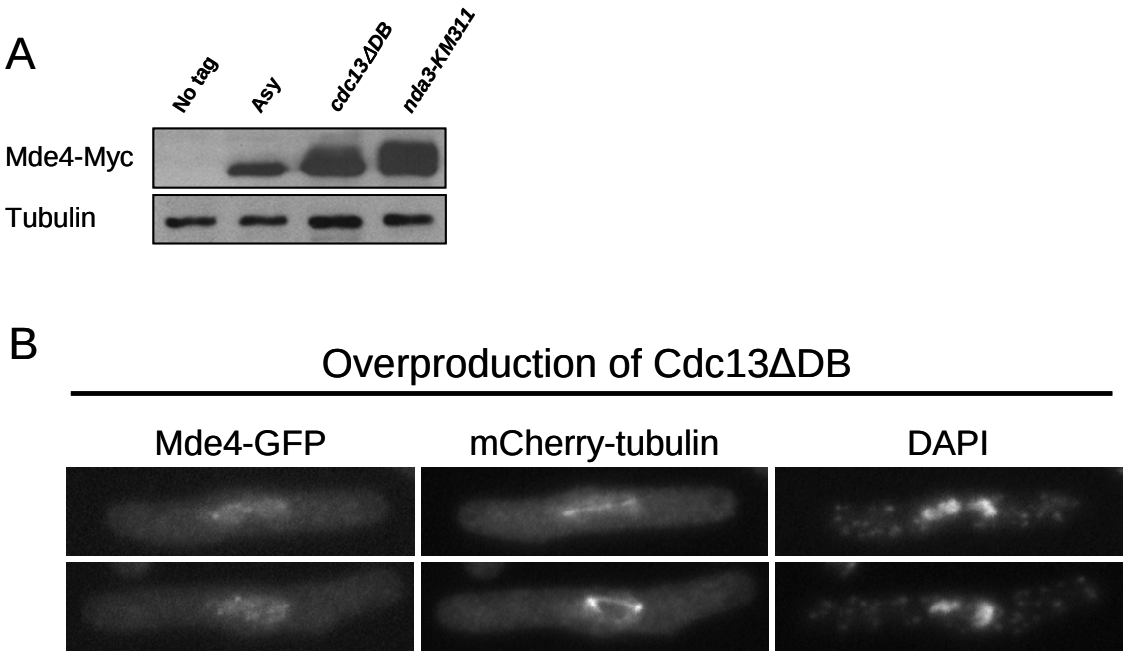
A
No tag
Asy
cdc13ΔDB
nda3-KM311
Mde4-Myc
Tubulin
B
Overproduction of Cdc13ΔDB
Mde4-GFP
mCherry-tubulin
DAPI

Figure 2-5: Overproduction of nondestructible Cdc13 Inhibits Loading of Monopolin onto the Spindle during Anaphase

(A) Gel migration of Mde4-13Myc was analyzed by immunoprecipitation followed by western blotting of Mde4-13Myc isolated from asynchronous (Asy) cells or cells overproducing Cdc13ΔDB for 19h (*cdc13ΔDB*) and cells arrested in prometaphase (M) via the *nda3-KM311* mutation (*nda3-KM311*). Lower panel shows the tubulin loading control. (B) Two examples of Mde4-GFP localization in anaphase were shown in *mde4-GFP mCherry-atb2* cells overproducing Cdc13ΔDB for 19h. Cells were fixed 19h after overexpression of Cdc13ΔDB, stained with DAPI, and imaged by fluorescence microscopy. Anaphase cells were picked as judged by DNA segregation via DAPI staining. The mitotic spindle was visualized by mCherry-atb2 (mCherry-tubulin).

Clp1 is not the only phosphatase to reverse Cdk1 phosphorylation on Mde4 during anaphase

To examine the contribution of Clp1 to Mde4 dephosphorylation in vivo, we synchronized wild-type and *clp1*Δ cells in prometaphase, then released them from the arrest and monitored Mde4 phosphorylation on SDS-PAGE. Although Mde4 is more highly phosphorylated at the prometaphase arrest point in *clp1*Δ cells, Mde4 still becomes dephosphorylated as these cells exit mitosis (Figure 2-6). Thus although Mde4 is specifically purified in a complex with the substrate trapping allele of Clp1, and can be dephosphorylated by Clp1 in vitro, this data indicate that other phosphatases are able to effect the dephosphorylation in vivo in the absence of Clp1. The identification of these phosphatases will be of considerable interest, and will be the subject of future studies. The ability of monopolin to localize faintly to the late anaphase spindles in *clp1*Δ mutant is consistent with this result showing that other phosphatases can compensate for the absence of Clp1. However, this experiment is not sufficient to show whether dephosphorylation of Mde4 is delayed in vivo at anaphase in *clp1*Δ mutant compared to wild type cell. The fission yeast stays at anaphase for about five minutes during cell cycle when grown at 30°C. Our data displayed a much larger window of anaphase duration (Figure 2-6) since first, synchronization using *nda3-KM311* mutation does not perfectly arrest cells in prometaphase and second, cells do not progress into anaphase at the same time after released from prometaphase arrest because cells in prolonged prometaphase caused by *nda3-KM311* mutation tend to have kinetochore-microtubule misattachments that can trigger the spindle assembly checkpoint (Radcliffe et al., 1998). We observed that Mde4 is

Figure 2-6

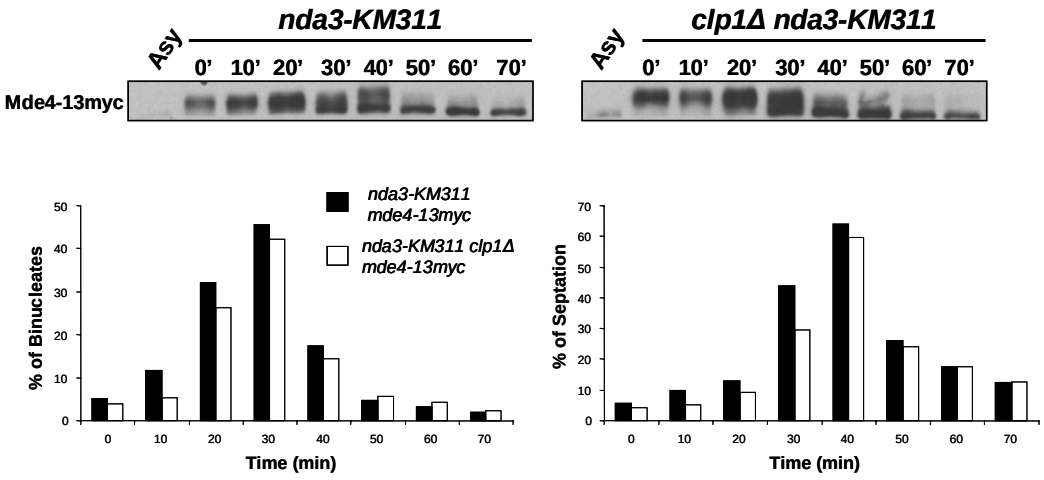
nda3-KM311
clp1Δ nda3-KM311
Asy
0' 10' 20' 30' 40' 50' 60' 70'
Mde4-13myc
nda3-KM311 mde4-13myc
nda3-KM311 clp1Δ mde4-13myc
% of Binucleates
% of Septation
Time (min)
Time (min)

Figure 2-6: Clp1 is not the only phosphatase to reverse Cdk1 phosphorylation on Mde4 during anaphase

mde4-13Myc nda3-KM311 and *mde4-13Myc clp1*Δ *nda3-KM311* cells were arrested at the restrictive temperature of 19°C for 6h to synchronize them in prometaphase, and were then shifted to the permissive temperature of 30°C. Samples were taken at the indicated time points and the migration shift of Mde4-13Myc (upper panel) and cell cycle progress (lower panel) were determined by western blot analysis and microscopy, respectively.

more highly phosphorylated at prometaphase in the absence of *clp1*$^{+}$(Figure 2-6 and Figure 2-3E). Although other phosphatases can reverse Cdk1 phosphorylation, it might take more time to completely dephosphorylate hyperphosphorylated Mde4 in *clp1*Δ mutants. That would be a reason why the monopolin complex does not localize on the spindle at early anaphase in *clp1*Δ cells.

Loss of Monopolin causes defects in microtubule attachment to kinetochores and activates the spindle checkpoint

To test whether spindle localization of the monopolin complex is important for spindle function, we examined spindle dynamics in monopolin mutants. The fission yeast spindle elongation can be divided into three distinct phases (Hagan, 1998; Khodjakov et al., 2004b; Nabeshima et al., 1998). During phase I, which begins when cells enter mitosis, the spindle forms and grows to span the nucleus at a length of 2.5~3μm. In phase II (metaphase/anaphase A), the spindle maintains the 2.5~3μm length until last chromosome is bi-oriented, and then elongates during phase III, which corresponds to anaphase B. This spindle elongation is mediated by sliding forces produced by motor proteins at the spindle midzone. Mitotic spindles were observed by time-lapse fluorescence microscopy in wild-type, *mde4*Δ, and *pcs1*Δ cells expressing GFP-α-tubulin. A comparison of the kinetics of spindle elongation in *mde4*Δ, *pcs1*Δ, and wild-type cells revealed that cells lacking monopolin spend significantly more time in phase II (Figure 2-7A). Wild-type cells stayed less than 20 min in phase II, but 8 of 14 *mde4*Δ cells, and 6 of 8 *pcs1*Δ cells showed a prolonged phase II suggesting a delay in metaphase. A metaphase delay is often observed

Figure 2-7

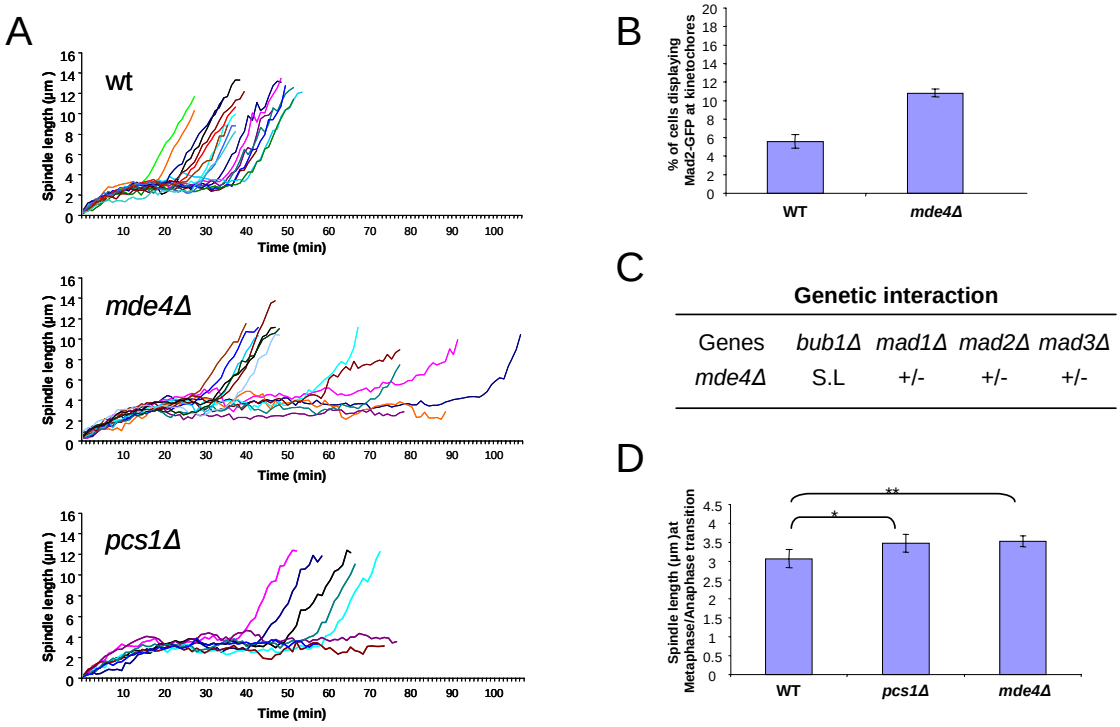
A
wt
mde4Δ
pcs1Δ
Spindle length (µm)
Time (min)
B
% of cells displaying Mad2-GFP at kinetochores
WT
mde4Δ
C
Genetic interaction
Genes bub1Δ mad1Δ mad2Δ mad3Δ
mde4Δ S.L +/- +/- +/-
D
Spindle length (µm) at Metaphase/Anaphase transition
WT
pcs1Δ
mde4Δ

Figure 2-7: Loss of Monopolin Causes Defects in Microtubule Attachment to Kinetochores and Activates the Spindle Checkpoint

(A) Spindle elongation was monitored in wild-type and monopolin mutant cells. Spindle length were measured every one minute from time-lapse sequences of asynchronous *GFP-atb2* (n=17), *GFP-atb2 mde4D* (n=14), and *GFP-atb2 pcs1D* (n=8) cells.
(B) Asynchronous wild-type (n=779) and *mde4*Δ (n= 901) cells expressing Mad2-GFP were scored for the presence of Mad2-GFP puncta at kinetochores. Error bars represent standard deviation (SD)
(C) Genetic interactions between the *mde4*Δ and spindle assembly checkpoint mutations. The *mde4*Δ mutants were crossed with the spindle assembly checkpoint mutants *bub1*Δ, *mad1*Δ, *mad2*Δ and *mad3*Δ. Genetic interactions are shown as synthetic lethality (S.L), strong growth defect (+/-).
(D) A comparison of spindle lengths of wild-type and monopolin mutant cells at the metaphase/anaphase transition. Mean spindle lengths were compared between wild-type (n=17) and *pcs1Δ* (n=8, single asterisks, $p<0.01$) and *mde4Δ* (n=14, double asterisk, $p<0.0001$) by a *t* test. Error bars represent standard deviation.

in cells when microtubule attachments to kinetochores are defective, which triggers the spindle checkpoint to inhibit anaphase onset. Observation of asynchronous wild-type and *mde4*Δ cells showed that an elevated percent of *mde4*Δ cells displayed spindle checkpoint activation as judged by the presence of Mad2 at kinetochores (Figure 2-7B). We tested for genetic interactions between the *mde4*Δ mutant and the spindle checkpoint mutants, *mad1*Δ, *mad2*Δ, *mad3*Δ and *bub1*Δ. The *mde4*Δ mutation was synthetic lethal with *bub1*Δ since no double mutants were recovered. Double mutants between *mde4*Δ and *mad1*Δ, *mad2*Δ or *mad3*Δ showed strong synthetic growth defects (Figure 2-7C), consistent with the notion that *mde4*Δ cells have defects in attachment of microtubules to kinetochores, which trigger spindle checkpoint dependent delays.

We observed another difference in spindle morphology in monopolin mutants. Spindle lengths at the phase II/III transition in *mde4*Δ and *pcs1*Δ mutants were longer, 3.52 ± 0.15 μm and 3.47 ± 0.23 μm respectively, than that of wild-type cells, 3.07 ± 0.23 μm (Figure 2-7D). Elongated phase II spindles have also been observed in *mis6* and *mis12* mutants, which are defective in kinetochore-microtubule attachment (Goshima et al., 1999), and cells defective in cohesion between sister chromatids (Toyoda et al., 2002). This may suggest that poorly attached kinetochores in monopolin mutants cause an imbalance of pushing and pulling forces in the spindle, leading a somewhat elongated metaphase spindle. Previous results have shown that monopolin is involved in preventing merotelic attachments (Gregan et al., 2007), which are not believed to be monitored by the spindle checkpoint. However our results suggest an additional role for monopolin in attachment of microtubules to kinetochores that is monitored by the spindle checkpoint. The monopolin

complex might be required for prevention of all microtubule mis-attachments at kinetochores or/and some merotelic attachments might be monitored by the spindle assembly checkpoint in vivo.

Monopolin may stabilize anaphase spindle microtubules to prevent chromosome co-segregation

The analysis of spindle elongation in *mde4*Δ cells revealed another novel function of monopolin in promoting anaphase spindle stability. In 6.4% (3 of 47) of *mde4*Δ cells, the spindles appeared to break and/or collapse (Figure 2-8A (Movie 1); Figure 2-8B (Movie3); Movie 2)(Movies are linked in Choi et al., 2009). Consistent with this, we found that about 8.5 % of septated *mde4*Δ cells showed chromosome co-segregation, in which one daughter cell inherited all of the chromosomes (Figure 2-8C). This phenotype likely arises because the nuclear envelope does not break down during mitosis in *S. pombe*. As a consequence of this, chromosomes collapse back into a single mass inside the nuclear envelope when the spindle breaks prematurely. Similar results have been observed when the mitotic spindle was cut using laser microsurgery (Khodjakov et al., 2004a; Tolic-Norrelykke et al., 2004). In those studies, when the mitotic spindle was cut in the middle, it completely collapsed since the laser destroyed anti-parallel microtubule structures at the spindle midzone. However, when the mitotic spindle was cut near either of the SPBs, it did not affect the structure of the spindle midzone. So, a sliding force generated by motor proteins at the spindle midzone elongates the spindle unidirectionally, with the end of the spindle lacking an SPB pushing out the nuclear envelope as it elongated, resulting in a finger-like extension

Figure 2-8

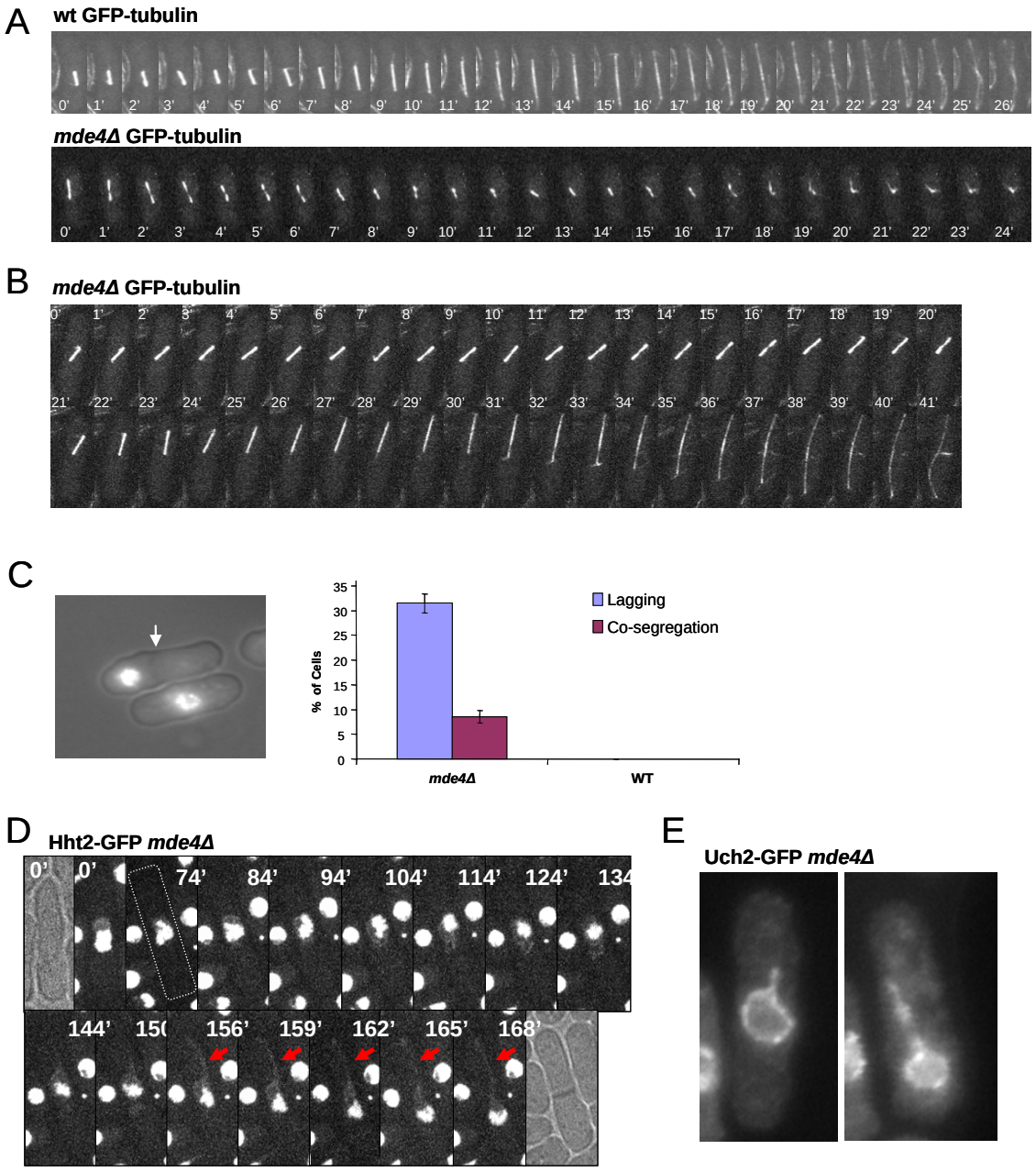
A
wt GFP-tubulin
0' 1' 2' 3' 4' 5' 6' 7' 8' 9' 10' 11' 12' 13' 14' 15' 16' 17' 18' 19' 20' 21' 22' 23' 24' 25' 26'
mde4Δ GFP-tubulin
0' 1' 2' 3' 4' 5' 6' 7' 8' 9' 10' 11' 12' 13' 14' 15' 16' 17' 18' 19' 20' 21' 22' 23' 24'
B
mde4Δ GFP-tubulin
0' 1' 2' 3' 4' 5' 6' 7' 8' 9' 10' 11' 12' 13' 14' 15' 16' 17' 18' 19' 20'
21' 22' 23' 24' 25' 26' 27' 28' 29' 30' 31' 32' 33' 34' 35' 36' 37' 38' 39' 40' 41'
C
% of Cells
35
30
25
20
15
10
5
0
Lagging
Co-segregation
mde4Δ
WT
D
Hht2-GFP mde4Δ
0' 0' 74' 84' 94' 104' 114' 124' 134
144' 150 156' 159' 162' 165' 168'
E
Uch2-GFP mde4Δ

Figure 2-8: Monopolin May Stabilize Anaphase Spindle Microtubules to Prevent Chromosome Cosegregation

(A) Time-lapse analysis using GFP-tubulin expressing wild-type (upper panel) and *mde4Δ* mutant cells (lower panel) is shown. Images were collected at one minute intervals.
(B) Time-lapse analysis using GFP-α-tubulin expressing *mde4*Δ cell is shown. The images were collected at one minute intervals.
(C) Left: an example of the chromosome co-segregation phenotype observed in *mde4Δ* cells (arrow indicates septum position). Right: the frequency of anaphase cells with lagging chromosomes and septated cells with cosegregated chromosomes for *mde4Δ* (anaphase cells (n=327) and septated cells (n=549)) and wild type (anaphase cells (n-=350) and septated cells (n=570)) cells. Error bar represent standard deviation.
(D) Time-lapse analysis using histone H3-GFP (hht2-GFP) expressing *mde4*Δ cell is shown. The images were collected at one minute intervals. A thin protrusion of nucleoplasmic staining of free Hht2-GFP is indicated (red arrow).
(E) Examples of nuclear envelope protrusion observed in *mde4*Δ cells using the nuclear envelope protein Uch2-GFP, which was visualized by fluorescence microscopy.

of the nuclear envelope (Figure 2-8E). Once the broken end of the spindle reached the end of the cell, it pushed against the cell tip causing the other spindle pole to move to the opposite end of the cell. Of the three cells that showed spindle elongation defects, two showed spindle breakage and collapse (Figure 2-8A (Movie1) and Movie 2) and one showed unidirectional spindle elongation, suggesting that the spindle may have broken near one pole (Figure 2-8B (Movie 3)). Another case of apparent spindle breakage near one SPB followed by chromosome co-segregation was observed by time-lapse analysis of *mde4*Δ cells expressing histone H3-GFP (Figure 2-8D). In this cell, chromosomes were condensed but co-segregated into one daughter cell after cytokinesis. Whole chromosomes started to move toward one side after a thin protrusion of nucleoplasmic staining of free histone H3-GFP reached the other side of the cell tip, probably due to the nuclear envelope extension by unidirectional spindle elongation (red arrow, Figure 2-8D). Furthermore, thin protrusions of the nuclear envelope possibly caused by broken spindle ends were also occasionally observed in *mde4*Δ but not in wild-type cells (Figure 2-8E). Taken together, our data suggest that monopolin may have a novel function in stabilization of anaphase spindles.

Characterization of nonphosphorylatable and phosphomimetic mutants of Mde4

To more clearly define the role of phosphorylation of Mde4 in regulating function of the monopolin complex, we constructed non phosphorylatable and phospho-mimetic mutants of Mde4. Although five of twelve potential Cdk1 sites on Mde4 were identified as

Figure 2-9

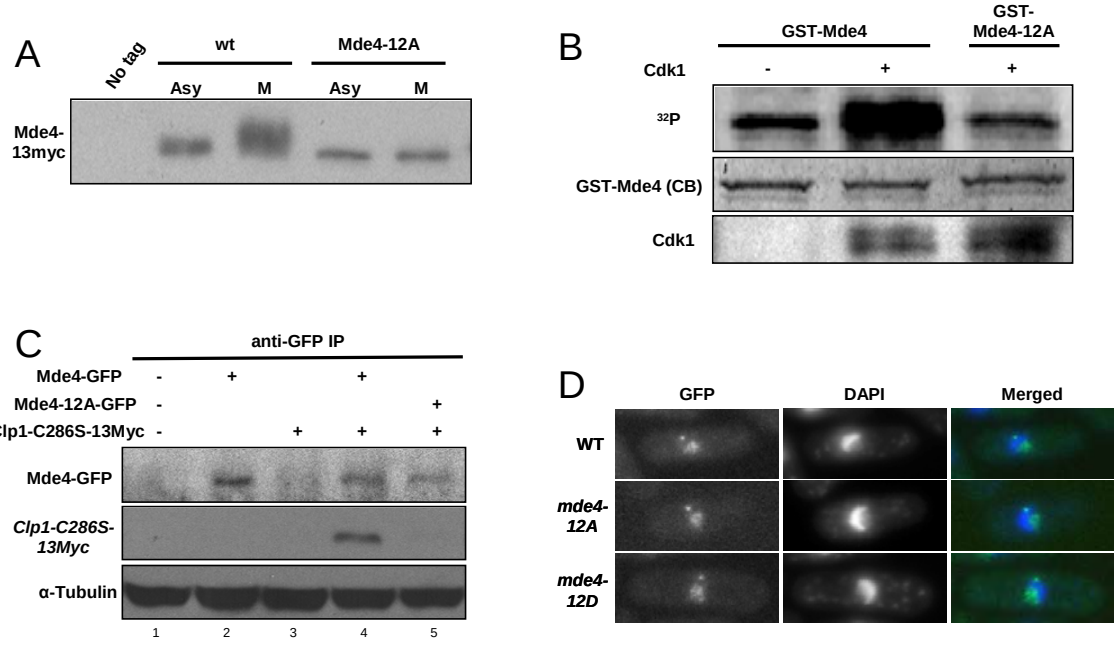
A
No tag
wt
Mde4-12A
Asy
M
Asy
M
Mde4-13myc
B
GST-Mde4
GST-Mde4-12A
Cdk1
-
+
+
32P
GST-Mde4 (CB)
Cdk1
C
anti-GFP IP
Mde4-GFP - + +
Mde4-12A-GFP - +
Clp1-C286S-13Myc - + + +
Mde4-GFP
Clp1-C286S-13Myc
α-Tubulin
1 2 3 4 5
D
GFP
DAPI
Merged
WT
mde4-12A
mde4-12D
E
Pcs1-GFP
DAPI
Merged
mde4Δ
mde4+
mde4-12A
mde4-12D

Figure 2-9: Characterization of *mde4-12A* and *mde4-12D*, Nonphosphorylatable and Phosphomimetic Mutants of Mde4

(A) Mde4 migration shift by phosphorylation was examined in wild-type (No tag), *mde4-13Myc* (wt) and *mde4-12A-13Myc* (12A) cells grown asynchronously (Asy) at 30°C or arrested at metaphase (M) by *nda3-KM311* block at 19°C. IP-Western blot is shown.
(B) In vitro Kinase assay were performed using purified Cdk1 from metaphase arrested *nda3-KM311* cells by Cdc13 (*S. pombe* Cyclin B) immunoprecipitation, and bacterially expressed GST-Mde4-137-421 or GST-Mde4-12A-137-421 were used as substrates. Protein labeled by γ-^{32}P-labeled protein was detected with a Phosphorimager (Molecular Dynamics), and the gel was stained with Coomassie blue (CB) as a loading control. The level of Cdk1 was determined by western blotting.
(C) Anti-GFP (upper panel) and anti-Myc (middle panel) western blots of anti-GFP immunoprecipitates from cell lysates of the following cultures are shown: wild-type (1), *mde4-GFP* (2), *clp1-C286S-13Myc* (3), *mde4-GFP clp1-C286S-13Myc* (4), *mde4-12A-GFP clp1-C286S-13Myc* (5). Lower panel shows the tubulin loading control from whole cell extracts prior to immunoprecipitation.
(D) Asynchronously growing cells expressing Mde4-GFP, Mde4-12A-GFP, and Mde4-12D-GFP were fixed, stained with DAPI, and DAPI and GFP signals were visualized using fluorescence microscopy. Interphase cells are shown.
(E) Asynchronously growing *mde4*Δ, *mde4*$^{+}$, *mde4-12A*, and *mde4-12D* cells expressing Pcs1-GFP were fixed, stained with DAPI, and DAPI and GFP signals were visualized using fluorescence microscopy. Interphase cells are shown. Note for (D) and (E) that the nucleolus is the non DAPI staining region of the nucleolus, and the spot at the nuclear periphery corresponds to the clustered kinetochores in interphase.

phosphorylated by our mass spectrometry analysis (Figure 2-3A), sequence coverage of Mde4 from our mass spectrometry was only about 30%, making it difficult to define all *in vivo* Cdk1 phosphorylation sites on Mde4. Therefore we mutated all twelve of the Cdk1 consensus sites to alanine (S/T to A) to prevent phosphorylation or to acidic residues (S to D and T to E) to create a phospho-mimetic mutant. We named them *mde4-12A* and *mde4-12D* respectively, and constructed strains where the endogenous *mde4*$^{+}$ locus was replaced by *mde4-12A* and *mde4-12D*. As expected, the Mde4-12A mutant protein was no longer hyperphosphorylated in metaphase-arrested cells (Figure 2-9A) and Mde4-12A was not phosphorylated by Cdk1 in vitro (Figure 2-9B), indicating that the major sites of mitotic phosphorylation by Cdk1 had been eliminated. Additionally, Mde4-12A did not interact with Clp1-C286S (Figure 2-9C), further confirming that phosphorylation is required for interaction with the Clp1-C286S substrate trapping allele. We do not believe that the 12A and 12D mutations grossly perturbed the Mde4 protein structure because they did not affect Mde4-GFP localization to kinetochores and the nucleolus in interphase cells (Figure 2-9D). Additionally, kinetochore and nucleolar localization of Pcs1-GFP was abolished in the absence of Mde4 (Figure 2-9E), but was retained in *mde4-12A* and *mde4-12D* mutants (Figure 2-9E) suggesting that the Cdk1 site mutations do not disrupt formation of the monopolin complex.

Phosphorylation of Mde4 is required to prevent monopolin localization to the prometaphase/metaphase spindle

Figure 2-10

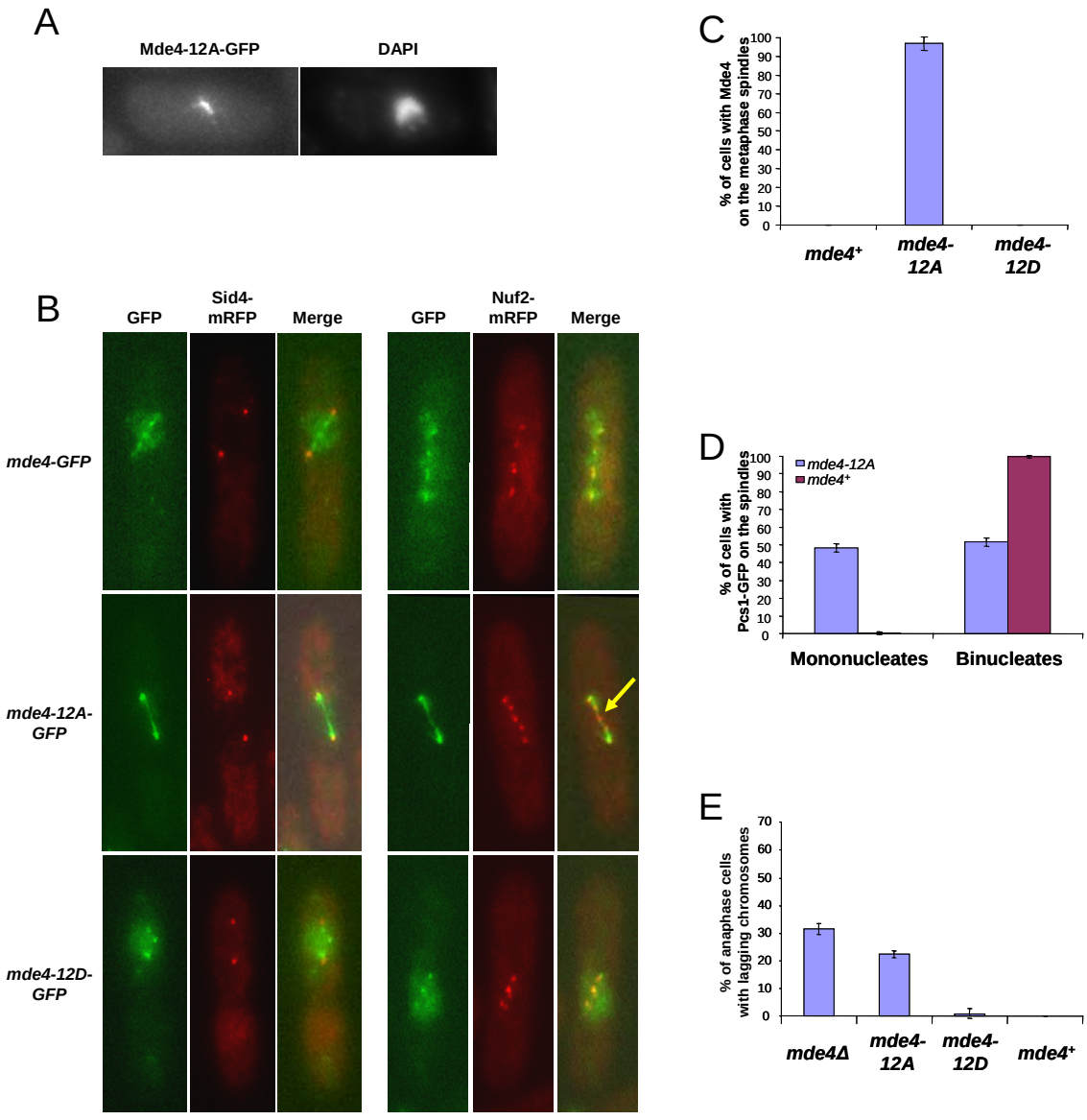
A
Mde4-12A-GFP
DAPI
B
GFP
Sid4-mRFP
Merge
GFP
Nuf2-mRFP
Merge
mde4-GFP
mde4-12A-GFP
mde4-12D-GFP
C
% of cells with Mde4 on the metaphase spindles
mde4+
mde4-12A
mde4-12D
D
% of cells with Pcs1-GFP on the spindles
mde4-12A
mde4+
Mononucleates
Binucleates
E
% of anaphase cells with lagging chromosomes
mde4Δ
mde4-12A
mde4-12D
mde4+

Figure 2-10: *Mde4-12A* Prematurely Localizes to the Spindle Instead of Kinetochores Before Anaphase Onset and Displays Lagging Chromosomes in Anaphase

(A) Pcs1-GFP localization is shown in *mde4-12A* cells in preanaphase. Cells were grown asynchronously, fixed, stained with DAPI, and imaged by fluorescence microscopy. Mitotic progression was determined by DNA condensation, segregation and spindle length.
(B) Localization of Mde4, Mde4-12A, and Mde4-12D at metaphase was examined in the following strains: *mde4-GFP sid4-mRFP, mde4-12A-GFP sid4-mRFP, mde4-12D-GFP sid4mRFP* (left panel), *mde4-GFP nuf2-mRFP, mde4-12A-GFP nuf2-mRFP,* and *mde4-12D-GFP nuf2-mRFP* (right panel). Cells were arrested in metaphase by overexpression of Mad2 using the pRFP3X-Mad2 plasmid for 19 hr in the absence of thiamine. Cells were fixed and imaged by fluorescence microscopy. The yellow arrow indicates a kinetochore that does not appear to label with Mde4-12A-GFP.
(C) The frequency of Mde4 localization to the metaphase spindle. *mde4-GFP sid4-mRFP, mde4-12A-GFP sid4-mRFP, mde4-12D-GFP sid4-mRFP* cells were arrested at metaphase by Mad2 overexpression for 19h. Cells showing spindle localization were counted among metaphase arrested cells exhibiting unseparated condensed chromosomes and separated spindle pole bodies. Error bars represent SD.
(D) Quantification of Pcs1 spindle localization in preanaphase and postanaphase *mde4*$^{+}$, and *mde4-12A* cells. *pcs1-GFP* and *pcs1-GFP mde4-12A* cells were grown asynchronously at 30°C then fixed and stained with DAPI. Of cells that showed Pcs1 spindle localization, the percentage that were mononucleate or binucleate is shown. Error bars represent SD.
(E) Frequency of lagging chromosomes in *mde4* mutants was determined by counting the percent of anaphase cells with lagging or unevenly segregated chromosomes from asynchronously growing *mde4Δ, mde4-12A, mde4-12D,* and wild-type cells. Error bars represent SD.

Unlike wild-type Mde4, Mde4-12A-GFP was often observed on the spindle in pre-anaphase cells (Figure 2-10A), suggesting that it may load onto the spindle prematurely. To examine this in greater detail, we arrested cells at metaphase by overexpressing the spindle assembly checkpoint protein Mad2, which prevents cyclin B and securin destruction by suppressing the activity of the APC/C^{Cdc20} complex (He et al., 1997). Under this condition, Mde4-GFP and Mde4-12D-GFP were observed as several faint dots between the two spindle pole bodies marked with Sid4-mRFP (Figure 2-10B left panel). These dots co-localized with a kinetochore protein, Nuf2-mRFP (Figure 2-10B right panel). In contrast, Mde4-12A-GFP localized prematurely to the metaphase spindle and did not appear to localize at kinetochores (Figure 2-10B, yellow arrow). Mde4-12A localized to the metaphase spindle in 97% (n = 115) of metaphase cells, in contrast to Mde4 (n = 126) and Mde4-12D (n = 103), which did not localize on the spindle in a single metaphase cell (Figure 2-10C). To examine how the *mde4-12A* mutation affects Pcs1 localization, we counted cells displaying spindle localization of Pcs1-GFP in asynchronous *mde4*$^{+}$ and *mde4-12A* cells and classified them into mononucleate (early mitosis) and binucleate cells (anaphase). In wild-type cells, Pcs1-GFP localization on the spindle was observed almost exclusively in anaphase cells (307 of 308). In *mde4-12A* cells, Pcs1-GFP localized to the spindle normally in anaphase cells but was also observed on the short spindle in preanaphase cells; specifically, 48% (n = 350) of cells exhibiting Pcs1-GFP localization to the spindle were mononucleates (Figure 2-10D). Thus, in each assay the non-phosphorylatable Mde4-12A mutant localizes the monopolin complex inappropriately to

the prometaphase/metaphase spindle, implying that Cdk1 phosphorylation on Mde4 acts to prevent premature localization of the Pcs1-Mde4 complex to the mitotic spindle.

Localization of monopolin at kinetochores has been proposed to prevent merotelic attachments, which cause lagging chromosomes in anaphase (Gregan et al., 2007; Rabitsch et al., 2003). We observed that 22% of *mde4-12A* cells (n = 304) exhibited lagging chromosomes in anaphase, comparable to the 31% observed in *mde4*Δ cells (n = 327) (Figure 2-10E). In contrast, less than 1% of *mde4-12D* cells (n = 311) in anaphase showed lagging chromosomes (Figure 2-10E). Our data shows that Cdk1 phosphorylation on Mde4 is important for the role of monopolin in preventing merotelic attachment of kinetochores to spindle microtubules. One explanation for this could be that Cdk1 phosphorylation promotes kinetochore localization of Mde4 by inhibiting premature localization of Mde4 to microtubules in prometaphase/metaphase.

Dephosphorylation of Mde4 promotes localization of monopolin to the anaphase spindle

We used the *mde4-12A* and *mde4-12D* mutants to explore the role of Mde4 dephosphorylation in monopolin localization to the anaphase spindle (Figure 2-11A). Mde4-GFP and Mde4-12A-GFP localized similarly to the spindle in early and late anaphase. In contrast, Mde4-12D-GFP showed a diffused nuclear signal in anaphase, with less than 10% of cells showing faint spindle localization. Pcs1-GFP localized in *mde4*$^{+}$, *mde4-12A*, and *mde4-12D* cells in the same way as each Mde4 mutant protein (Figure 2-11A lower panels), further confirming that the phosphorylation status of Mde4 regulates

Figure 2-11

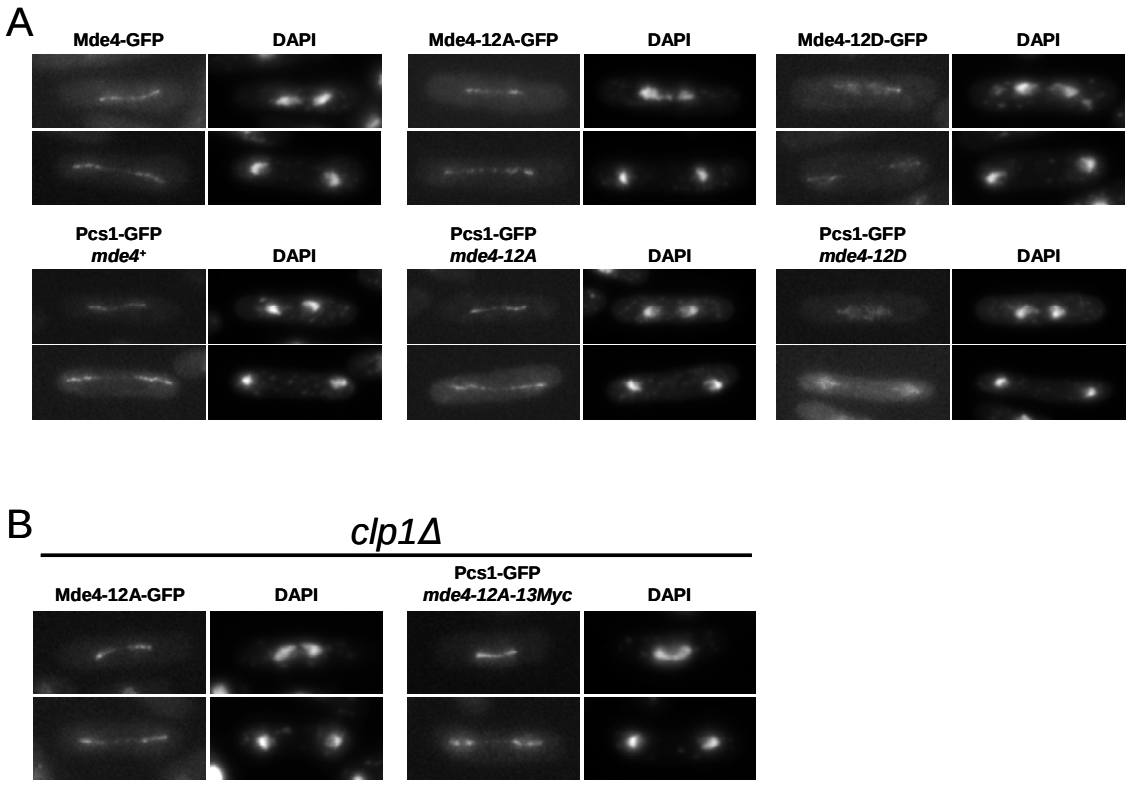
A
Mde4-GFP
DAPI
Mde4-12A-GFP
DAPI
Mde4-12D-GFP
DAPI
Pcs1-GFP
mde4+
DAPI
Pcs1-GFP
mde4-12A
DAPI
Pcs1-GFP
mde4-12D
DAPI
B
clp1Δ
Mde4-12A-GFP
DAPI
Pcs1-GFP
mde4-12A-13Myc
DAPI

Figure 2-11: Mde4-12D Weakly Localizes on Anaphase Spindles and Produces Chromosome Co-segregation

Cells were grown asynchronously, fixed and imaged by fluorescence microscopy.
(A) Early- (top row) and late-anaphase (bottom row) localization of wild-type Mde4-GFP, Mde4-12A-GFP, Mde4-12D-GFP (upper panels), and Pcs1-GFP in *mde4*$^{+}$, *mde4-12A*, and *mde4-12D* cells (lower panels).
(B) Early- (top row) and late-anaphase localization (bottom row) of Mde4-12A-GFP in *clp1Δ* and Pcs1-GFP in *mde4-12A clp1Δ* cells.

localization of the monopolin complex to the spindle. The poor localization of Mde4-12D to the spindle is similar to that observed for wild-type Mde4 in *clp1*Δ cells (see Figure 2-4C), presumably because Mde4 is not dephosphorylated as rapidly in *clp1*Δ cells. If this is the case, then disruption of Mde4 phosphorylation should rescue the Mde4 spindle localization defect in *clp1*Δ cells. This proved to be the case, since Mde4-12A localized strongly to the anaphase spindles in *clp1*Δ cells (Figure 2-11B). Together these results show that Cdk1 phosphorylation must be removed to allow Mde4 to localize to the anaphase spindles.

Both *mde4-12A* and *mde4-12D* cells display distinct defects in spindle elongation

To better characterize spindle dynamics in *mde4-12A* and *mde4-12D* mutants, spindle elongation was observed by time-lapse microscopy in these cells. Spindle elongation in *mde4-12A* cells resembled that seen in *mde4*Δ cells (compare Figure 2-12A with Figure 2-7A), in that 50% of *mde4-12A* cells (10 of 20) stayed longer at phase II than *mde4*$^{+}$ cells. However unlike *mde4*Δ cells, we did not observe spindle collapse or breakage in *mde4-12A* cells. The extended phase II in *mde4-12A* cells suggests that, like *mde4*Δ cells, they have microtubule attachment defects that trigger a spindle assembly checkpoint-dependent delay. To test this notion, we first compared the frequency of spindle checkpoint activation by monitoring the presence of Mad2 at kinetochores in cycling cells. *mde4-12A* cells displayed a similar level of checkpoint activation as *mde4*Δ cells (Figure 2-12B). Then we crossed *mde4-12A* to various spindle checkpoint mutants. The *mde4-12A* mutant was synthetic lethal with the *mad1*Δ, *mad2*Δ, *mad3*Δ and *bub1*Δ checkpoint mutants (Figure 2-12C) since

Figure 2-12

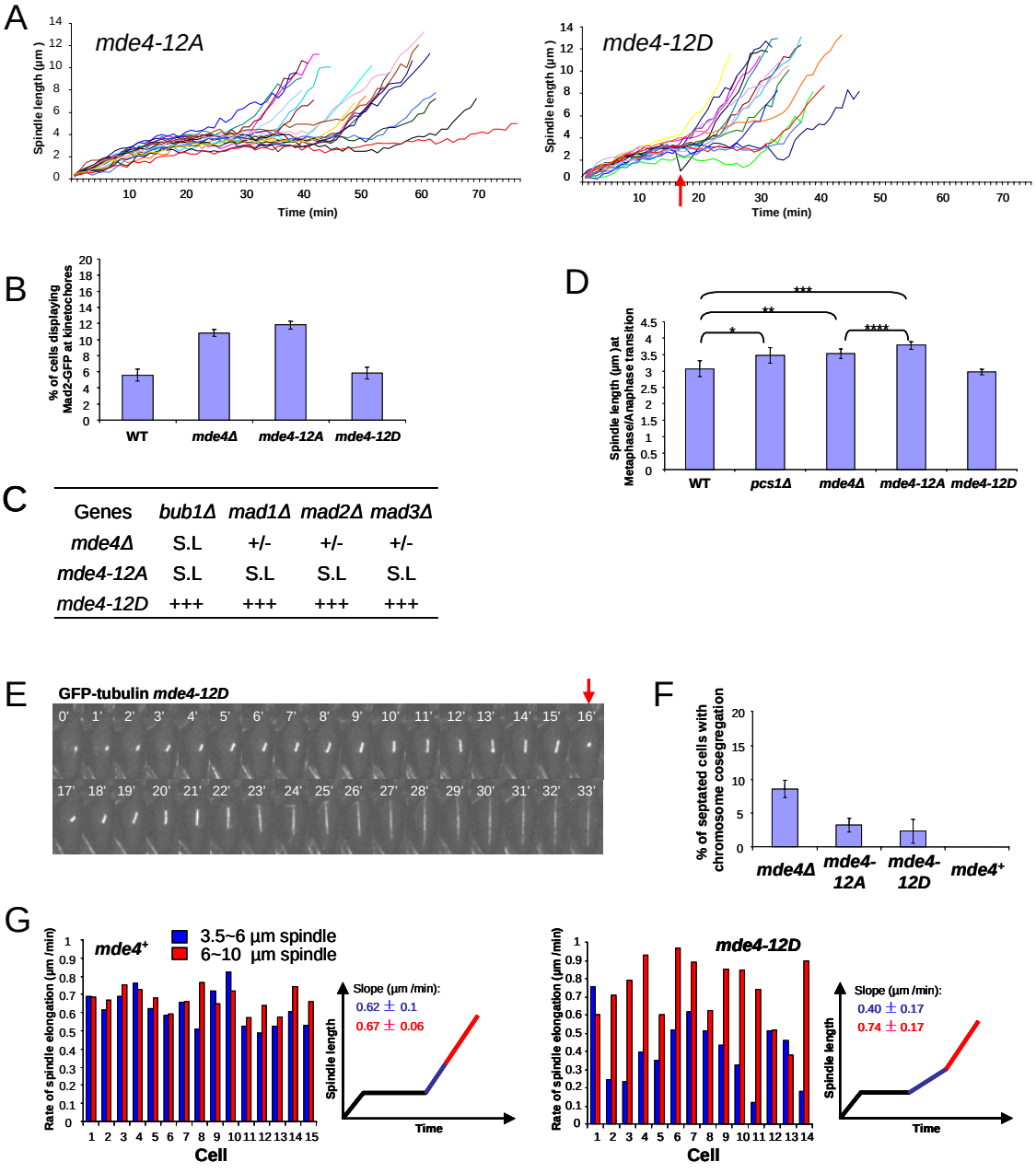

Genes	*bub1Δ*	*mad1Δ*	*mad2Δ*	*mad3Δ*
mde4Δ	S.L	+/-	+/-	+/-
mde4-12A	S.L	S.L	S.L	S.L
mde4-12D	+++	+++	+++	+++

Figure 2-12: Both *mde4-12A* and *mde4-12D* Cells Display Distinct Defects in Spindle Elongation

(A) Spindle elongation was monitored in *mde4-12A* and *mde4-12D* cells. Spindle length was measured every one minute from time-lapse sequences of asynchronous *GFP-atb2 mde4-12A* (n=20) and *GFP-atb2 mde4-12D* (n=17) cells. Arrow indicates spindle collapse in the cell shown in (E).
(B) Asynchronous wild-type (n=779) and *mde4*Δ (n=901), *mde4-12A* (n=662), *and mde4-12D* (n=651) cells expressing Mad2-GFP were scored for the presence of Mad2-GFP puncta at kinetochores.
(C) Genetic interactions between the *mde4*Δ, *mde4-12A*, and *mde4-12D* mutations and spindle assembly checkpoint mutations. The *mde4*Δ, *mde4-12A* and *mde4-12D* mutants were crossed with the spindle assembly checkpoint mutants *bub1*Δ, *mad1*Δ, *mad2*Δ and *mad3*Δ. Genetic interactions are shown as synthetic lethality (S.L), strong growth defect (+/-) and normal growth (+++).
(D) A comparison of spindle lengths of wild-type (n=17) and monopolin mutant *pcs1Δ* (n=8), *mde4Δ* (n=14), *mde4-12A* (n=20), and *mde4-12D* (n=16) cells at the metaphase/anaphase transition. The mean lengths of the spindle were compared between wild-type and *pcs1Δ* (single asterisk, $p<0.01$), *mde4Δ* (double asterisks, $p<0.01$) or *mde4-12A* (triple asterisk $p<0.0001$) by a *t* test. Error bars represent standard deviation.
(E) Spindle collapse and re-elongation was observed in 1 of 17 the *GFP-atb2 mde-12D* cells shown in (A). Images were collected every minute and spindle collapse was reconfirmed by examining a 3D view of the spindle from stacked images (data not shown) at the time point of spindle shortening (red arrow).
(F) Frequency of chromosome co-segregation in *mde4* mutants was determined by counting the percent of septated cells with a single DNA mass in only one daughter cell. Error bar represent SD. (n=549, 554, 561, 570 in *mde4Δ, mde4-12A, mde4-12D* and wild-type cells respectively)
(G) Comparison of spindle elongation rate between $mde4^{+}$ (n=15) and *mde4-12D* (n=14) cells. Spindle elongation rates were obtained by measuring the slope of plots of spindle length over time via linear regression in individual $mde4^{+}$ and *mde4-12D* anaphase cells. Slopes were calculated for early- (spindle lengths of 3.5-6um, shown as a blue bar) and late-anaphase (spindle lengths of 6-10 um, shown as a red bar). Each pair of red and blue bars represents an individual cell.

no double mutants were recovered, suggesting that the extended duration at phase II in *mde4-12A* cells is due to the activation of the spindle checkpoint. Notably, this interaction is even stronger than that observed for *mde4*Δ, since *mde4*Δ was only lethal with *bub1*Δ. Additionally, *mde4-12A* cells displayed much longer spindle at the phase II/III transition (3.78±0.12μm) than wild-type cells and even slightly longer than *mde4*Δ cells (Figure 2-12D). These results suggest that *mde4-12A* mutants may have greater defects in microtubule attachment to kinetochores than *mde4*Δ cells. This could be explained if the defects in *mde4-12A* cells are due not just to loss of Mde4 from the kinetochores in metaphase, but also to premature localization of Mde4 to the spindle.

Overall *mde4-12D* cells showed spindle behavior similar to wild-type cells but most cells (14 of 16) displayed slightly shorter phase II which is not statistically significant by *t*-test (Figure 2-12A and Figure 2-7A). Spindle lengths at the phase II/III transition in *mde4-12D* cells were 2.97 ± 0.09 μm, which is similar to that of wild-type cells (Figure 2-12D), and *mde4-12D* cells did not show negative genetic interactions with the spindle checkpoint mutants, *mad1*Δ, *mad2*Δ, *mad3*Δ and *bub1*Δ (Figure 2-12C), suggesting that microtubule attachment in *mde4-12D* cells is as normal as wild type. Consistent with Mde4 spindle localization being important for spindle stability, we found one *mde4-12D* cell that showed spindle collapse followed by recovery (Figure 2-12E). In addition, 2.3% of *mde4-12D* cells display chromosome co-segregation (Figure 2-12F) suggesting that reduced levels of Mde4 on the spindle may make the spindle less stable resulting in chromosome co-segregation due to spindle collapse. Unexpectedly, we also found that *mde4-12D* cells display slowed spindle elongation in early anaphase B (Figure 2-12G). We measured the spindle

elongation rate during early (from 3.5 to 6 μm length of the spindle) and late (from 6 to 10 μm length of the spindle) phase III. Although in wild-type cells the rate of spindle elongation (~0.65 μm/min) was the same in early and late phase III, in *mde4-12D* cells the rate of spindle elongation was slower during early phase III (~0.40 μm/min) but was similar to wild-type cells in late phase III (0.74 μm/min). Taken together, our data suggest that dephosphorylation of Mde4 by Clp1 triggers spindle localization of monopolin, which promotes proper spindle elongation in early anaphase and enhances spindle stability.

Discussion Chapter II

For faithful segregation of genetic material, chromosomes must be attached to microtubules in a bi-oriented manner at metaphase, and segregated to each daughter cell through spindle elongation at anaphase. Our studies show that regulated phosphorylation of the monopolin complex allows it to carry out discrete functions in each of these steps (Figure 2-13). When cells enter mitosis, the Mde4-Pcs1 complex is released from the nucleolus and Mde4 becomes phosphorylated on Cdk1 sites. Mde4 phosphorylation does not appear to cause release of Mde4 from the nucleolus, since Mde4-12A is still released from the nucleolus in early mitosis. Instead, phosphorylation of Mde4 is required to prevent localization of the Mde4-Pcs1 complex to the metaphase spindle. Furthermore, the Mde4-12A protein not only localizes prematurely to the spindle, it also appears to localize poorly to the kinetochores. This could either be because monopolin localization to kinetochores requires Mde4 phosphorylation, or because the Mde4-12A protein has higher affinity for the spindle than for the kinetochores. We prefer the later model, since the Mde4-12A protein localizes normally to kinetochores in interphase when there is no spindle in the nucleus to compete with the kinetochores for binding to Mde4. In any case, Mde4 phosphorylation serves the dual function of (1) allowing monopolin to localize to kinetochores, where it can carry out its function in promoting proper chromosome attachment, and (2) blocking premature localization of monopolin to the spindle, which might interfere with metaphase spindle dynamics. After anaphase onset, Clp1 along with other phosphatases dephosphorylate

Figure 2-13

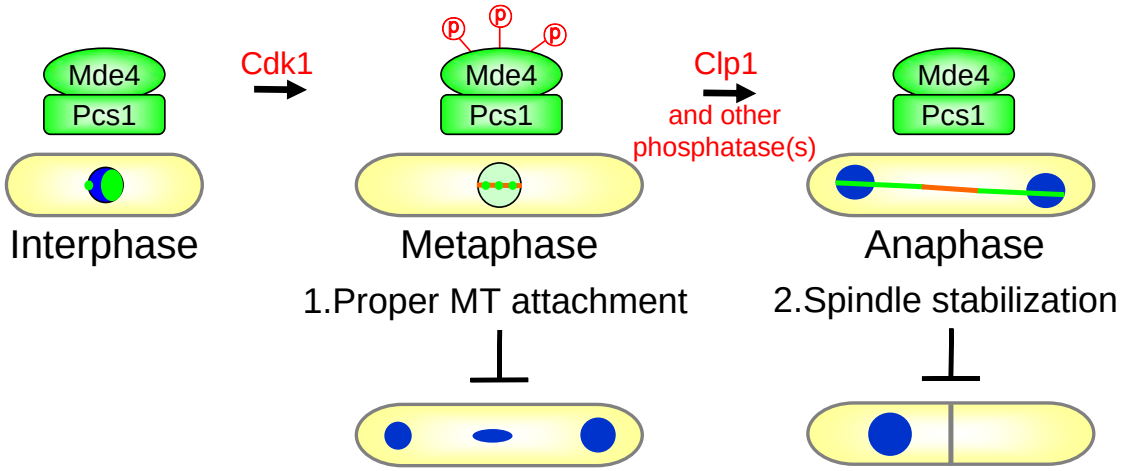
Mde4
Pcs1
Cdk1
Mde4
Pcs1
Clp1
and other
phosphatase(s)
Mde4
Pcs1
Interphase
Metaphase
Anaphase
1.Proper MT attachment
2.Spindle stabilization

Figure 2-13: A Model of Phosphorylation-Dependent Regulation of Chromosome Segregation by the Monopolin Complex

Left: Mde4 and Pcs1 (green) localize to the nucleolus (large green spot in nucleus) and the clustered kinetochores (smaller green spot at periphery of the nucleus) in interphase. Middle: in early mitosis, Mde4 becomes phosphorylated (probably by Cdk1), which is required to maintain Pcs1-Mde4 at kinetochores (three small green spots) to promote proper attachment of microtubules (MTs) to kinetochores to prevent lagging chromosomes in anaphase. Right: in anaphase, Clp1 and other phosphatases dephosphorylate Mde4 to promote loading of monopolin onto the spindle (shown in orange) to stabilize it and allow for proper elongation to prevent chromosome cosegregation.

Mde4 to allow the monopolin complex to load onto the anaphase spindle where it is required for both spindle stability and proper spindle elongation.

Monopolin function at kinetochores

Previous studies in budding and fission yeast led to a model for monopolin function which proposed that the monopolin complex acts to clamp microtubule binding sites together at a pair of sister kinetochores (budding yeast) and at same kinetochores (fission yeast) to ensure that they attach to microtubules from the same spindle pole in *S. cerevisiae* meiosis I for chromosome mono-orientation and from the opposite pole in *S. pombe* mitosis and mitosis II for chromosome bi-orientation (Gregan et al., 2007; Monje-Casas et al., 2007; Petronczki et al., 2006; Rabitsch et al., 2003). Further work in budding yeast showed that monopolin may also function to clamp the rDNA repeats together (Huang et al., 2006) and tether rDNA to the nuclear envelope through the interaction with inner nuclear membrane proteins to keep them in register and prevent unequal crossing over (Mekhail et al., 2008). The budding yeast monopolin requires separate adapters to target it to the meiosis I kinetochores and the rDNA repeats. These results suggest that monopolin can act as a crosslinker for different structures through the use of unique adapter molecules. Many crosslinking molecules such as the microtubule crosslinker Ase1 (PRC1 in humans) form multimeric complexes (Loiodice et al., 2005; Schuyler et al., 2003). Consistent with this, we have found that Mde4 and Pcs1 not only form heterodimers (Figure 2-14A), but may form either hetero-tetramers or higher order multimers since Mde4-GFP pulled down Mde4-13Myc from cell lysates from diploid cells expressing both tagged proteins (Figure

Figure 2-14

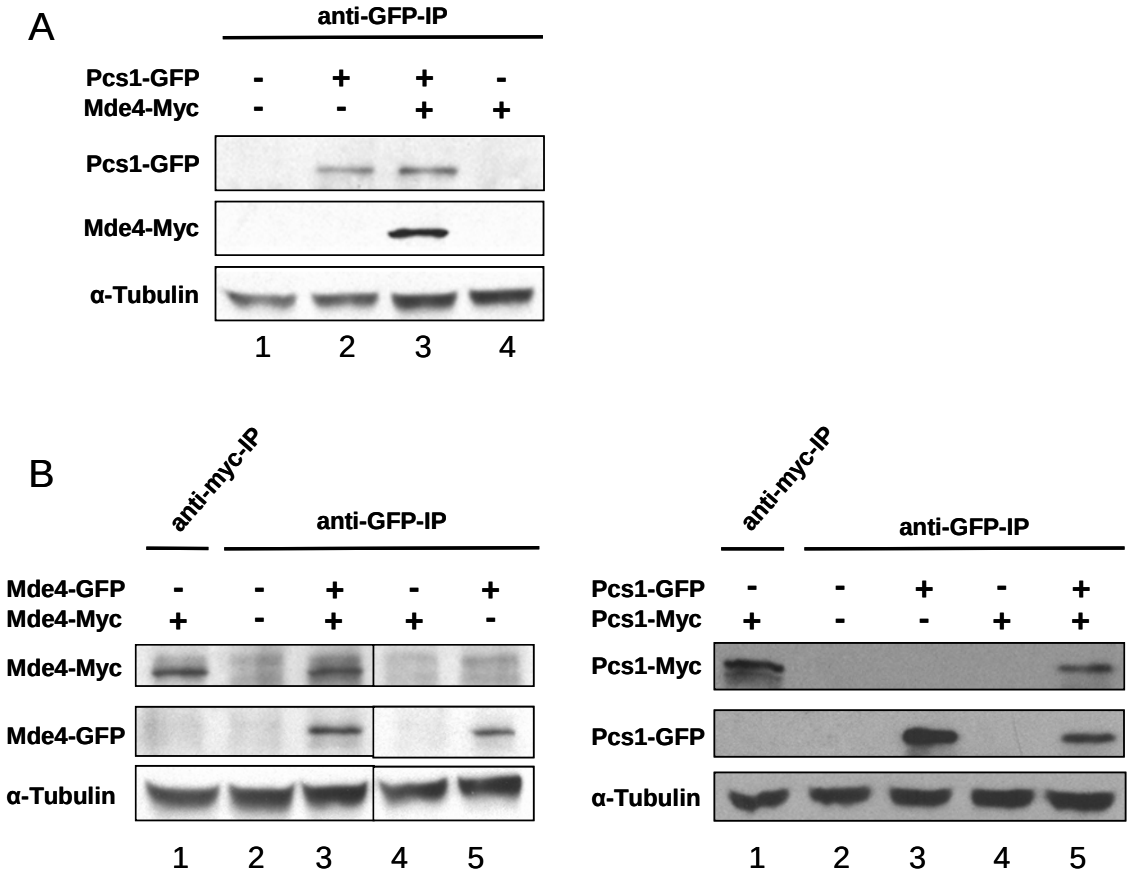
A
anti-GFP-IP
Pcs1-GFP - + + -
Mde4-Myc - - + +
Pcs1-GFP
Mde4-Myc
α-Tubulin
1 2 3 4
B
anti-myc-IP
anti-GFP-IP
Mde4-GFP - - + - +
Mde4-Myc + - + + -
Mde4-Myc
Mde4-GFP
α-Tubulin
1 2 3 4 5
anti-myc-IP
anti-GFP-IP
Pcs1-GFP - - + - +
Pcs1-Myc + - - + +
Pcs1-Myc
Pcs1-GFP
α-Tubulin
1 2 3 4 5

Figure 2-14: Mde4 and Pcs1 May Form Heterodimers and Possibly Heterotetramers in vivo

(A) Interaction between Mde4 and Pcs1 was determined by immunoprecipitation followed by western blotting using cell lysates from the following cultures: wild-type (1), *pcs1-GFP* (2), *pcs1-GFP mde4-13Myc* (3), *mde4-13Myc* (4). Lower panel shows the tubulin loading control from whole cell extracts prior to immunoprecipitation.
(B) Multimerization of Mde4 and Pcs1 was determined by immunoprecipitation followed by western blotting using diploid cell lysates from cultures of the following strains: (left panel) *mde4-13Myc* haploid (1), wild-type haploid (2), *mde4-GFP mde4-13Myc* diploid (3), *mde4-13Myc* haploid (4), *mde4-GFP* haploid (5) (left panel), (right panel) *pcs1-13Myc* haploid (1), wild type haploid (2), *pcs1-GFP* haploid (3), *pcs1-13Myc* haploid (4), *pcs1-GFP pcs1-13Myc* diploid (5) (right panel). Samples in left panel were run in the same gel, with nonrelevant lanes excised.

2-14B). Similar results were observed for cells expressing two different tagged versions of Pcs1 (Figure 2-14B). Thus it is possible that in *S. pombe* the Mde4-Pcs1 complex acts to cross-link microtubule binding sites, spindle microtubules, and possibly rDNA repeats. However, candidate adapter molecules for these locations have not been identified. TAP-purification of Mde4 and Pcs1 did not identify other kinetochore or microtubule binding proteins that could serve as adapters for Mde4-Pcs1 at these locations (Gregan et al., 2007 and appendix A).

In addition, our finding that monopolin mutants have extended metaphase delays and depend on the spindle checkpoint for normal growth suggests that monopolin may have an additional function to promote attachment of microtubules to kinetochores, since merotelic attachments are not thought to trigger the spindle checkpoint (Cimini, 2007). One way to reconcile this data with the earlier model would be to suppose that monopolin acts to clamp together and stabilize parallel microtubule ends at kinetochore. Thus, monopolin could both stabilize attachments and favor kinetochore binding to microtubules from the same pole. Alternatively, monopolin could carry out separate functions in preventing merotelic attachments and promoting or stabilizing microtubule attachment to kinetochores.

Role of monopolin function in spindle elongation

Our work identified a novel function of monopolin in promoting elongation and stability of the mitotic spindle. The spindle breakage phenotype we observed in *mde4*Δ cells indicates that Mde4 may have a structural role in maintaining spindle integrity. The *mde4-12D* mutant, which localizes poorly to the mitotic spindle, also has spindle integrity defects as

judged by the chromosome cosegregation phenotype observed in fixed cells, and the occasional spindle collapse observed in time-lapse analysis. Both the exclusion of monopolin from anti-parallel microtubules in the spindle midzone, and the spindle breakage phenotype could be explained if monopolin prefers to bind to and crosslink only parallel microtubules. By crosslinking spindle microtubules, monopolin could promote spindle stability much like the spindle midzone crosslinker Ase1 (Loiodice et al., 2005; Schuyler et al., 2003). In an attempt to study the microtubule binding properties of monopolin in vitro, we were able to produce small amounts of the Mde4-Pcs1 complex in bacteria, however the bacterially produced protein complex did not bind to microtubules in vitro (unpublished data), suggesting that monopolin either does not bind to microtubules directly or that it requires other proteins or secondary modifications that are only present in vivo. In addition to the spindle collapse defect, we also found that *mde4*-12D mutant cells display slowed spindle elongation in early anaphase. We also observed a slowed rate of spindle elongation in *mde4*Δ cells (data not shown), however the phenotype in these cells may be complex since, unlike the *mde4-12D* mutant cells, *mde4*Δ cells have a high incidence of lagging chromosomes, which also slows spindle elongation (Pidoux et al., 2000). The cause of slowed spindle elongation in *mde4-12D* cells is not known, but could be explained if monopolin has a role in loading and/or activation of microtubule motors on the spindle in early anaphase.

Reversal of Cdk1 phosphorylation and anaphase spindle function

Upon entry into mitosis, Cdk1 phosphorylation, either directly or indirectly, drives disassembly of the interphase microtubule cytoskeleton and assembly of the mitotic spindle. However, cells are able to maintain a mitotic spindle even when Cdk1 activity drops in anaphase. This and other studies have shown that anaphase spindle stability is accomplished at least in part by the loading of certain proteins onto the spindle specifically in anaphase (Choi et al., 2009; Fu et al., 2009; Khmelinskii et al., 2007; Pereira and Schiebel, 2003; Woodbury and Morgan, 2007). Tightly coupling the localization and/or activity of these proteins to the level of Cdk1 activity seems to be a common strategy, as spindle binding affinity of a number of spindle-associated proteins is inhibited in early mitosis by Cdk1 activity and then enhanced by dephosphorylation in anaphase. Examples include the budding yeast Sli15 (human INCENP), Ase1, Fin1 and the fission yeast Ase I and kinesin-6 Klp9 (Fu et al., 2009; Khmelinskii et al., 2007; Pereira and Schiebel, 2003; Woodbury and Morgan, 2007). Dephosphorylation by Cdc14 promotes spindle localization of Sli15 and Fin1 (Pereira and Schiebel, 2003; Woodbury and Morgan, 2007), enhances the activity of Ase1 (Khmelinskii et al., 2007) and initiates Klp9 interaction with Ase1 on the spindle (Fu et al., 2009). Similar to our findings with non-phosphorylatable Mde4, non-phosphorylatable variants of Sli15 and Fin1 localize prematurely to the mitotic spindle, which results in chromosome segregation defects (Pereira and Schiebel, 2003; Woodbury and Morgan, 2007 and this study). Premature localization of monopolin to the metaphase spindle also seems to cause additional defects in spindle dynamics or microtubule attachment to kinetochores since double mutants between *mde4-12A* and spindle

checkpoint mutants such as *mad2*Δ were lethal, in contrast to *mde4*Δ *mad2*Δ mutants that were sick but viable. It would be interesting to test whether Mde4-12A stabilizes the dynamic early mitotic spindle using fluorescence recovery after photobleaching of the metaphase spindle. That experiment may give an answer to another question of whether it is important to keep monopolin off spindle microtubules prior to anaphase.

Chapter III

A role of Cdk1 activity in chromosome bi-orientation

Unpublished data

Summary

Merotelic kinetochore orientation, in which a single kinetochore binds microtubules emanating from both poles, is the most problematic kinetochore-microtubule misattachment during mitosis since it is not detected by the spindle assembly checkpoint (SAC). Merotelic attachments produce lagging chromosomes, a leading cause of aneuploidy in mammalian tissue cultured cells. In *Schizosaccharomyces pombe*, monopolin and heterochromatin mutants show high frequencies of lagging chromosomes in anaphase. We found that either deletion of *clp1*$^{+}$ (the *S. pombe* Cdc14-family phosphatase) or mild overexpression of wild type or nondestructible cyclin B can rescue the lagging chromosome phenotype observed in monopolin and/or heterochromatin mutants. These results suggest that substrates of Cdk1 and Clp1 have a role in correcting merotelic attachments. Candidate substrates include INCENP, Survivin and Borealin because they were identified as the most abundant proteins purified with Clp1 from mitotic cells (appendix A). A mild overexpression of the fission yeast Aurora kinase also reduces lagging chromosome production in *mde4Δ* cells. Aurora is important for correction of merotelic attachments and raises the possibility that deletion of *clp1*$^{+}$ rescues the lagging chromosome phenotype in *mde4Δ* cells by enhancing Aurora function. However, other results suggest that Cdk1 and Clp1 may influence merotelic attachments through regulation of tension generated by the metaphase spindle. Lack of Mde4 causes an increase in the length of metaphase spindle due to microtubule attachment defects. Interestingly, the metaphase spindle length of *clp1Δ mde4Δ* returns to that of wild type, but the double mutant still displays a metaphase delay indicating that the reduced

length of the spindle was not due to rapid correction of misattachments. The suppression of merotely in monopolin and heterochromatin mutants is also observed when they are combined with mutations in kinesin-6 motor *klp9*$^{+}$ or Kinesin-5/bimC motor *cut7*$^{+}$, whose functions are required for spindle elongation. Taken together, these findings suggest that higher Cdk1 activity in *clp1Δ* may facilitate correction of merotelic kinetochores before anaphase onset by affecting Aurora kinase dynamics toward kinetochores and/or reducing the pulling force by altering the activity of microtubule motors or associating proteins, thus resulting in reduced tension applied on merotelically oriented kinetochores which might be detected and corrected by Aurora kinase more efficiently.

Introduction Chapter III

Equal segregation of the duplicated chromosomes to daughter cells during mitosis depends on chromosome bi-orientation at metaphase. Failure to do so leads to aneuploidy, which is often associated with cancer. All eukaryotic cells have a ubiquitous safety device called the spindle assembly checkpoint (SAC) to monitor kinetochore-microtubule attachment and tension, which stops cell cycle progression into anaphase until all sister kinetochores establish bipolar attachment (Musacchio and Salmon, 2007). Merotelic kinetochore orientation, in which a single kinetochore binds microtubules from both spindle poles rather than just one, occurs frequently in early mitosis in mammalian cells (Cimini et al., 2003). It is the most problematic type of kinetochore-microtubule misattachment since it is not detected by the SAC. Cells progress into anaphase with merotelic attachments and merotelically attached chromosomes are observed as lagging chromosomes, which are a major cause of aneuploidy in tissue cultured cells (Cimini et al., 2002; Cimini et al., 2001; Musacchio and Salmon, 2007). Interestingly many chromosomes with merotelic attachments can be corrected before anaphase by Aurora kinase (Cimini et al., 2006; Knowlton et al., 2006), and during anaphase by anaphase spindle mechanics (Cimini et al., 2004; Courtheoux et al., 2009). However, it is still elusive how Aurora kinase detects and corrects merotelic orientations.

It has been suggested that the monopolin complex functions as a clamp to bundle different microtubule binding sites on kinetochores to align them so that they bind only microtubules emanating from their facing pole (Choi et al., 2009; Gregan et al., 2007;

Petronczki et al., 2006; Rabitsch et al., 2003; Toth et al., 2000). Lack of monopolin in fission yeast produces a high frequency of lagging chromosomes in anaphase (Choi et al., 2009; Gregan et al., 2007; Rabitsch et al., 2003). We showed that monopolin has dual roles in both metaphase and anaphase for chromosome bi-orientation and spindle elongation and/or integrity respectively. Its dual function is sequentially and spatially regulated by phosphorylation on the Mde4 subunit by Cdk1 and dephosphorylation by the *S. pombe* Cdc14 phosphatase, Clp1. Moreover, Mde4 is more highly phosphorylated at prometaphase in *clp1Δ* cells than wild-type cells suggesting that Clp1 may alter the steady state level of Cdk1 phosphorylation of key substrates in metaphase. In addition to monopolin, heterochromatin is also required for prevention of merotelic kinetochore orientation in fission yeast (Gregan et al., 2007). As in higher eukaryotes, outer repeat sequences of the *S. pombe* centromeres recruit Swi6, the HP1 homolog, and are modified as heterochromatin, which promotes further incorporation of the fission yeast cohesin Rad21 to establish and maintain the function of centromere (Bernard et al., 2001; Lachner et al., 2001).

Pre-anaphase spindles maintain a certain length depending on the balance of forces between interpolar microtubules, which couple to motors that drive spindle elongation, and microtubules attached to kinetochores, which antagonize spindle elongation forces (Glotzer, 2009). In fission yeast, the forces generated by interpolar microtubules in early mitosis mainly depend on two different motor activities, plus-end directed kinesin-5 (also called bimC family) Cut7, and minus-end directed kinesin-14 proteins, Klp2 and Pkl1 (Hagan and Yanagida, 1992; Pidoux et al., 1996; Troxell et al., 2001). Ase1/Prc1 microtubule bundlers were also well known protein to localize at the spindle midzone and bundle antiparallel

microtubules to stabilize the spindle midzone. Combined with help from well conserved kinesin-5/bimC motors, Ase1 promotes spindle elongation during anaphase by generating sliding forces to push opposite poles towards the cell cortex (Loiodice et al., 2005; Mollinari et al., 2002; Schuyler et al., 2003). In fission yeast, deletion of *ase1*$^{+}$ interferes with spindle elongation. *ase1Δ* mutant cells undergo frequent spindle collapse in early mitosis and do not fully elongate the anaphase spindle (Loiodice et al., 2005). Ase1 function in the spindle midzone in budding yeast is regulated by Cdk1 and Cdc14 (Khmelinskii et al., 2007). A recent fission yeast study suggested that kinesin-5 Cut7 functions to elongate the early mitotic spindle but is dispensable for anaphase spindle elongation; instead, Clp1 dependent binding of kinesin-6 Klp9 to Ase1 at the spindle midzone mediates anaphase spindle elongation (Fu et al., 2009).

The *S. pombe* Cdc14 phosphatase Clp1 regulates multiple cell cycle events such as mitotic entry, chromosome segregation, contractile ring assembly, spindle elongation, and coordination of mitosis with cytokinesis (Choi et al., 2009; Clifford et al., 2008; Cueille et al., 2001; Fu et al., 2009; Trautmann et al., 2004; Trautmann et al., 2001; Wolfe and Gould, 2004; Wolfe et al., 2006). Despite the previously described role of Clp1 in chromosome bi-orientation, *clp1Δ* does not show negative genetic interactions with monopolin and heterochromatin mutants. Instead, we show that maintenance of higher Cdk1 activity through deletion of *clp1*$^{+}$ or other manipulations suppresses the frequency of lagging chromosomes in monopolin and heterochromatin mutants possibly due to change of both the dynamics of aurora kinase at kinetochores and/or altered balance of forces on the early mitotic spindle.

Results Chapter III

Relative levels of Cdk1 activity may regulate correction of merotelic orientation of kinetochores

Work in budding yeast has suggested that the Cdc14 phosphatase primarily acts to antagonize Cdk1 phosphorylation in anaphase for proper mitotic exit (Stegmeier and Amon, 2004). Unlike budding yeast, which release Cdc14 after anaphase onset, the fission yeast Cdc14 phosphatase Clp1 is released at mitotic entry as in mammalian cells, and therefore might have the ability to regulate early mitotic events such as chromosome attachment and spindle dynamics. (Choi et al., 2009; Clifford et al., 2008; Cueille et al., 2001; Fu et al., 2009; Trautmann et al., 2004; Trautmann et al., 2001; Wolfe and Gould, 2004; Wolfe et al., 2006). Despite an apparent positive role of Clp1 in chromosome bi-orientation (Trautmann et al., 2004), we found that *clp1Δ* does not show negative genetic interactions with monopolin and heterochromatin mutants both of which have defects in chromosome bi-orientation and produce high frequencies of lagging chromosomes in anaphase (Gregan et al., 2007). Surprisingly we found that deletion of $clp1^{+}$ significantly reduces the lagging chromosome frequency in both monopolin and heterochromatin mutants. We observed that only 6.9% of *mde4Δ clp1Δ* cells (n = 313) exhibited lagging chromosomes or uneven segregation of chromosomes to two poles (as illustrated in Figure 3-1A, hereafter referred to lagging chromosomes) in anaphase, compared to 31.5% in *mde4Δ* (n =327) and 0.3 % in *clp1Δ* (n = 325) single mutants (Figure 3-1A left panel). Lack of Clp1 also reduced lagging chromosome production in both *mde4-12A*, a nonphosphorylatable mutant of Mde4 (Choi

et al., 2009), and *swi6Δ*, from 19.2 % in *mde4-12A* (n = 360) to 10.8 % in *mde4-12A clp1Δ* (n = 390) (Figure 3-1A middle panel) and from 9.6 % in *swi6Δ* (n=320) to 1.4 % of *swi6Δ clp1Δ* (n = 337) (Figure 3-1A right panel). One simple explanation for these results could be that deletion of *clp1*$^{+}$ results in higher level of Cdk1 phosphorylation of certain substrates involved in correction of merotelic attachment.

To address the question of whether the reduced frequency of lagging chromosomes is caused by higher Cdk1 activity in the absence of Clp1 at early mitosis, wild-type, *mde4Δ* and *mde4Δ clp1Δ* cells were transformed by a plasmid containing the *S. pombe* cyclin B, Cdc13, whose expression is controlled by its endogenous promoter. Expression of Cdc13 from multicopy plasmids did not produce lagging chromosomes in wild-type cells (0%, n = 410) and cells were not arrested in anaphase and no defect in behavior of chromosomes were detected (data not shown). However, the frequency of lagging chromosomes was suppressed by this mild expression of Cdc13 from 28.5 % in untransformed *mde4Δ* (n = 365) to 11.1 % in transformed *mde4Δ* (n = 387), but did not further reduced lagging chromosome production in transformed *mde4Δ clp1Δ* (6.3 %, n = 351) compared to 6.9% in untransformed *mde4Δ clp1Δ* (n= 313) (Figure 3-1B left panel). To further confirm this data we used a strain which expresses nondestructible cyclin B, Cdc13*Δ*DB, under the control of thiamine-suppressible nmt1 promoter (*nmt1-Cdc13ΔDB*), which had been integrated into chromosomal *leu1*$^{+}$ locus. Although over production of Cdc13*Δ*DB in wild-type fission yeast cells causes high levels of Cdk1 activity and arrests cells in anaphase with segregated chromosomes (Chang et al., 2001), residual expression of Cdc13*Δ*DB when the nmt1 promotor is repressed, did not cause severe chromosome segregation defects including

Figure 3-1

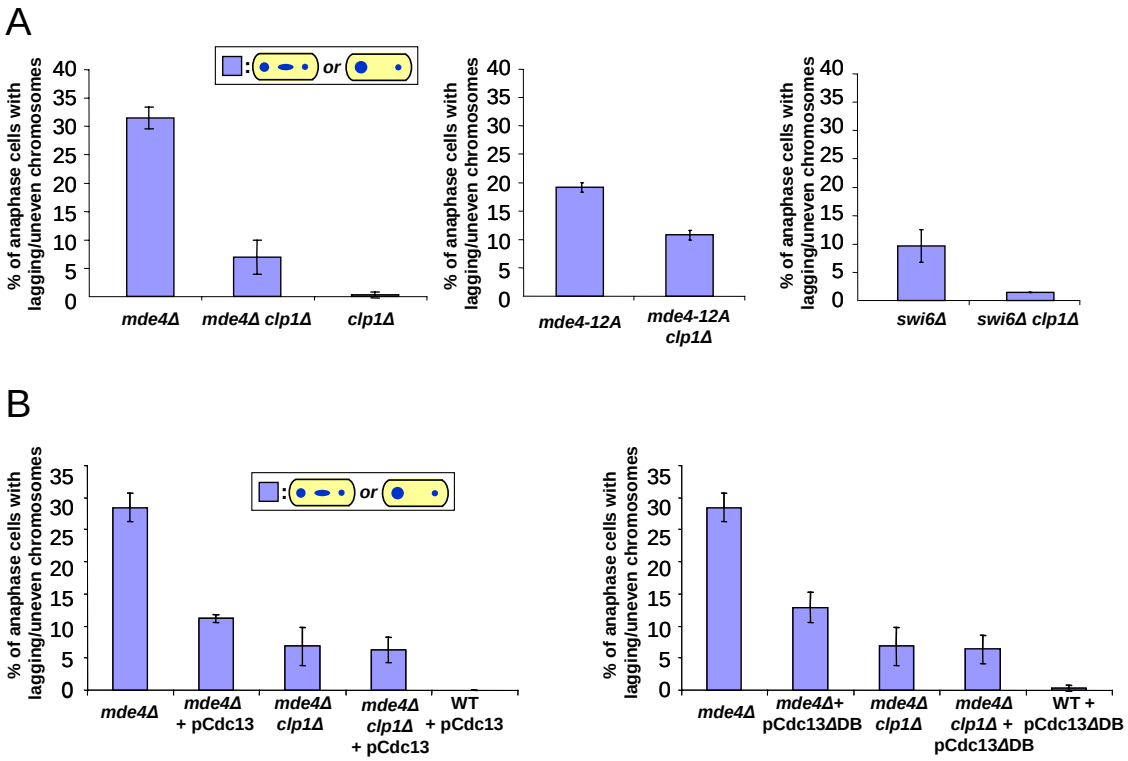
A
% of anaphase cells with lagging/uneven chromosomes
or
mde4Δ
mde4Δ clp1Δ
clp1Δ
mde4-12A
mde4-12A clp1Δ
swi6Δ
swi6Δ clp1Δ
B
mde4Δ
mde4Δ + pCdc13
mde4Δ clp1Δ
mde4Δ clp1Δ + pCdc13
WT + pCdc13
mde4Δ+ pCdc13ΔDB
mde4Δ clp1Δ
mde4Δ clp1Δ + pCdc13ΔDB
WT + pCdc13ΔDB

Figure 3-1: Cdk1 activity promotes correction of merotelic orientation of kinetochores in monopolin and heterochromatin mutants

(A) The frequency of lagging chromosomes in *mde4* mutants and the *swi6Δ* mutant in the presence or absence of $clp1^{+}$ was determined by counting the percent of anaphase cells with lagging or unevenly segregated chromosomes from asynchronously growing cells. Cells were fixed and stained with DAPI and calcofluor white to visualize DNA and cells wall respectively. Error bars represent standard deviation.

(B) The frequency of lagging chromosomes was determined as in (A) in *mde4Δ, mde4Δ clp1Δ* mutants and wild-type cells carrying a plasmid with a genomic clone of the S. pombe Cyclin B, Cdc13 (pCdc13) or an integrated copy of nondestructible cyclin B (pCdc13ΔDB). Cells were grown in thiamine containing rich media to suppress over expression of nondestructible cyclin B (Cdc13ΔDB), thus Cdc13ΔDB was mildly produced by leaky expression of nmt1 promoter. Error bars represent standard deviation.

lagging chromosomes (0.3%, WT + pCdc13*Δ*DB, n = 364). However this mild expression of Cdc13*Δ*DB in the presence of thiamine suppressed the lagging chromosome production with *mde4Δ* mutation to 12.9 % (n = 367), but this Cdc13*Δ*DB expression did not further reduced lagging chromosome production in *mde4Δ clp1Δ* (6.4 %, n = 362) compared to 6.9% in control *mde4Δ clp1Δ* (n= 313). Consistent with reduction of lagging chromosome in the absence of Clp1 (Figure 3-1), these data suggest that more highly phosphorylated substrates of Cdk1 and Clp1 might play a role in correcting merotelic kinetochore orientation in monopolin and heterochromatin mutants. It was interesting that mild expression of both wild-type (6.3 %) and nondestructible cyclin (6.4 %) in *mde4Δ clp1Δ* mutant did not further suppress the frequency of lagging chromosome than *mde4Δ clp1Δ* alone (6.9 %) indicating that some of merotelic attachments might not be overcome by higher Cdk1 activity.

Aurora Kinase might be a Cdk1 target for correction of merotelic attachments

As shown in appendix A, the fission yeast chromosome passenger complex (CPC) components INCENP (Pic1), Survivin (Bir1), and Borealin (Nbl1) were purified as the most abundant proteins interacting with Clp1 in mitotic arrested cells and some of their Cdk1 sites were identified as phosphorylated (9 of 17 sites in Pic1, 9/19 sites in Bir1, and 0/1 in Nbl1). Aurora kinase B has been known to fix maloriented kinetochore-microtubule attachments in various organisms (Andrews et al., 2004; Cimini et al., 2006; Lampson et al., 2004; Tanaka et al., 2002). Translocalization of Aurora B from kinetochores to the spindle midzone is dependent on Cdk1 and Cdc14 phosphatase (Murata-Hori et al., 2002; Pereira

and Schiebel, 2003).The *S. pombe* Ark1 is only Aurora kinase identified to date and it function similar to mammalian Aurora kinase B in chromosome condensation, chromosome bi-orientation, the spindle assembly checkpoint response, and cytokinesis (Bohnert et al., 2009; Kawashima et al., 2007; Leverson et al., 2002; Petersen and Hagan, 2003). In fission yeast, Clp1 localizes at kinetochores during early mitosis and functions in chromosome bi-orientation (Trautmann et al., 2004). Thus, early mitotic Cdk1 activity may compete for the CPC with Clp1 at the kinetochore to regulate the activity of the *S. pombe* Ark1 directly or by changing its dynamics to kinetochores. Therefore higher Cdk1 activity in *clp1Δ* cells could enhance Aurora kinase activity to correct merotelic orientations in monopolin mutants. Before addressing this question, we first transformed a plasmid containing the *S. pombe* Aurora kinase (Ark1-GFP) under the control of thiamine suppressible nmt1 promoter to test whether increasing the pool of Ark1 in cells can suppress lagging chromosome production in the *mde4Δ* mutant. Mild expression of Ark1-GFP from multicopy plasmids in the presence of thiamine did not produce lagging chromosomes in wild type cells (0%, n=334) (Figure 3-2A). In contrast, the frequency of lagging chromosomes was reduced by this mild expression of Ark1-GFP to 12.5 % in *mde4Δ* (n = 374) from 24.6 % for empty vector transformed *mde4Δ* cells (n=310). Expression of Ark1 did not further suppress the lagging chromosome frequency in *mde4Δ clp1Δ* (6.2 %, n =324) (Figure 3-2A). Previous studies in mammalian cells suggest that Aurora kinase is enriched at merotelic attachment sites and promotes the correction of merotelic attachments before anaphase onset (Cimini, 2007; Cimini et al., 2006; Knowlton et al., 2006). Thus we tested for genetic interaction between *mde4Δ* or *swi6Δ* and the CPC mutants, *ark1-T7*,

Figure 3-2

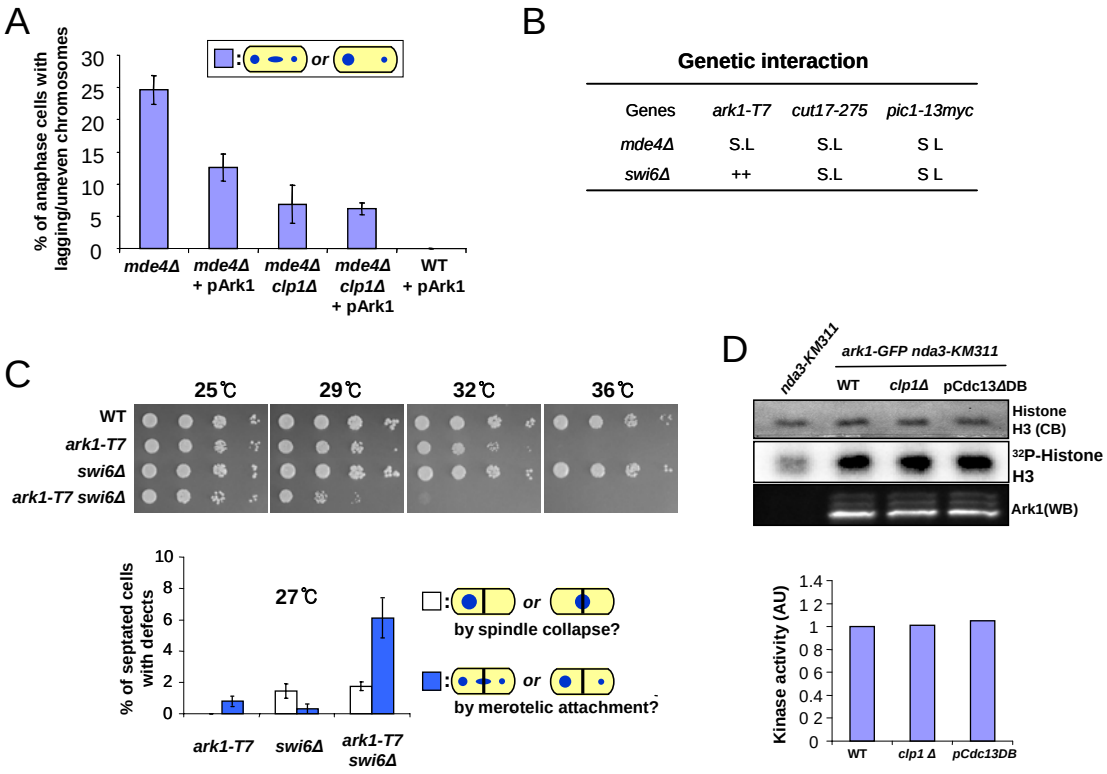
A
% of anaphase cells with lagging/uneven chromosomes
30
25
20
15
10
5
0
: or
mde4Δ
mde4Δ + pArk1
mde4Δ clp1Δ
mde4Δ clp1Δ + pArk1
WT + pArk1
B
Genetic interaction
Genes | ark1-T7 | cut17-275 | pic1-13myc
mde4Δ | S.L | S.L | S L
swi6Δ | ++ | S.L | S L
C
25℃
29℃
32℃
36℃
WT
ark1-T7
swi6Δ
ark1-T7 swi6Δ
% of septated cells with defects
10
8
6
4
2
0
27℃
ark1-T7
swi6Δ
ark1-T7 swi6Δ
: or
by spindle collapse?
: or
by merotelic attachment?
D
nda3-KM311
ark1-GFP nda3-KM311
WT
clp1Δ
pCdc13ΔDB
Histone H3 (CB)
32P-Histone H3
Ark1(WB)
Kinase activity (AU)
1.4
1 2
1
0 8
0 6
0.4
0 2
0
WT
clp1 Δ
pCdc13DB

Figure 3-2: Aurora kinase is important for correction of merotelic attachments

(A) The frequency of lagging chromosomes was determined by counting the percent of anaphase cells with lagging or unevenly segregated chromosomes from asynchronously growing *mde4Δ, mde4Δ clp1Δ,* and wild type cells which were transformed with pREP1-ark1-GFP. Ark1-GFP transformed cells (shown as + pArk1) mildly produce Ark1-GFP under the suppressed state of nmt1 promoter in the presence of thiamine. Error bars represent standard deviation.
(B) Genetic interactions between the *mde4*Δ, *swi6*Δ and the chromosome passenger complex mutations. The *mde4*Δ and *swi6*Δ mutants were crossed with the chromosome passenger complex mutants, Aurora kinase *ark1-T7*, Survivin *cut17-275* and INCENP *pic1-13myc*. Genetic interactions are shown as synthetic lethality (S.L) and mild growth (++).
(C) (top) *swi6*Δ cells show a synthetic growth defect with the *ark1-T7* mutation. Wild-type (WT), *ark1-T7*, *swi6*Δ and *ark1-T7 swi6*Δ cells were grown in YE at 25°C, and then serial dilution were spotted on YE plates and incubated at the indicated temperatures for 3-5 days. (Bottom) The percentage of cells with a septum showing defects in chromosome segregation were displayed at indicated temperatures. Asynchronously growing *ark1-T7*, *swi6*Δ and *ark1-T7 swi6*Δ cells were fixed then stained with DAPI for DNA and calcofluor for septum. Error bars represent standard deviation.
(D) (top) In vitro kinase assays (n=1) were performed with immunoprecipitated Ark1-GFP from metaphase arrested *nda3-KM311* cells with different genetic backgrounds: wild-type (WT), *clp1*Δ, wild-type cells mildly expressing Cdc13ΔDB (pCdc13ΔDB) and commercially available (NEB) recombinant human Histone H3.2 as a substrate. Protein labeled by γ-^{32}P was detected with a phospho imager (Molecular Dynamics), and the gel was stained with Coomassie Blue (CB) as a loading control. The protein level of Ark1-GFP used for this assay was determined using western blot (Kodak 4000MM image station)(bottom). Relative kinase activity (AU, arbitrary unit) was measured by subtracting the background and then normalizing for Ark1 protein level compared to wild type whose kinase intensity was set of 1.

cut17-275 (Survivin) or *pic1-13myc* which show lagging chromosomes and chromosome condensation defects at high temperature. We checked whether reduced activity of Aurora kinase in the CPC mutants affect cell viability in monopolin and heterochromatin mutants. Double mutants were not recovered with the exception of the double mutant between *swi6Δ* and *ark1-T7* (Figure 3-2B), consistent with the CPC being important for correcting lagging chromosomes. This double mutant was probably recovered because *swi6Δ* cells produce a much lower percentage of lagging chromosomes than *mde4Δ* cells (Figure 3-1) and the *ark1-T7* mutant has the mildest phenotype at its permissive temperature of 25°C (Figure 3-2C) compared to *cut17-275* and *pic1-13myc*, which show over 20% of cells in anaphase possessing lagging chromosomes and a more severe DNA condensation problem at the same temperature. To characterize the genetic interaction between *swi6Δ* and *ark1-T7* in more detail, we tested viability at different temperatures (Figure 3-2C top panel). In contrast to *swi6Δ* and wild-type which showed normal growth in all temperature we tested, *ark1-T7* started to show a growth defect at 32°C and could not grow at 36°C. Interestingly, the *ark1-T7 swi6Δ* double mutant displayed a synthetic growth defect at 29°C suggesting that Ark1 activity is required for viability of *swi6Δ* at 29°C. To examine this further, we looked at chromosome behavior of the *ark1-T7 swi6Δ* double mutant. At a temperature of 29°C or higher, the *ark1-T7* mutant itself showed DNA condensation defects with high frequency of stretched chromatin which inhibited our measurement of frequency of lagging chromosomes. However examination of phenotypes at 27°C, where *ark1-T7* cells did not have condensation defects, the *ark1-T7 swi6Δ* cells had greatly enhanced rates of lagging chromosomes and missegregation (data not shown). To examine the consequence of

lagging and unevenly segregated chromosomes shown in anaphase, we measured the frequency of chromosome segregation defects amongst cells with septa. The chromosome segregation defects were classified into two classes: (1) chromosome co-segregation into either of daughter cells or unsegregated chromosomes that were cut by the septum (shown as a white box in Figure 3-2C bottom panel and hereafter referred to *co-segregation*). Some of this phenotype might be caused by spindle collapse. (2) lagging chromosome cut or unevenly segregated chromosomes (shown as a blue box in Figure 3-2C bottom panel and hereafter referred to *cut*). This second phenotype is probably caused by lagging chromosomes in anaphase. At 27°C, 0.2 % of *co-segregation* and 2.2% of *cut* (n = 633) were observed in the *ark-T7* mutant. In contrast, the *ark1-T7 swi6Δ* mutants displayed a much increased frequency of *cut* (6.1 %, n = 621) compared to *swi6Δ* mutation (0.3%, n =612). However, the frequencies of co-segregation were similar between the *swi6Δ* and *ark1-T7 swi6Δ* mutants (1.5 % in *swi6Δ* and 1.8 % in *ark1-T7 swi6Δ*) (Figure 3-2 bottom panel). These data support a role of Aurora kinase in correction of merotelic oriented kinetochores in the fission yeast as shown previously in mammalian cells (Cimini et al., 2006; Knowlton et al., 2006).

Next we returned to address the effect of enhanced Cdk1 activity in *clp1Δ* cells on the activity of Aurora kinase Ark1. We first tested whether Ark1 kinase activity is changed in conditions where Cdk1 activity is higher than wild-type such as in *clp1Δ* cells or in wild-type cells mildly expressing nondestructible Cdc13ΔDB. To compare the kinase activity of Ark1 in wild-type, *clp1Δ* and Cdc13ΔDB expressing cells, we first purified active mitotic Ark1-GFP by immunoprecipitation from the three different cell types that were arrested in

prometaphase by *nda3-KM311* mutation. Then we carried out in vitro kinase assays using Histone H3 as a substrate (Figure 3-2D top panel). We observed no significant change of Ark1 activity in higher Cdk1 states (Figure 3-2D bottom panel) suggesting that higher Cdk1 phosphorylation on the CPC might not increase the activity of Aurora kinase directly in fission yeast. Another possible mechanism of regulating Aurora kinase by Cdk1 and Clp1 is that Cdk1 phosphorylation on the CPC may change the kinetochore dynamics of the CPC. Though Cdk1 activity did not change the enzymatic activity of Ark1 directly (Figure 3-2D), it might increase Ark1 activity locally at kinetochores to deal with mal-oriented kinetochores by affecting the dynamics of Ark1 localization at the kinetochore. Fluorescence recovery after photobleaching (FRAP) experiment may give us clues about this possibility. I constructed stains to test this hypothesis and will carry out FRAP experiments in the near future to check whether Ark1-GFP recovers more slowly in *clp1Δ* cells which might mean that Cdk1 phosphorylation on the CPC makes it bind kinetochores more stably.

Lack of Clp1 reduces the length of the metaphase spindle in *mde4Δ* cells but does not rescue the metaphase delay

Since we observed that lack of Clp1 reduced the frequency of lagging chromosome in the monoplin and heterochromatin mutants, we wanted to examine how *clp1Δ* promoted correction of merotelic attachments by monitoring spindle elongation using GFP-tubulin expressing cells by time lapse microscopy. Our previous studies had shown that *mde4Δ* cells undergo a prolonged checkpoint-dependent delay in metaphase, which indicated that

mde4Δ cells have defects in attachment of kinetochores to microtubules. To see whether deletion of *clp1*$^{+}$ was enhancing attachment, we tested whether the metaphase delay in *mde4Δ* cells was observed if *clp1*$^{+}$ was also deleted. The length of time in phase II (metaphase) was estimated by measuring time for cells to spend for spindle elongation from 2.0 μm to 3.5 μm. The *mde4Δ clp1Δ* mutants showed a delay in phase II similar to *mde4Δ* cells, suggesting that deletion of *clp1*$^{+}$ is not correcting the attachment defects in *mde4Δ* cells (Figure 3-3A). Consistent with this, loss of the spindle checkpoint was lethal in *mde4Δ clp1Δ* cells (Figure 3-3B). These genetic interactions with the SAC mutants were more severe than *mde4Δ* single mutation, but *clp1Δ* did not show negative interaction with the SAC mutants (Figure 3-3B). This is probably due to function of Clp1 in chromosome bi-orientation since previous work from our lab showed that *clp1Δ* has minor effect in normal chromosome segregation but shows a defect in chromosome bi-orientation after release from mitotic arrest by *nda3-KM311* mutation (Trautmann et al., 2004). We conclude that higher Cdk1 activity in *clp1Δ* does not efficiently suppress triggering of the SAC caused by *mde4Δ* mutation presumably due to syntelic attachment despite its ability to suppress merotelic attachment.

Although deletion of *clp1*$^{+}$ did not affect the metaphase delay in *mde4Δ* cells, it did cause a change in the length of the metaphase spindle. The mean length of the phase II spindle in the *mde4Δ clp1Δ* mutant (2.60 ± 0.14 μm) was restored to the level of wild-type and *clp1Δ* cells (2.56 ± 0.05 μm and 2.57 ± 0.08 μm respectively), compared to *mde4Δ* cells, which showed a longer metaphase spindle (2.93 ± 0.05 μm). In spite of no significant difference in metaphase spindle length between wild type and *clp1Δ* in our study (Figure 3-

Figure 3-3

A

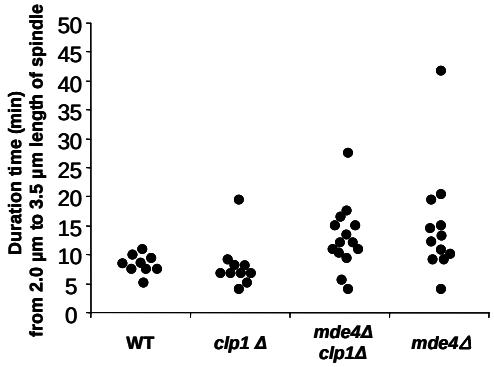

B

Genetic interaction

Genes	*bub1Δ*	*mad1Δ*	*mad2Δ*	*mad3Δ*
mde4Δ	S.L	+/-	+/-	+/-
clp1Δ	+++	+++	+++	+++
mde4Δ clp1Δ	S.L	S.L	S.L	S.L

C

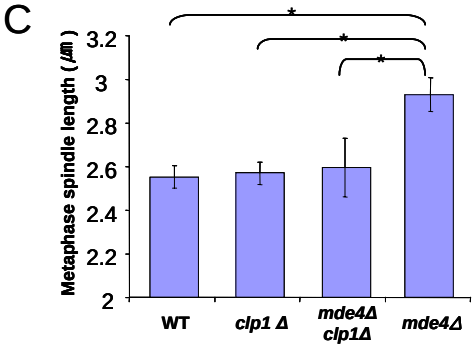

Figure 3-3: Lack of Clp1 reduces the length of the metaphase spindle in *mde4Δ* but still requires the spindle assembly checkpoint for viability

(A) Spindle elongation was monitored in wild-type (WT), *clp1*Δ, *mde4*Δ *clp1*Δ and *mde4*Δ cells. Spindle length were measured every one minute from time-lapse sequences of asynchronous *GFP-atb2* (n=9), *GFP-atb2 clp1*Δ (n=10), *GFP-atb2 mde4*Δ *clp1*Δ (n=14) and *GFP-atb2 mde4Δ* (n=13) cells. The duration time in phase II is estimated by measuring the time cells display spindle lengths between from 2.0 µm to 3.5 µm. Each dot represents the length of phase II in an individual cell.
(B) Genetic interactions between the *mde4*Δ, *clp1*Δ, *mde4*Δ *clp1*Δ and the spindle assembly checkpoint mutations. The *mde4*Δ, *clp1*Δ and *mde4*Δ *clp1*Δ mutants were crossed with the spindle assembly checkpoint mutants, *bub1*Δ, *mad1*Δ, *mad2*Δ and *mad3*Δ and 48 tetrads were dissected. Genetic interactions are shown as synthetic lethality (S.L), strong growth defect (+/-) and normal growth (+++).
(C) A comparison of metaphase spindle lengths of wild-type, *clp1Δ*, *mde4Δ clp1Δ* and *mde4Δ* cells. The mean lengths of the phase II spindle were compared between *mde4Δ* and wild-type (WT), *clp1Δ* or *mde4Δ clp1Δ* (all marked as single asterisk $p<0.0001$) by unpaired *t* test. Differences between WT and *clp1Δ* or *mde4Δ clp1Δ* were not statistically significant by unpaired *t* test ($p=0.4393$ and $p=0.3577$ respectively).

3C), recent study in the fission yeast showed that the spindle length at anaphase B onset is comparably shorter in *clp1Δ* (2.67 ± 0.53 μm) than wild type (3.34 ± 0.42 μm) (Fu et al., 2009). Taken together, these data suggest that the reduction of lagging chromosome production in *mde4Δ clp1Δ* cells might be caused by altering metaphase spindle dynamics by elevating Cdk1 activity, which could shift the balance between forces driving spindle elongation and resistance to those forces by microtubules attached to kinetochores. We hypothesize that reduction of forces driving spindle elongation would result in less tension at sister kinetochores which might allow merotelic attachments to be detected and corrected by Aurora kinase more efficiently. Therefore, we next investigated whether reduction of pulling force on sister kinetochores caused by the spindle midzone mutants can suppress lagging chromosome production in anaphase in the *mde4Δ* or *swi6Δ* mutants.

The reduction of pulling force generated from the spindle midzone suppresses the frequency of lagging chromosome in monopolin and heterochromatin mutants

To reduce the pulling force on sister kinetochores at metaphase, we decided to use the kinesin-6 *klp9Δ* and kinesin-5/bimC *cut7-24* mutants, which have defects in spindle elongation (Fu et al., 2009) In contrast to the *klp9Δ* mutant, which did not produce lagging chromosomes (0%, n = 314), the percentage of lagging chromosome in anaphase was significantly reduced in *mde4Δ klp9Δ* mutation (4.7 %, n =320) compared to *mde4Δ* mutation (27.1%, n =310) (Figure 3-4A). Similar reduction was observed in *swi6Δ klp9Δ* mutation (5.2%, n =314) compared to *swi6Δ* mutation (10.2%, n =328) (Figure 3-4A).

Figure 3-4

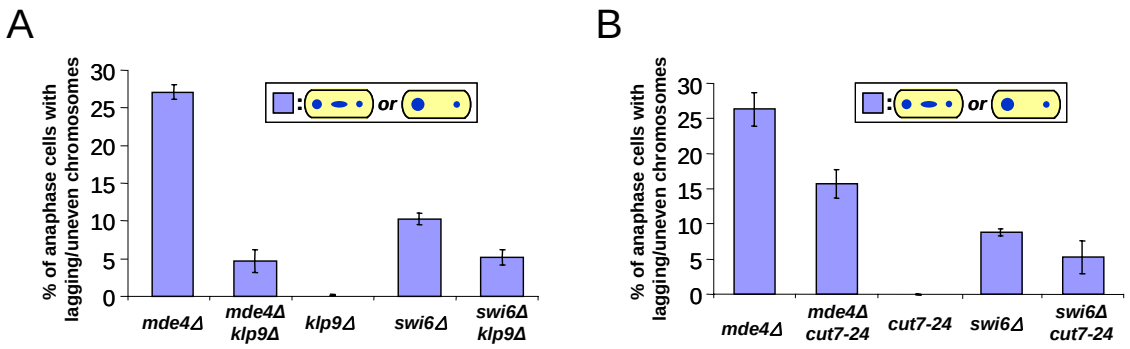
A
% of anaphase cells with lagging/uneven chromosomes
30
25
20
15
10
5
0
: or
mde4Δ
mde4Δ klp9Δ
klp9Δ
swi6Δ
swi6Δ klp9Δ
B
% of anaphase cells with lagging/uneven chromosomes
30
25
20
15
10
5
0
: or
mde4Δ
mde4Δ cut7-24
cut7-24
swi6Δ
swi6Δ cut7-24

Figure 3-4: Reduction of pulling force generated from the spindle midzone suppresses the frequency of lagging chromosomes in monopolin and heterochromatin mutants

(A) The frequency of lagging chromosomes from asynchronously growing *mde4Δ, mde4Δ klp9Δ, klp9Δ, swi6Δ* and *swi6Δ klp9Δ* cells at 30°C is shown. Error bars represent standard deviation.

(B) The frequency of lagging chromosomes from asynchronously growing *mde4Δ, mde4Δ cut7-24, cut7-24, swi6Δ* and *swi6Δ cut7-24* cells at 25°C is shown. Error bars represent standard deviation.

The kinesin-5/bimC motor Cut7 only functions in early mitosis and is dispensable for anaphase spindle elongation in fission yeast (Fu et al., 2009). A temperature sensitive allele *cut7-24* analyzed at the permissive temperature reduced lagging chromosome production in monopolin and heterochromatin mutants, albeit to a lesser extent than *klp9Δ* mutant possibly because it was analyzed at permissive temperature to avoid spindle breakage, which occurs at restrictive temperature (Figure 3-4B). *cut7-24* itself did not produce lagging chromosomes (n = 313), but this mutation reduced the frequency of lagging chromosomes to 15.7% in *mde4Δ cut7-24* (n = 311) from 26.3% in *mde4Δ* (n = 315). Similar results were observed when *cut7-24* was combined with the *swi6Δ* mutation: 8.8% of anaphase *swi6Δ* cells showed lagging chromosomes in contrast to 5.26% in *swi6 Δcut7-24*.

Taken together, our results suggest that reduction of pulling force generated from the spindle midzone protein mutants, *klp9Δ* and *cut7-24*, may promote correction of lagging chromosomes before anaphase onset perhaps by bringing merotelically attached kinetochores into proximity with Aurora kinase which can break the improper connections. It was previously shown that mutations at a Cdk1 site in the bimC box of Cut7 did not affect its association with the mitotic spindle in fission yeast (Drummond and Hagan, 1998) despite the importance of Cdk1 phosphorylation at the same site in the *Xenopus* and human homolog Eg5 (Blangy et al., 1995; Sawin and Mitchison, 1995). In contrast, localization of Klp9 to the spindle is negatively regulated by Cdk1 phosphorylation in fission yeast (Fu et al., 2009). Thus it is possible that increasing Cdk1 activity promotes correction of merotelic attachments by negatively regulating Klp9.

Discussion Chapter III

In mammalian cells, merotelically-oriented kinetochores are observed with high frequency during early mitotic stage before anaphase onset. They are aligned normally at the metaphase plate, but do not appear parallel to the spindle equator. Instead, they are shown as tilted and stretched in both live and fixed cells (Cimini et al., 2004; Cimini et al., 2001; Cimini et al., 2003). However, the frequency of lagging chromosomes in anaphase cells is much lower than that of merotelically oriented kinetochores, and prolonging metaphase reduces the frequency of anaphase cells with lagging chromosomes, suggesting that two different error correction mechanisms act in metaphase and anaphase, respectively (Cimini et al., 2003). The spindle mechanics in anaphase B might be have a role in solving lagging chromosomes depending on the ratio of microtubules to the correct versus incorrect pole (Cimini et al., 2004). The same author also showed that Aurora kinase B promotes the correction of merotelic attachments before anaphase onset (Cimini et al., 2006). However, it has not been clear how Aurora B detects merotelic attachments. Here we proposed that higher Cdk1 activity might regulate both dynamics of the Aurora kinase complex and the mitotic spindle, and thus facilitate correction of merotelic kinetochore orientations (Figure 3-5): (1) higher Cdk1 activity could cause of the Aurora kinase complex to associate more stably with kinetochores and may expand the region of Aurora kinase. More persistent local activity of Aurora kinase could promote detection and destabilization of merotelically attached kinetochores. Alternatively, (2) higher Cdk1 activity may drive early mitotic spindle dynamics toward shrinkage, resulting in less tension applied to merotelic

Figure 3-5: Hypothetical model for correction of merotelic attachment in *clp1Δ* cells

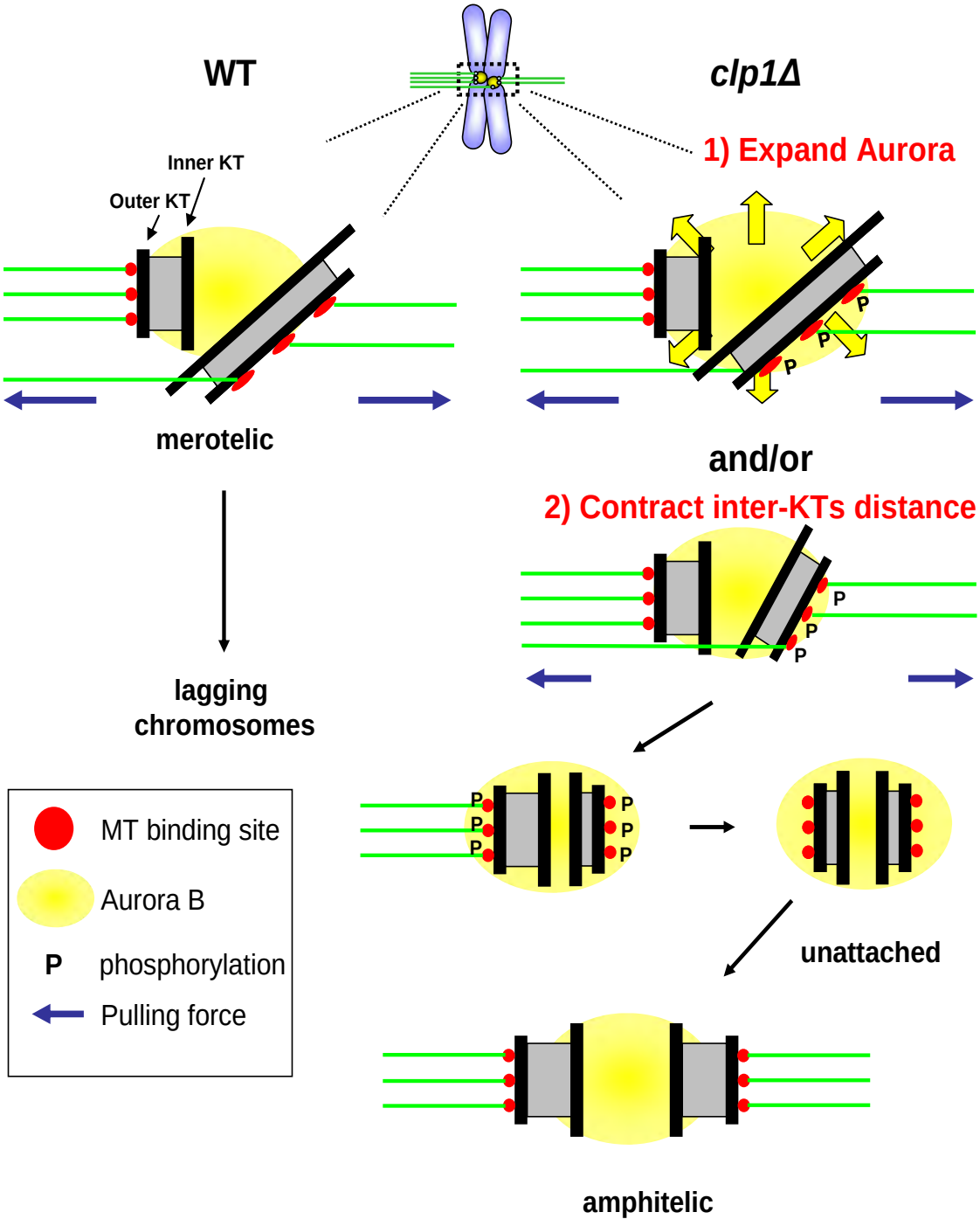

Figure 3-5: Hypothetical model for correction of merotelic attachment in *clp1Δ* cells

Higher Cdk1 activity might regulate both dynamics of the Aurora kinase complex and the mitotic spindle, and thus facilitate correction of merotelic kinetochore orientation: (1) higher Cdk1 activity could drive the dynamics of the Aurora kinase complex toward kinetochores to associate more stably with them and expand the zone of Aurora kinase. Thus more persistent local activity of Aurora kinase could detect and disconnect merotelic attachments more efficiently. Reattachments of newly growing microtubules from opposite poles establish kinetochore bi-orientation. (2) Higher Cdk1 activity bias early mitotic spindle dynamics toward shrinkage, resulting in less tension applied to merotelic kinetochores by reduced pulling force from opposite poles. Now merotelically bound kinetochores can not avoid Aurora kinase activity in the inner centromeres and are efficiently corrected by Aurora kinase.

kinetochores by reduced pulling force from opposite poles. Now merotelic kinetochores can not avoid Aurora kinase activity and are efficiently corrected by Aurora kinase.

To test these possibilities, following experiments are required as further studies: for first hypothesis, examination of Aurora kinase intensity and dynamics of Aurora kinase at kinetochores in *clp1Δ* mutant would show whether the zone of Aurora kinase is expanded in the absence of Clp1. To test second hypothesis, i) tension applied on sister kinetochores and frequency of stretched kinetochores, which is a possible marker for merotelically attached kinetochores, would be measured using a strain in which the *S. pombe* centromere 2 is labeled by LacI-GFP. This experiment would show whether conditions with higher Cdk1 activity reduce the tension and merotelic attachment at metaphase. ii) we could carry out time lapse filming using Histone-GFP combined with tubulin-mCherry in different mutants to show what percentage of mutant cells actually show lagging chromosomes in anaphase and what frequency of lagging chromosomes leads to *cut* or *co-segregation* to test whether conditions with higher Cdk1 activity actually reduce merotelic attachments in monopolin and heterochromatin mutants before anaphase onset.

Then we can move to the next question of what the important Cdk1 substrates are. Klp9 would be a great candidate. It was identified recently as a Clp1 substrate in fission yeast (Fu et al., 2009) and we also found Klp9 in our TAP purification results using a substrate trapping allele Clp1-C286S. The currently defined function of Klp9 is its role in spindle elongation at anaphase. Klp9 diffuses in the nucleus during early mitosis and localizes at the spindle midzone through the interaction with Ase1 (Fu et al., 2009). Its role in early mitosis is unknown. In contrast, Cut7 might not be a target. Cut7 has a consensus

Cdk1 site on its bimC motor region, whose phosphorylation is known to be important for microtubule binding affinity of its homolog Eg5 in *Xenopus* and human (Blangy et al., 1995; Sawin and Mitchison, 1995). Unlike with Eg5, Cdk1 phosphorylation did not show any effect on Cut7 affinity for microtubules in fission yeast (Drummond and Hagan, 1998).

Regulation of metaphase spindle length has not been studied well. Studies in drosophila S2 cells suggest that many kinesin motors in the spindle midzone and plus ends of kinetochore-microtubules, and microtubule associating proteins (MAP) such as EB1, Dis1/TOG, and CLSAP control the length of metaphase spindle (Goshima and Vale, 2003; Goshima et al., 2005). In addition to Cut7 and Klp9, fission yeast has six kinesin motors (Pkl1, Klp2, Klp5, Klp6, Klp8, Tea2) and three major MAPs, Mal3 (EB1), Dis1 (Dis1/TOG), and Cls1 (CLSAP). Unlike with one of two *S. pombe* kinesin-14/Kar3 Pkl1, all other proteins listed above have conserved Cdk1 sites on their amino acid sequence. So it would be interesting for future study to test the role of Cdk1 phosphorylation on those proteins in regulation of metaphase spindle length.

Our results suggest that the correction mechanism of merotelic kinetochore orientation might be regulated by altering local activity of Aurora kinase at kinetochores and/or affecting early mitotic spindle dynamics. Chromosome bi-orientation is established by complex mechanisms. In addition to possible tension sensors INCENP and Survivin (Sandall et al., 2006), other tension sensing protein candidates such as Sgo1, Sgo2 (Shugoshin 1 and 2) and PICH (Plk1-interacting checkpoint helicase) were reported by several studies (Baumann et al., 2007; Gomez et al., 2007; Indjeian et al., 2005; Salic et al., 2004). These tension sensors may pull microtubule binding sites composed of Ndc80

complex on merotelically oriented kinetochores toward the inner centromere region where full Aurora kinase B activity exists, then Aurora B may destabilize interaction between microtubules and the Ndc80 complex (Cimini, 2007) probably by Aurora B phosphorylation in N-terminal tail of Ndc80(Cheeseman et al., 2006; Ciferri et al., 2008; DeLuca et al., 2006). These studies raise the possibility that Cdk1 activity may regulates those tension sensors directly to promote kinetochore bi-orientaion. It has not been shown why monopolin mutants have a longer metaphase spindle. Lack of clamping microtubule binding sites on same kinetochores caused by the mutation may induce tensionless sister kinetochores leading to more separated metaphase spindle due to lack of resistance at kinetochore microtubule against pulling force from opposite poles. The examination of tension between sister kinetochores by measuring the distance between Cen2-GFPs at metaphase arrested monopolin mutants could be used to test this idea.

Chapter IV

General Discussion

The accurate and timely segregation of duplicated chromosomes is an essential aspect of mitotic cell division. To achieve this goal, chromosomes must be attached to microtubules emanating from opposite poles in a bi-oriented manner at metaphase, and separated through spindle elongation at anaphase. Our study in chapter II showed that timely regulated phosphorylation of the monopolin complex allows it to carry out discrete functions at the kinetochores in metaphase and the spindle in anaphase. However, detailed mechanisms to explain how the monopolin complex localizes at kinetochores and the spindle are elusive due to lack of information about its interacting partners at each of these locations though kinetochore partners have been unveiled by recent studies. In chapter III, we used monopolin and heterochromatin mutants as a model system producing lagging chromosomes to study the detailed correction mechanism of merotelic kinetochore orientation. Studies in chapter III provide some clues about a role for early mitotic Cdk1 activity in correction mechanisms for merotelically attached kinetochores possibly through Aurora kinase and early mitotic spindle dynamics. Since monopolin was found recently and has been analyzed by just a few studies, a more complete study of its function and regulation may allow us to gain a better understanding of correction mechanisms for merotelic kinetochore attachments.

Conservation of monopolin function at kinetochore?

The large number of microtubule binding sites at each mammalian kinetochore suggests that they should be particularly vulnerable to merotelic attachments. Consistent with this, time-lapse analysis of cultured mammalian cells showed that merotelic attachments are a major cause of chromosome mis-segregation (Cimini et al., 2001). Therefore we expect that mammalian cells have mechanisms to prevent merotely. In maize plant cells, Mis12-Ndc80 forms a bridge between adjacent homologous kinetochores to promote mono-orientation of homologous kinetochores during meiosis I, raising the possibility that monopolin like mechanism also exists in higher eukaryotes (Li and Dawe, 2009). Although monopolin-like proteins have not been identified in maize and vertebrate, a monopolin-like clamping mechanism can be one of strong candidate to suppress merotelic attachments, though prevention of merotely could be achieved by other mechanisms such as clamping only plus ends of kinetochore microtubules together or enhancing structural rigidity in centromeres to keep more efficient back to back position of sister kinetochores.

Vertebrate centromeres form a centromeric protein network called CCAN (constitutive centromere associated network), which is composed of a alphabet group of 19 CENPs including histone H3 variant CENP-A (reviewed in Przewloka and Glover, 2009). Although fission yeast has the smaller regional centromeres than vertebrate, it also contains the Sim4 complex (CCAN homolog), which comprises at least 16 proteins, whereas it has been known to date that *Drosophila* and *C. elegans* centromeres form the much simpler complex with only two key proteins, CENP-A and CENP-C (Przewloka and Glover, 2009).

Microtubule binding site are composed by conserved KMN network (KNL-1/Mis12 complex/Ndc80 complex) at outer kinetochores and fission yeast has a functional homolog of KMN network, called the Spc7/Mind/Ndc80 complex (Przewloka and Glover, 2009)(Figure 4-1).

A recent fission yeast study showed that monopolin component Pcs1 interacts with *S. pombe* CENP-C homolog, Cnp3 (Tanaka et al., 2009) and a structural study unveiled that the *S. cerevisiae* Csm1/Lrs4 complex and *S. pombe* Mde4/Pcs1 complex form a distinct V-shaped structure with two globular heads, which share a fold with Spc24/Spc25 of the Ndc80 complex (Corbett et al., 2009) and the authors also demonstrated a physical interaction between the globular head domains of Csm1/Lrs4 and the outer kinetochore Mis12 complex. Consistent with our finding that monopolin forms a multimeric complex (see Figure 2-14B), Gregan's lab found that monopolin forms multimers when Mde4 is phosphorylated during mitosis (personal communication). Taken together, the monopolin complex might localize to kinetochore in interphase as a linker between Cnp3 and Mis12 (Figure 4-1) since Pcs1 localization is abolished at kinetochore, but not in the nucleolus in *cnp3Δ* mutant (Tanaka et al., 2009). After cell enter mitosis, mitotic phosphorylation on the monopolin complex may form a hetero-tetramer or higher order to clamp neighboring microtubule binding sites together (Figure 4-1). Although fission yeast has a conserved KMN network, it has different mechanism to build the complex. For example, in contrast to KNL-1 that is required for loading of both the Mis12 complex and the Ndc80 complex to kinetochore, the *S. pombe* KNL-1 homolog Spc7 is required for proper localization of Mis12 at kinetochore, but not for Ndc80 (Kerres et al., 2007). Given that monopolin links

Figure 4-1: A hypothetical clamp model for monopolin function at kinetochore

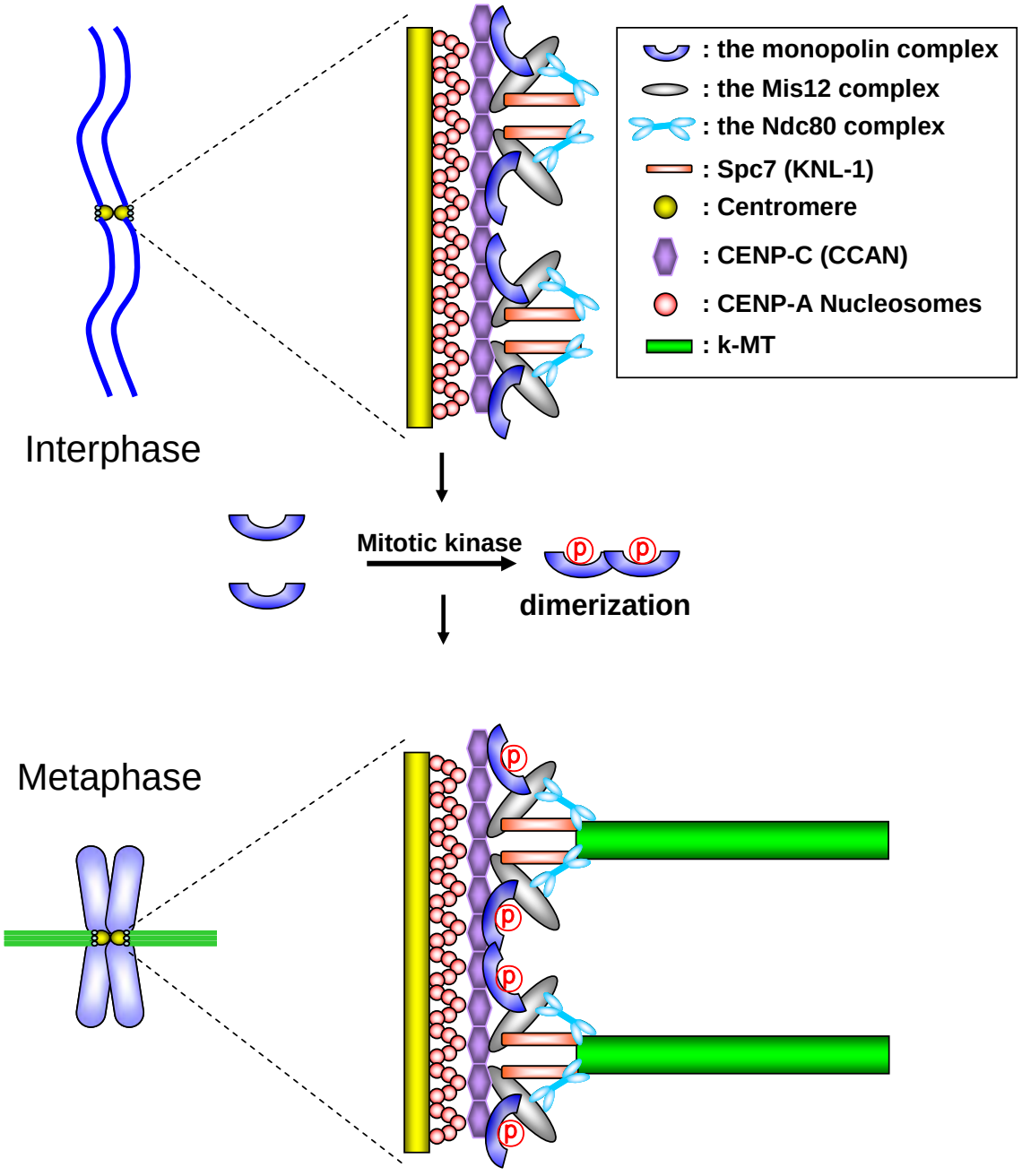

Figure 4-1: A hypothetical clamp model for monopolin function at kinetochore

In contrast to the vertebrate, which forms the stable KMN (KNL-1/Mis12 complex/Ndc80 complex) network at kinetochore during mitosis, the fission yeast KMN homolog, Spc7/Mind complex/Ndc80 complex components constitutively localize at kinetochore throughout the cell cycle. In interphase (top), monopolin links the KMN network to CENP-C (Cnp3) of the inner kinetochore CCAN through physical interaction with both proteins, Mis12 and Cnp3. Upon entry into mitosis (bottom), monopolin might be dimerized presumably by mitotic phosphorylation, resulting in clamping the neighboring Mis12 complex to form stable and aligned microtubule binding sites on CENP-C.

between Mis12 and Cnp3 of the CCAN, monopolin may promote stable and proper kinetochore-microtubule attachment by crosslinking the KMN network of outer kinetochores to the CCAN of inner kinetochores. It would be interesting to examine whether monopolin may affect the loading of outer kinetochore components in the Spc7/Mind/Ndc80 complex.

Moreover, the additional functions of monopolin in protecting repetitive sequences such as rDNA repeats from recombinational loss as well as in spindle elongation raise the possibility of existence of functional homologs in other organisms (Choi et al., 2009; Huang et al., 2006; Khmelinskii and Schiebel, 2009; Mekhail et al., 2008). It will be interesting in future studies to identify structural or functional homologs of monopolin in mammalian cells. We found the monopolin complex by TAP purification followed by mass spectrometry using a substrate trapping allele of Clp1. If phosphorylation dependent regulation of monopolin function is conserved, a similar proteomics approach would be a good possible way to identify the monopolin homologs in mammalian cells.

Monopolin functions as parallel microtubule bundler?

We showed that monopolin localizes at both ends of the anaphase spindle after removal of Cdk1 phosphorylation on Mde4 in chapter II. In the future, several questions regarding the association of monopolin with microtubules should be addressed. First, monopolin localizes to the ends of the anaphase spindle and is excluded from the spindle midzone. It is unknown whether monopolin is prevented from localization to the spindle midzone, or it prefers to bind to the parallel microtubules outside the midzone. Though many proteins

have been known to be loaded in the spindle midzone (reviewed in Glotzer, 2009), a parallel microtubule bundler, which localizes to both ends of the anaphase spindle has not been identified. In addition, it is not clear whether monopolin binds directly to microtubules or uses an adapter protein because we used a small amount of the Mde4-Pcs1 complex for in vitro microtubule binding assay due to the difficulty to get enough amount of soluble recombinant Mde4 from *E. coli*. We carried out TAP purification of Mde4 using tubulin mutant *nda3-KM311*, which may eliminate proteins that function on the spindle. Thus synchronization at other mitotic phases with the spindle may be helpful to identify possible adaptor molecules to reveal spindle localization mechanism of monopolin. Another question is whether it is important to keep monopolin off spindle microtubules prior to anaphase. In chapter II, we showed that Mde4-12A prematurely localizes at early mitotic spindles. *mde4-12A* mutant produces an even longer metaphase spindle than *mde4Δ* cells and shows more severe genetic interactions with the spindle checkpoint mutants suggesting that the *mde4-12A* mutant may have negative gain of function. It would be interesting to test whether Mde4-12A stabilizes the dynamic early mitotic spindle using fluorescence recovery after photobleaching of the metaphase spindle in a manner similar to a mutant form of the budding yeast INCENP Sli15 that lacks Cdk1 phosphorylation sites (Pereira and Schiebel, 2003). It would be also interesting to examine whether *mde4-12A* is a dominant negative mutation by following experiments: i) measuring the frequency of lagging chromosome in *mde4-12A* mutant, in which wild-type copy of $mde4^{+}$ is integrated into genome to test whether lagging chromosome production is reduced, and ii) examination of genetic interaction of the mutant, which have both copies of *mde4-12A* and

mde4^{+}, with the SAC mutants to define whether premature localization of Mde4-12A still trigger the SAC despite the proper function of wild type Mde4 at kinetochore.

Prevention of merotelic kinetochore orientations

As studied by chromatin immunoprecipitation previously, monopolin localizes at the central core region of centromeres (Gregan et al., 2007), but heterochromatin forms on the outer repeat regions of the centromere in fission yeast (Pidoux and Allshire, 2004). Heterochromatin further recruits the cohesin molecule Rad21 and provides structural rigidity to this region to support back to back orientation of sister kinetochores. The heterochromatin region is also important as a site for the chromosome passenger protein localization (Kawashima et al., 2007; Vanoosthuyse et al., 2007). The *S. pombe* shugoshin Sgo2 is required for the Aurora kinase complex localization to heterochromatin via the interaction with Survivin Bir1 (Kawashima et al., 2007). These authors showed that the chromosome passenger complex (CPC) is loaded on the heterochromatin region of the centromere, and its loading to heterochromatin was significantly reduced in the absence of Sgo2. Despite a significant reduction in the CPC loading to kinetochores, *sgo2Δ* cells showed a similar frequency of lagging chromosomes to wild-type cells indicating that the reduced level of Aurora is enough to deal with mal-oriented kinetochore-microtubules unless additional disruption in kinetochore bi-orientation is applied. Alternatively, misattached chromosomes may only occur at very low frequencies in unperturbed *S. pombe* cells, making reduced levels of Aurora not an issue. Combined mutation of *sgo2Δ* with *swi6Δ* showed synthetic growth defect caused by high production of lagging chromosomes

in anaphase (Kawashima et al., 2007). This growth defect in *sgo2Δ swi6Δ* cells is reduced by forced localization of Survivin (Bir1) to heterochromatin using ectopic expression of Bir1-GFP-2CD, in which Bir1 was fused to two chromo domains of Swi6 (Kawashima et al., 2007).

We observed that mild ectopic expression of Ark1-GFP suppresses the frequency of lagging chromosomes in *mde4Δ* mutant (Figure 3-2A). However, expression of wild type Bir1 or Bir1-GFP-2CD in *mde4Δ* cells did not cause any reduction of lagging chromosomes in *mde4Δ* mutant (data not shown). Previous observation of monopolin localization to the central core region of centromeres (Gregan et al., 2007) suggests that lack of monopolin might not affect heterochromatin structure, which is required for Aurora kinase loading to inner centromeres. Taken together our data indicate that the level of the CPC at heterochromatin region is might not be affected significantly by *mde4Δ* mutation compared to that of wild-type cells. All other non-enzymatic components of the CPC function to load Aurora kinase to the places where the enzymatic activity is required. In fully loaded state such as *mde4Δ* cells, forced localization of Bir1 or increasing the pool of Bir1 in cells by expressing Bir1-GFP-2CD or wild-type Bir1 might not have a big effect on the ability of Aurora to break merotelic attachments that had been pulled away from the region of the inner centromere with Aurora. In contrast, direct increase in the cellular pool of Ark1 by expressing Ark1-GFP may allow it to reach the more distal merotelic attachments.

Are some merotelic attachments not correctable?

We observed a suppression of lagging chromosomes in monopolin and heterochromatin mutants by mutations in Clp1, mutations in kinesin motor proteins, increased expression of Cyclin B, or increased expression Aurora kinase Ark1. It is interesting that combined expression of Cyclin B or Ark1 with *clp1Δ* do not further reduce the frequency of lagging chromosomes below the level observed in *clp1Δ* single mutant. It might suggest that there is a threshold in correction of merotely by elevated Cdk1 activity. For example, amongst the 30% of lagging chromosomes in the *mde4Δ* mutant, about 5 to 6 % of the merotelic attachments may be really problematic (see Figure 3-1) and not easily corrected by cellular mechanisms. In contrast to monotely and syntely, which are all or nothing attachments, merotely may have various tensions depending on the ratio of attached microtubules from opposite poles, which might impact how easily they are corrected.

Phosphorylation dependent regulation by Cdk1 and Cdc14 during early mitosis

Recent progress in quantitative phospho-proteomics is facilitating identification of putative Cdk1 substrates (Dephoure et al., 2008; Holt et al., 2009; Ubersax et al., 2003; Wilson-Grady et al., 2008) but the particular regulatory role of Cdk1 phosphorylation on individual substrates needs to be defined. Before our study started, only limited numbers of Cdk1 substrates were characterized such as Ase1, Fin1 and INCENP Sli15 (Higuchi and Uhlmann, 2005; Khmelinskii et al., 2007; Pereira and Schiebel, 2003; Woodbury and Morgan, 2007). In addition to those, we and another group put Mde4 and Klp9 into the list (Choi et al., 2009; Fu et al., 2009). They are all spindle localized proteins and their

translocation to the spindle occurs after anaphase onset by reversing Cdk1 phosphorylation by the Cdc14 phosphatases. Those data further confirmed the role of Cdc14, which is mainly believed to function after Cdk1 activity drops to reverse Cdk1 phosphorylation for proper mitotic exit. In contrast to budding yeast, which activates Cdc14 after anaphase onset by releasing it from nucleolar inhibitor Net1, the fission yeast Clp1 is released from the nucleolus at mitotic entry as in mammalian cells, indicating that Clp1 could have an additional role in early mitosis. At metaphase, it localizes at kinetochores, suggesting that it has substrates at kinetochores. Cdk1 phosphorylates Clp1 to suppress its enzymatic activity (Wolfe et al., 2006), but Clp1 still may compete for substrates with Cdk1 by concentrating its localization to specialized spots such as kinetochores. Our studies in Chapter II and III provide an insight for a novel regulatory role of Cdc14 phosphatases in early mitosis: competing with highly active Cdk1 for the CPC components and possibly molecular motor proteins to mediate correction of merotelic attachment. It has been well known that hundreds of proteins are involved in DNA condensation, early mitotic spindle dynamics, and maturation of kinetochore structure to capture microtubules during early mitosis to accomplish chromosome bi-orientaion. These events occur precisely during the period of peak Cdk1 activity, and results of various quantitative phospho-proteomics studies suggest that most mitotic phosphorylation is mediated by Cdk1. Thus, a phosphorylation dependent switch by highly active Cdk1 and spatially regulated Clp1 could serve as a key regulatory factor in during early mitosis to precisely control complex and dynamic error correction mechanism in sister kinetochore bi-orientation.

Appendix A

List of proteins interacting with Clp1 phosphatase and the monopolin Mde4

A-1 and A-2: List of proteins copurified with Clp1-C286S-TAP from prometaphase (by cold sensitive tubulin mutation *nda3-KM311*), metaphase (by temperature sensitive proteasome mutation *mts3-1*), late anaphase (released from G2 arrest by *cdc25-22* mutation) and asynchronously growing cells. Purified protein complex was analyzed by tandem mass spectrometry.

A-3: List of proteins copurified with Mde4-TAP from prometaphase arrested *clp1-C286S-GFP nda3-KM311* cells.

Apparent ribosomal proteins, translational initiation and elongation factors, metabolic enzymes and tRNA ligases are not listed in A-1, A-2, and A-3.

A-1. Proteins shown in all three conditions

Proteins	*S. pombe* DB Accs	prometa/metaphase		late anaphase		Asynchronous	
		Coverage rate	Peptide count	Coverage rate	Peptide count	Coverage rate	Peptide count
Clp1	SPAC1782.09c	79.70%	1138	75.70%	1271	74.60%	1084
Bir1, Survivin	SPCC962.02c	30.20%	81	58.90%	142	43.10%	89
Pic1, INCENP	SPBC336.15	27.70%	52	39.90%	255	38.40%	109
Heat shock protein sks2	SPBC1709.05	40.10%	51	42.70%	53	32.60%	48
Probable heat shock protein ssa2	SPCC1739.13	30.10%	49	65.30%	226	54.20%	128
Borealin homolog Nbl1	SPBC725 12	28.40%	20	52.60%	18	50.50%	17
LEM domain protein Man1, Sad1 interacting factor	SPAC14C4.05c	15.60%	17	17.20%	13	17.70%	17
U3 snoRNP protein Nop58	SPAC23G3.06	25.40%	15	12.80%	6	7.10%	3
Serine/threonine-protein kinase shk1/pak1	SPBC1604.14c	23.10%	14	17.20%	12	25.70%	16
Bip1, 78 kDa glucose-regulated protein homolog	SPAC22A12.15c	21.10%	14	35.90%	80	37.00%	62
Heat shock protein 90 homolog Swo1	SPAC926.04c	17.90%	13	21.00%	14	11.80%	9
Actin	SPBC32H8.12c	25.90%	12	45.90%	23	29.10%	22
heat shock protein Ssa1 (predicted)	SPAC13G7.02c	17.40%	12	49.80%	118	39.20%	75
U3 snoRNA-associated protein 10 Utp10	SPBC23E6.04c	10.10%	12	2.30%	4	3.00%	3
Rad24, 14-3-3 protein	SPAC8E11.02c	42.20%	11	53.30%	31	47.80%	25
Heat shock 70 kDa protein, mitochondrial	SPAC664.11	20.80%	11	50.60%	62	34.60%	26
Pumilio homology domain family member 6	SPCP1E11.11	10.40%	11	15.70%	11	17.40%	12
rRNA 2'-O-methyltransferase fibrillarin fib1	SPBC2D10.10c	39.70%	10	23.60%	6	7.50%	2
Rad25, 14-3-3 protein	SPAC17A2.13c	37.80%	10	23.00%	6	27.40%	8
YTH domain-containing protein mmi1	SPCC736.12c	18.50%	10	50.10%	53	47.40%	28
Probable nucleolar GTP-binding protein 1 Nog1	SPBC651.01c	18.10%	8	14.00%	11	14.00%	9
ATP-dependent RNA helicase dbp2	SPBP8B7.16c	17.10%	8	10.20%	5	3.50%	2
Mde4, monopolin complex component	SPBC6B1.04	17.60%	6	46.60%	42	43.00%	27
Clp1-interacting protein Nsk1	SPAC3G9.01	10.80%	6	53.00%	133	39.20%	76
MT organizer Mto1	SPCC417.07c	7.40%	6	5.50%	5	6.20%	5
Forkhead protein sep1	SPBC4C3.12	6.90%	6	25.90%	29	41.20%	40
Start control protein cdc10	SPBC336.12c	6.40%	6	51.60%	75	45.80%	71
Switch-activating protein 1 Sap1	SPCC1672.02c	23.60%	5	35.40%	9	10.60%	2
Calmodulin	SPAC3A12.14	13.30%	5	43.30%	8	32.70%	12
Checkpoint serine/threonine-protein kinase bub1	SPCC1322.12c	6.70%	5	19.90%	20	13.20%	17
Importin subunit beta-3 Sal3	SPCC1840.03	5.00%	5	11.80%	10	10.60%	9

Probable mitochondrial phosphate carrier protein	SPBC1703.13c	16.40%	4	8.70%	2	8.00%	2
DUF1776 family protein	SPBC106.03	15.70%	4	20.20%	6	26.30%	7
Mitochondrial protein import protein mas5	SPBC1734.11	11.30%	4	18.70%	8	14.00%	4
Protein slt1	SPAC17G6.13	9.50%	4	33.90%	25	21.50%	8
DNAJ domain protein Mdj1 (predicted)	SPCC4G3.14	8.70%	4	8.30%	6	7.00%	2
DNAJ domain protein Caj1/Djp1 type	SPAC4H3.01	7.10%	4	7.90%	4	16.60%	8
Rho-type GTPase activating protein Rga6	SPBC354.13	6.40%	4	5.30%	4	3.70%	2
RhoGEF Rgf3	SPCC645.06c	4.90%	4	2.60%	2	2.60%	2
Pcs1, monopolin complex component	SPAC11E3.03	14.90%	3	49.50%	41	48.60%	30
19S proteasome regulatory subunit Rpt6	SPBC23G7.12c	10.20%	3	8.70%	3	6.20%	2
U3 snoRNP-associated protein Utp21	SPCC1672.07	5.80%	3	4.30%	3	3.20%	2
Cell wall integrity protein scw1	SPCC16C4.07	5.30%	3	3.60%	3	11.10%	4
GTP binding protein (predicted)	SPBC428.15	6.60%	2	16.90%	5	7.00%	2
sequence orphan	SPBC2G2.14	5.40%	2	17.60%	10	20.50%	7
MBF transcription factor complex subunit Res2	SPAC22F3.09c	5.00%	2	29.40%	27	41.20%	55
Mitotic checkpoint protein bub3	SPAC23H3.08c	4.40%	2	23.40%	6	13.40%	4
kinesin-like protein Klp6	SPBC1685.15c	4.20%	2	29.70%	39	29.20%	37
N-acetyltransferase Nat10	SPAC20G8.09c	3.10%	2	2.40%	2	2.60%	3
Cell division cycle-related protein res1/sct1	SPBC725.16	2.70%	2	49.30%	95	38.60%	47

A-2. Protein shown in one or two of three conditions

Proteins	S. pombe DB Accs	pro/metaphase		late anaphase		Asynchronous	
		Coverage rate	Peptide count	Coverage rate	Peptide count	Coverage rate	Peptide count
ATP-dependent RNA helicase ded1	SPCC1795.11	33.30%	48			29.40%	15
cell surface glycoprotein (predicted)	SPBPJ4664.02	0.70%	44				
P-type proton ATPase Pma1	SPAC1071.10c	23.90%	41				
ubiquitin Ubi4	SPBC337.08c	6.50%	40				
WD repeat protein Lub1	SPBC887.04c	4.30%	35				
ribonucleoside reductase large subunit Cdc22	SPAC1F7.05	26.10%	30			3.60%	2
SWI/SNF complex subunit Snf5	SPAC2F7.08c	1.70%	25				
P-type proton ATPase Pma2	SPCC1020.01c	7.60%	22				
cell division control protein Cdc15	SPAC20G8.05c	15.10%	21	9.00%	6		
tubulin-tyrosine ligase (predicted)	SPAC12B10.04	7.70%	21				
Ribosome biosynthesis protein Sik1	SPBC646.10c	36.80%	20			8.50%	3
Kinesin-like protein 5	SPBC2F12.13			24.30%	20	24.60%	26
AAA family ATPase ELf1	SPAC3C7.08c	18.50%	17				
Transcription factor nrm1	SPBC16A3.07c			31.60%	15	30.40%	13
ADP,ATP carrier protein Anc1	SPBC530.10c	29.80%	14			10.60%	4
hypothetical protein	SPBC36B7.06c	22.50%	14				
two-component GAP Cdc16	SPAC6F6.08c	10.70%	14				
translation elongation regulator Gcn1 (predicted	SPAC18G6.05c	7.50%	14				
Centromere-binding factor 5 homolog Cbf5	SPAC29A4.04c	17.50%	13			10.80%	2
transcription factor	SPCC320.03			9.30%	13	6.90%	2
karyopherin Kap123	SPBC14F5.03c	9.40%	12				
RNA-binding protein Snd1	SPCC645.08c	6.20%	12				
U5 snRNP complex subunit Brr2 (predicted)	SPAC9.03c	2.90%	12				
kinesin-like protein Klp9	SPBC15D4.01c			9.50%	12	25.40%	20
MBF complex negative regulatory component Yox1	SPBC21B10.13c			38.30%	12	32.80%	13
glycine hydroxymethyltransferase (predicted)	SPAC24C9.12c	25.70%	11				
cell wall protein Gas5, 1,3-beta-glucanosyltransferase (predicted)	SPAC11E3.13c	19.60%	11				
acetohydroxyacid reductoisomerase	SPBC56F2.12	21.30%	10				
cytoplasmic threonine-tRNA ligase Trs1 (predicted)	SPBC25H2.02	11.50%	10				
vigilin	SPCC550.14	11.50%	10	4.10%	3		
pentafunctional aromatic polypeptide Aro1 (predicted)	SPAC1834.02	8.40%	10				
MAP kinase kinase kinase Byr2	SPBC1D7.05	1.20%	10				
F1-ATPase beta subunit Atp2	SPAC222.12c	25.90%	9				

clathrin heavy chain Chc1 (predicted)	SPAC26A3.05	8.50%	9				
pig-Q	SPBC30D10.11	6.40%	9				
1,3-beta-glucan synthase subunit Bgs4	SPCC1840.02c	5.10%	9				
zuotin (predicted)	SPBC1778.01c	16.50%	8				
NADH dehydrogenase	SPAC3A11.07	14.70%	8			6.70%	3
chaperonin-containing T-complex zeta subunit Cct6	SPBC646.11	13.10%	8				
secretory pathway protein Sec18 (predicted)	SPAC1834.11c	12.80%	8	4.70%	2		
transcription factor Ste11	SPBC32C12.02	7.90%	8				
U3 snoRNP-associated protein Rrp5	SPCC1183.07	7.20%	8				
nuclear export receptor Crm1	SPAC1805.17	3.20%	8				
P-type ATPase (predicted)	SPAC821.13c	3.10%	8				
Transcription factor tau subunit sfc1	SPAC6F12.11c			16.00%	8	10.30%	3
BRCT domain protein mug176	SPBC3H7.14			13.50%	8		
Protein phosphatase 2B catalytic subunit PPb1	SPBP4H10.04			12.60%	8	18.80%	9
chaperonin-containing T-complex delta subunit Cct4	SPBC106.06	17.50%	7				
mitochondrial heat shock protein Hsp60/Mcp60	SPAC12G12.04	10.50%	7	12.50%	6		
epimarase (predicted)	SPCC757.02c	7.70%	7				
alpha-1,4-glucan synthase Ags1	SPCC1281.01	4.00%	7				
glutathione S-conjugate-exporting ATPase Abc2	SPAC3F10.11c	3.50%	7				
guanyl-nucleotide exchange factor (predicted)	SPBC211.03c	3.10%	7				
MutS protein homolog	SPCC285.16c	2.90%	7	2.20%	2		
hypothetical protein	SPAPB15E9.01c	2.30%	7				
DASH complex subunit Dad3	SPAC14C4.16			45.30%	7		
elongator subunit Iki3	SPBC36.07			6.40%	7	1.80%	2
RACK1 ortholog Cpc2	SPAC6B12.15	24.50%	6				
protein disulfide isomerase (predicted)	SPAC17H9.14c	20.90%	6				
AAA family ATPase Rvb1	SPAPB8E5.09	17.30%	6				
AAA family ATPase Cdc48	SPAC1565.08	11.80%	6				
chaperonin-containing T-complex beta subunit Cct2	SPAC1D4.04	11.40%	6				
GTPase Grn1	SPBC26H8.08c	10.90%	6	8.30%	3		
vacuolar transporter chaperone (VTC) complex subunit (predicted)	SPCC1322.14c	10.70%	6				
nucleocytoplasmic transport chaperone Srp40 (predicted)	SPBC1711.05	6.90%	6				
proteasome component	SPAC1782.01	4.50%	6				
CCR4-Not complex subunit Not1 (predicted)	SPAC20G8.06	4.40%	6				
RNA-binding protein	SPAC644.16	3.10%	6				
MutS protein homolog 2	SPBC19G7.01c	2.50%	6				

dynein heavy chain Dhc1	SPAC1093.06c	1.60%	6				
Sm snRNP core protein Smd2	SPAC2C4.03c			25.20%	6		
Hypothetical protein	SPBC11C11.06c			22.50%	6		
serine/threonine protein phosphatase PP1 Dis2	SPBC776.02c	16.20%	5				
ATP-dependent RNA helicase Ste13	SPBC776.09	15.70%	5				
ribosome export GTPase (predicted)	SPAC6F6.03c	14.70%	5	5.80%	2		
ATP-dependent RNA helicase dbp3	SPBC17D1.06	14.40%	5	8.50%	3		
tubulin alpha 1 nad2	SPBC16A3 15c	14.30%	5				
elongator complex, histone acetyltransferase subunit Elp3 (predicted)	SPAC29A4.20	13.60%	5				
adenosylhomocysteinase (predicted)	SPBC8D2.18c	13.40%	5				
mitochondrial ATP-dependent RNA helicase Mss116 (predicted)	SPBC691.04	12.70%	5				
sulfate adenylyltransferase	SPBC27.08c	11.40%	5				
exocyst complex subunit Exo70 (predicted)	SPBC106.20	11.10%	5				
ER membrane DUF1682 family protein	SPBC2G5.01	10.40%	5			8.60%	2
vacuolar protein Vac8	SPBC354.14c	9.10%	5				
karyopherin Kap109	SPBC30B4.05	8.20%	5				
RNA-binding protein	SPAC4G8.03c	6.30%	5				
DEAD/DEAH box helicase	SPAC694.02	5.30%	5				
Pof6 interacting protein Sip1, predicted AP-1 accessory protein	SPBC27B12.08	5.00%	5				
RNA-binding protein Puf3 (predicted)	SPAC1687.22c	4.60%	5				
ATP-dependent DNA helicase Hrp3	SPAC3G6.01	4.50%	5				
sec14 cytosolic factor family	SPCC23B6.04c	3.50%	5				
alpha-1,4-glucan synthase Mok14	SPCC63.04	3.40%	5				
phosphatidylinositol kinase (predicted)	SPBC577.06c	3.30%	5				
HECT-type ubiquitin ligase E3 Ptr1	SPAC19D5.04	2.60%	5				
chorein homolog	SPBC16C6.02c	2.10%	5				
Nucleolar protein gar2	SPAC140.02			14.20%	5	5.60%	3
U3 snoRNP-associated protein Cic1/Utp30 family (predicted)	SPAC8F11.04			6.20%	5		
DNA topoisomerase 2-associated protein pat1	SPBC19G7.10c			10.10%	5	12.80%	12
U3 snoRNP protein Nop14 (predicted)	SPBC3F6.04c			6.20%	5		
transcription factor TFIIIC complex subunit Sfc9	SPBC8D2.07c			8.20%	5	6.10%	2
Uncharacterized FAD-binding protein	SPAC17H9.12c	27.80%	4			19.90%	4
GTPase Rbg1 (predicted)	SPAC9.07c	16.90%	4				
U3 snoRNP-associated protein Sof1	SPBC1A4.07c	15.80%	4				
serine palmitoyltransferase complex subunit (predicted)	SPBC18E5.02c	14.50%	4				
FKBP-type peptidyl-prolyl cis-trans isomerase (predicted)	SPAC27F1.06c	14.40%	4				
coatomer epsilon subunit (predicted)	SPBC24C6.05	14.20%	4				
kinesin-like protein Klp8	SPAC144.14	13.90%	4				
peroxisomal biogenesis factor 11	SPBC582.09	13.90%	4				

hypothetical protein	SPCC132.03	13.60%	4				
homoisocitrate dehydrogenase	SPAC31G5.04	13.50%	4				
DNAJ/TPR domain protein DNAJC7 family	SPBC543.02c	13.40%	4				
6-phosphogluconate dehydrogenase, decarboxylating	SPBC660.16	11.40%	4			6.50%	2
dipeptidyl peptidase (predicted)	SPAC3A11.10c	10.80%	4				
pescadillo-family BRCT domain protein	SPBC19F5.05c	10.20%	4	7.10%	3		
SWI/SNF and RSC complex subunit Arp9	SPAC1071.06	9.40%	4				
WD repeat protein (predicted)	SPBC1711.16	9.30%	4				
delta-1-pyrroline-5-carboxylate dehydrogenase	SPBC24C6.04	8.20%	4				
signal recognition particle subunit Srp72	SPCC320.10	8.20%	4				
karyopherin Cut15	SPCC962.03c	8.10%	4				
U3 snoRNP-associated protein Utp1	SPBC713.04c	7.80%	4				
Blt1	SPBC1A4.05	7.70%	4	7.40%	3		
COPII-coated vesicle component Sfb3 (putative)	SPBC4.03c	7.20%	4				
U3 snoRNP-associated protein Utp3 (predicted)	SPBC3B8.09	6.90%	4				
DNA binding factor Trf1	SPBC19G7.13	6.80%	4				
19S proteasome regulatory subunit Mts4	SPBP19A11.03c	6.50%	4	3.90%	2		
19S proteasome regulatory subunit Rpn2 (predicted)	SPBC17D11.07c	6.30%	4				
serine/threonine protein kinase Ksp1 (predicted)	SPBC16E9.13	5.90%	4				
serine/threonine protein kinase Cdc7	SPBC21.06c	5.50%	4				
hypothetical protein	SPBC27.04	5.50%	4				
Rad7 homolog Rhp7	SPCC330.02	5.50%	4				
transcription factor TFIIIC complex B box binding subunit Sfc3	SPBC336.07	5.00%	4				
ribosome biogenesis ATPase, Arb family ABCF1-like (predicted)	SPCC825.01	5.00%	4				
C-1-tetrahydrofolatesynthase	SPBC2G2.08	4.90%	4				
ribosome biogenesis protein Noc1 (predicted)	SPAC4F10.09c	4.80%	4	3.50%	2		
cohesin-associated protein Pds5	SPAC110.02	4.60%	4				
RNB-like protein Sts5	SPCC16C4.09	4.60%	4	5.40%	4		
peptidase (predicted)	SPCC1259.02c	4.40%	4				
nucleoporin Nup157/170	SPAC890.06	4.00%	4				
mediator of replication checkpoint 1	SPAC694.06c	3.70%	4				
heat shock protein Hsp104 (predicted)	SPBC16D10.08c	3.60%	4				
phospholipase (predicted)	SPAC1786.02	3.40%	4				
nucleoporin Nup146	SPAC23D3.06c	3.40%	4				
DUF221 family protein implicated in Golgi to plasma membrane transport	SPAC24H6.13	3.40%	4				
DNA polymerase delta catalytic subunit Cdc6	SPBC336.04	3.40%	4				
M phase inhibitor protein kinase Wee1	SPCC18B5.03	3.40%	4				

Dopey family protein	SPAPB21F2.02	3.30%	4				
ribosome biogenesis protein Urb1	SPCC14G10.02	3.30%	4				
cytoskeletal protein binding protein Sla1 family, Shd1 (predicted)	SPAC16E8.01	2.70%	4				
adherin, cohesin loading factor Mis4	SPAC31A2.05c	2.70%	4				
ubiquitin-protein ligase E3 (predicted)	SPBC21D10.09c	2.50%	4				
phosphatidylinositol kinase-related protein Tra2	SPAC1F5.11c	2.30%	4				
morphogenesis protein Mor2	SPBP19A11.04c	2.30%	4				
P-type ATPase P5 type (predicted)	SPCC1672.11c	2.20%	4				
nuclear pore complex associated protein	SPCC162.08c	1.60%	4				
ferrichrome synthetase Sib1	SPAC23G3.02c	1.50%	4				
Heat shock protein homolog pss1	SPAC110.04c			9.00%	4	4.60%	2
Cell polarity protein tea3	SPAC6G10.02c			6.10%	4	7.00%	6
sterol binding ankyrin repeat protein	SPBC2F12.05c			4.10%	4		
mitochondrial heatshock protein Hsp78	SPBC4F6.17c			7.30%	4		
pho88 family protein	SPBC16H5.04	28.40%	3				
snoRNP pseudouridylase complex protein Gar1	SPBC20F10.01	24.20%	3				
human LYHRT homolog	SPBC215.06c	22.50%	3				
V-type ATPase V0 subunit c (proteolipid subunit)	SPAC1B3.14	21.70%	3				
histone H2A beta	SPAC19G12.06c	21.40%	3				
histone H2A alpha	SPCC622.08c	21.20%	3				
Prohibitin Phb2	SPCC1322.16	19.70%	3			8.60%	2
ribosome biogenesis protein Rrs1 (predicted)	SPBC29A3.16	18.70%	3				
ubiquitin protease cofactor (predicted)	SPBP8B7.11	14.50%	3				
ubiquitin C-terminal hydrolase Ubp3	SPBP8B7.21	12.30%	3				
ribosome biogenesis protein Nop6	SPBP16F5.06	11.50%	3				
RSC complex subunit Rsc58	SPAC1F3.07c	11.40%	3				
MatE family transporter (predicted)	SPAC11D3.06	11.00%	3				
gamma-glutamyl phosphate reductase Pro1	SPAC821.11	10.90%	3			5.80%	2
19S proteasome regulatory subunit Rpn501	SPAC1420.03	10.80%	3				
19S proteasome regulatory subunit Rpn502	SPAPB8E5.02c	10.80%	3				
CCR4/nocturin family endoribonuclease	SPBC9B6.11c	10.80%	3				
signal recognition particle subunit Srp54	SPCC188.06c	10.50%	3				
rRNA processing protein Enp2 (predicted)	SPCC330.09	10.40%	3				
mitochondrial m-AAA protease	SPBC543.09	10.20%	3				
D-3 phosphoglycerate dehydrogenase (predicted)	SPCC364.07	10.10%	3				
ZIP zinc transporter 1	SPAP8A3.03	9.70%	3				
WD repeat protein, human WDR68 family	SPBC17D11.08	9.70%	3	8.50%	2		

serine/threonine protein kinase Cka1	SPAC23C11.11	9.60%	3				
ATP-dependent RNA helicase Dbp8 (predicted)	SPBC543.06c	9.30%	3				
19S proteasome regulatory subunit Rpn6 (predicted)	SPAC23G3.11	8.30%	3				
cortical component Lsb5 (predicted)	SPBC31F10.07	8.20%	3				
HRD ubiquitin ligase complex subunit (predicted)	SPBC28F2.08c	7.90%	3				
DNA polymerase alpha-associated DNA helicase A (predicted)	SPCC737.07c	7.40%	3				
serine/threonine protein kinase Ppk15 (predicted)	SPAC823.03	7.10%	3				
Noc complex subunit Noc2 family (predicted)	SPAC1142.04	6.90%	3	6.50%	3		
protein phosphatase regulatory subunit Pab1	SPAC227.07c	6.90%	3				
GTP binding protein (predicted)	SPAC27E2.03c	6.90%	3				
protein phosphatase regulatory subunit Paa1	SPAP8A3.09c	6.90%	3				
tubulin alpha 2	SPBC800.05c	6.50%	3				
medial ring protein Mid2	SPAPYUG7.03c	6.40%	3				
fork head transcription factor Fhl1	SPAC1142.08	6.20%	3				
GTPase activating protein Sec23a	SPCC31H12.07	6.20%	3				
P-type ATPase, calcium transporting Cta3	SPBC839.06	6.00%	3				
chaperonin-containing T-complex alpha subunit Cct1	SPBC12D12.03	5.80%	3				
mitochondrial ribosomal protein subunit S35	SPBC14C8.16c	5.70%	3				
meiotic recombination protein Rec10	SPAC25G10.04c	5.60%	3				
cytoplasmic isoleucine-tRNA ligase Irs1 (predicted)	SPBC8D2.06	5.60%	3				
dynamin Dnm1	SPBC12C2.08	5.40%	3				
AAA family ATPase Gcn20 (predicted)	SPBC29A3.09c	5.40%	3				
chaperonin-containing T-complex gamma subunit Cct3	SPBC1A4.08c	5.30%	3				
DNA polymerase alpha accessory factor Mcl1	SPAPB1E7.02c	5.20%	3				
ATP-dependent RNA helicase Dbp9 (predicted)	SPCC1494.06c	5.20%	3				
transcription elongation factor Spt5	SPAC23C4.19	5.10%	3				
glucosidase (predicted)	SPAC17G6.11c	4.90%	3				
GTPase Cwf10	SPBC215.12	4.80%	3	3.10%	2		
actin cortical patch protein (predicted)	SPBC29B5.04c	4.80%	3				
ATP-dependent RNA helicase Dbp5	SPBC12C2.06	4.60%	3				
ENTH/VHS domain protein	SPBC19F8.03c	4.60%	3				
DNA-directed RNA polymerase III complex large subunit Rpc1	SPBC651.08c	4.60%	3				
U3 associated protein Utp25 (predicted)	SPCC1827.01c	4.60%	3				

tuberin	SPAC630.13c	4.20%	3				
nucleoporin Nup189	SPAC1486.05	3.90%	3				
GTP binding protein Bms1	SPBC31E1.06	3.60%	3				
ER to Golgi tethering factor Uso1 (predicted)	SPAC29E6.03c	3.50%	3				
cell surface glycoprotein (predicted)	SPAPB2C8.01	3.50%	3				
serine/threonine protein kinase Ppk19	SPBC119.07	3.50%	3				
SNF2 family helicase Ino80	SPAC29B12.01	3.40%	3				
actin binding protein, coronin Crn1	SPAC23C4.02	3.20%	3				
ATP-dependent RNA helicase, TRAMP complex subunit Mtr4	SPAC6F12.16c	3.20%	3				
karyopherin Kap113	SPCC1322.06	3.20%	3				
SWI/SNF complex subunit Sol1	SPBC30B4.04c	3.10%	3				
Tre1 family protein (predicted)	SPBC354.09c	3.10%	3				
cell polarity factor Rax2	SPAC6F6.06c	3.00%	3				
secretory pathway protein Sec39 (predicted)	SPAC7D4.11c	3.00%	3				
brefeldin A efflux transporter Bfr1	SPCC18B5.01c	2.90%	3				
nucleoporin Nup132	SPAC1805.04	2.80%	3				
ATR checkpoint kinase Rad3	SPBC216.05	2.80%	3				
human THADA ortholog	SPCC1494.07	2.80%	3				
Smc5-6 complex SMC subunit Smc6	SPCC5E4.06	2.50%	3	4.30%	3		
Sec7 domain protein, ARF GEF (predicted)	SPAC30.01c	2.40%	3				
fun thirty related protein Fft3	SPAC25A8.01c	2.20%	3				
RecQ type DNA helicase	SPAC212.11	2.10%	3				
multidomain vesicle coat component Sec16	SPAC29B12.07	2.10%	3				
C2 domain protein Git1	SPBC21C3.20c	2.10%	3				
nucleoporin Nup186	SPCC290.03c	1.90%	3				
U3 snoRNP protein Utp20	SPBC56F2.04	1.70%	3				
Probable mitochondrial transport protein fsf1	SPAC17G6.15c			12.00%	3	7.40%	2
Dynein light chain Dlc1	SPAC1805.08			22.50%	3	22.50%	3
RNA-binding protein Rsd1	SPAC19G12.07c			4.10%	3		
serine palmitoyltransferase Lcb2	SPAC21E11.08			7.30%	3		
Rho guanine nucleotide exchange factor gef2	SPAC31A2.16			3.70%	3	3.50%	4
Transcription factor BTF3 homolog	SPAC4F10.14c			26.50%	3	26.50%	2
DASH complex subunit spc34	SPAC8C9.17c			13.40%	3	14.60%	2
serpine1 related protein	SPBC16A3.08c			9.50%	3	12.30%	2
striatin homolog	SPBC1773.01			8.00%	3	4.90%	2
transcription factor TFIID complex subunit Taf10	SPBC21H7.02			15.80%	3		
DASH complex subunit ask1	SPBC27.02c			16.90%	3	21.50%	4
Rho-type GTPase activating protein Rga4	SPBC28E12.03			3.50%	3		
19S proteasome regulatory subunit Rpt2	SPBC4.07c			8.30%	3	5.80%	2
clathrin light chain Clc1	SPBC9B6.08			19.70%	3	20.10%	2
ubiquitin-protein ligase E3 Brl1	SPCC1919.15			8.20%	3	6.40%	3

Mitochondrial import inner membrane translocase subunit tim13	SPAC17C9.09c	22.10%	2			32.60%	2
heat shock protein Hsp16	SPBC3E7.02c	16.80%	2	36.40%	4		
Probable vesicular-fusion protein sec17	SPAC959.02	12.50%	2	16.30%	3		
U3 snoRNP-associated protein Utp11	SPAC18G6.06	12.40%	2	13.30%	2		
hypothetical protein	SPAC9E9.05	10.90%	2	7.70%	3		
cyclin-dependent protein kinase Cdk1/Cdc2	SPBC11B10.09	9.10%	2	13.10%	3		
Brix domain protein Rpf2	SPAC926.08c	8.80%	2	14.50%	5	16.40%	7
mitochondrial serine hydrolase (predicted)	SPCC5E4.05c	8.50%	2	14.00%	2		
19S proteasome regulatory subunit Rpt3	SPCC576.10c	8.20%	2	8.20%	4		
GNS1/SUR4 family protein	SPAC1B2.03c	7.80%	2	13.20%	2		
nucleosome assembly protein Nap1	SPCC364.06	7.40%	2	8.70%	2		
ubiquitin-protein ligase E3 Brl2	SPCC970.10c	5.60%	2			3.20%	2
RNA-binding protein	SPBC4F6.14	5.50%	2	5.20%	2		
mitochondrial TOM complex subunit Tom70 (predicted)	SPAC6B12.12	5.00%	2	15.20%	7		
RNA-binding protein Mrd1	SPBP22H7.02c	4.60%	2	4.60%	3		
central kinetochore associated family protein (predicted)	SPCC1442.02	4.30%	2	4.40%	2		
M phase inducer phosphatase Cdc25	SPAC24H6.05	4.20%	2			5.00%	2
RNAPII degradation factor	SPBC354.10	4.20%	2			3.90%	2
coatomer alpha subunit (predicted)	SPBPJ4664.04	2.70%	2	3.00%	2		
Ras GTPase-activating-like protein rng2	SPAC4F8.13c	2.30%	2			1.30%	2

A-3. Proteins co-purified with Mde4-TAP from prometaphase arrested *clp1-C286S-GFP nda3-KM311* cells

Protein	*S. pombe* DB Accs	Coverage rate	Peptide count
Clp1	SPAC1782.09c	39.10%	126
Probable heat shock protein ssa2	SPCC1739.13	23.80%	46
Mde4, monopolin complex component	SPBC6B1.04	30.60%	38
Bip1, 78 kDa glucose-regulated protein homolog	SPAC22A12.15c	6.80%	10
Pcs1, monopolin complex component	SPAC11E3.03	12.20%	6
Vesicular-fusion protein sec18	SPAC1834.11c	8.50%	5
Heat shock protein 90 homolog Swo1	SPAC926.04c	3.40%	5
RNA-binding protein Snd1	SPCC645.08c	2.50%	4
mitochondrial serine hydrolase (predicted)	SPCC5E4.05c	11.10%	3
DNAJ domain protein Caj1/Djp1 type	SPAC4H3.01	6.60%	3
cargo-transport protein Ypp1 (predicted)	SPAC637.04	3.90%	3
Increased rDNA silencing protein 4 Irs4	SPAC1687.09	2.20%	3
transcription factor (predicted)	SPAC105.03c	1.00%	3
cytosolic thioredoxin Trx1	SPAC7D4.07c	25.50%	2
Probable RNA-binding protein sce3	SPBC18H10.04c	11.10%	2
electron transfer flavoprotein beta subunit (predicted)	SPAC1805.02c	11.00%	2
ribosome biogenesis protein Nsa2 (predicted)	SPCP1E11.08	10.40%	2
Histone H2A-alpha	SPCC622.08c	6.90%	2
Histone H2A-beta	SPAC19G12.06c	6.90%	2
Rad24, 14-3-3 protein	SPAC8E11.02c	6.70%	2
Heat shock protein 60, mitochondrial	SPAC12G12.04	5.00%	2
Heat shock protein homolog pss1	SPAC110.04c,	3.30%	2
PSP1 family protein	SPBPB7E8.02	3.10%	2
diacylglycerol binding protein (predicted)	SPCC297.05	2.60%	2
DNA topoisomerase II	SPBC1A4.03c	1.30%	2
ferrichrome synthetase Sib1	SPAC23G3.02c	0.40%	2

Appendix B

Material and Methods

Chapter II

Strains and plasmids

Strains used in this study are listed in Supplemental Table S1. Genetic crosses and general yeast techniques were performed as described previously (Moreno et al., 1991). Carboxy-terminal green fluorescent protein (GFP), and 13-Myc epitope tagging of *pcs1*$^+$, *mde4*$^+$, *mde4-12A* and *mde4-12D* was done by PCR-based gene targeting (Bahler et al., 1998). A substrate trapping allele *clp*$^+$, *clp1-C286S* and *mde4*$^+$ were TAP tagged for tandem affinity purification by same way. To construct the *mde4*Δ strains, the entire *mde4*$^+$ coding region was replaced with the *ura4*$^+$ gene cassette by homologous recombination. The *mde4*$^+$ genomic clone (pDM1061), which includes 1kb of 5' UTR and 0.5kb of 3' UTR, was cloned into the pENTR^{TM}/SD/D-Topo plasmid (Invitrogen). The *mde4-12A* (S/T to A) and *mde4-12D* (S/T to D/E) clones were created from the genomic clone pDM1061 using a combination of site-directed mutagenesis to mutate S147, minigene synthesis (Integrated DNA Technologies Inc.) to mutate S242, S247, S252, S270, T275, S290, S295, S316, S349, S354, and primer-directed mutagenesis to change S401. Using LR recombination, the mutated genomic clones were transferred into pIRT2-GW, which is a gateway destination plasmid constructed for this study that is based on the pIRT2 vector. pIRT2-mde4-12A and

pIRT2-mde4-12D were transformed into *mde4*Δ::*ura4*$^{+}$ strain and the resulting transformants were then plated on Edinburgh minimal medium (EMM -Leu) plates including 5-FOA to select for the *mde4-12A* and *mde4-12D* gene replacement strains. Expression of mRFP-tubulin and Mad2 from the thiamine repressible *nmt1* promoter was either repressed or induced by growing cells in EMM with or without 5 μg/ml of thiamine respectively.

TAP purification

Tandem affinity purification (TAP) of Clp1-CS-TAP was carried out as previously described (Gould et al., 2004) to isolate Clp1-C286S together with associated proteins from asynchronous cells, metaphase arrested cells by *nda3-KM311* and *mts3-1* block, and anaphase cells (60 min after released from *cdc25-22* block). Mde4-TAP was also purified from metaphase arrested cells by *nda3-KM311* block. Purified proteins were separated on SDS-PAGE gels and silver-stained. In parallel, samples were subjected to analysis by tandem mass spectrometry. Results from *nda3-KM311* and *mts3-1* block were combined to present in appendix A. Proteins co-purified with Clp1-C286S from all three conditions were listed in Appendix A-1 and proteins shown in one or two of above conditions were listed in Appendix A-2. Due to huge numbers of identified proteins isolated from prometaphase/metaphase arrested cells, we cut off proteins which were found by less than two hits in that condition, unless those proteins were detected in other cell cycle stages as well.

Microscopy

GFP- and mRFP-fusion proteins were observed either after fixation with –20°C methanol or in live cells. DNA was visualized with 4', 6-diamidino-2-phenylindole (DAPI; Sigma-Aldrich) at 2 µg/ml. Photomicrographs were obtained using a Nikon Eclipse E600 fluorescence microscope coupled to a cooled charge-coupled device camera (ORCA-ER; Hamamatsu, Bridgewater, NJ), and image processing and analysis were carried out using IPLab Spectrum software (Signal Analytics, Vienna, VA). For time-lapse studies, exponentially growing cells were concentrated, and 1.8 µl of cell suspension was placed on a microscope slide with a 2% YE agar slab. Time-lapse experiments were made at 24°C by acquiring epi-fluorescence images in Z-planes and 2 x 2 binning. Cells were viewed on a spinning disk microscope (Zeiss Axiovert 200 microscope with Argon ion laser system (Mellers Griot)). Images were captured using an IEEE1394 digital CCD camera C4742-80-12AG (Hamamatsu) and UltraVIEW^{TM}RS confocal imaging system software (PerkinElmer).

Immunoprecipitation and TAP purification

Immunoprecipitation was done as described (Sparks et al., 1999) in the presence of phosphatase inhibitors (1 mM $NaVO_4$ and 5 mM NaF). Mouse monoclonal anti-GFP (A-11120, Molecular Probes) and anti-Myc (sc-40, Santa Cruz Biotechnology) antibodies were used for immunoprecipitation, and mouse monoclonal anti-GFP (sc-9996, Santa Cruz Biotechnology) and rabbit polyclonal anti-Myc (SC-789, Santa Cruz Biotechnology) antibodies were used for Western blotting.

In vitro phosphatase assay

In vitro phosphatase assays were performed as described (Wolfe et al., 2006). Immunoprecipitated Mde4-13Myc from *clp1*Δ cells arrested at metaphase using the *nda3-km311* mutation was incubated in the presence of recombinant MBP-Clp1 or Lambda phosphatase at 30°C for 30 min in phosphatase assay buffer (50 mM Imidazole [pH 6.9], 1 mM EDTA, 1 mM DTT). Reactions were terminated by the addition of sample buffer and boiling, followed by separation on SDS-PAGE and visualization by western blotting.

In vitro kinase assay

In vitro kinase assays were performed as described (Sparks et al., 1999). Recombinant 6His-Mde4, GST-Mde4-137-421, and GST-Mde4-12A-137-421 purified from *E. coli* were incubated at 30°C for 30 min with γ-^{32}P labeled ATP in the presence or absence of Cdc2 immunoprecipitated from metaphase arrested *nda3-KM311* cells using anti-Cdc13 antibodies. Protein labeled by γ-^{32}P was detected with a phospho imager (Molecular Dynamics)

Chapter III

Microscopy

Chromosome segregation defects were observed in cells after fixation with -20°C methanol. DNA and cell wall materials were visualized by DAPI (Sigma-Aldrich) at 2 μg/ml and calcofluor white (CW: Sigma-Aldrich) at 50 μg/ml, respectively. Photomicrographs were

obtained using a Nikon Eclipse E600 fluorescence microscope coupled to a cooled charge-coupled device camera (ORCA-ER; Hamamatsu, Bridgewater, NJ), and image processing and analysis were carried out using IPLab Spectrum software (Signal Analytics, Vienna, VA). For time-lapse studies, 1.5 ml of log-phase cells was concentrated by centrifugation and suspended in 100 µl of medium (YE) and 30 µl of the cell suspension was mixed with 30 µl of 1 mg/ml soybean lectin (L1395; Sigma-Aldrich), placed in 35-mm glass-bottomed culture dishes (P35-1.5-10-C; MatTek), and immersed in 3 ml of medium (YE) for time-lapse imaging. Time-lapse experiments were made at 25°C by acquiring epifluorescence images in z planes and 1 x 1 binning. Cells were then viewed on a microscope (Axiovert 200; Carl Zeiss, Inc.) with an argon ion laser system (Melles Griot). Images were captured using an IEEE 1394 digital charge-coupled device camera (C4742-80-12AG; Hamamatsu Photonics) and UltraVIEW RS confocal imaging system software (PerkinElmer). Maximal projected images were loaded into IPLab software (BD) and the spindle length labeled by GFP-atb2 was measured for further analysis.

In vitro kinase assay

In vitro kinase assays were performed as described (Sparks et al., 1999). 1 µg or 5 µg of commercially available recombinant Histone H3.2 (NEB) was used as a substrate were incubated at 30°C for 30 min with γ-^{32}P labeled ATP in the presence or absence of Ark1-GFP immunoprecipitated from metaphase arrested wild type, *clp1*Δ, wild-type cells mildly expressing Cdc13ΔDB using *nda3-KM311* mutation by anti-GFP antibodies. Protein labeled by γ-^{32}P was detected with a phospho imager (Molecular Dynamics) and the gel

was stained with Coomassie Blue as a loading control. The protein level of Ark1-GFP used for this assay was determined using western blot (Kodak 4000MM image station). Relative kinase activity was measured by subtracting the background and then normalizing for Ark1 protein level compared to wild type whose kinase intensity was set of 1.

References

Adams, R. R., Carmena, M., and Earnshaw, W. C. (2001). Chromosomal passengers and the (aurora) ABCs of mitosis. Trends Cell Biol *11*, 49-54.

Andrews, P. D., Ovechkina, Y., Morrice, N., Wagenbach, M., Duncan, K., Wordeman, L., and Swedlow, J. R. (2004). Aurora B regulates MCAK at the mitotic centromere. Dev Cell *6*, 253-268.

Bahler, J., Wu, J. Q., Longtine, M. S., Shah, N. G., McKenzie, A., 3rd, Steever, A. B., Wach, A., Philippsen, P., and Pringle, J. R. (1998). Heterologous modules for efficient and versatile PCR-based gene targeting in Schizosaccharomyces pombe. Yeast *14*, 943-951.

Bassermann, F., Frescas, D., Guardavaccaro, D., Busino, L., Peschiaroli, A., and Pagano, M. (2008). The Cdc14B-Cdh1-Plk1 axis controls the G2 DNA-damage-response checkpoint. Cell *134*, 256-267.

Baumann, C., Korner, R., Hofmann, K., and Nigg, E. A. (2007). PICH, a centromere-associated SNF2 family ATPase, is regulated by Plk1 and required for the spindle checkpoint. Cell *128*, 101-114.

Berdougo, E., Nachury, M. V., Jackson, P. K., and Jallepalli, P. V. (2008). The nucleolar phosphatase Cdc14B is dispensable for chromosome segregation and mitotic exit in human cells. Cell Cycle *7*, 1184-1190.

Bernard, P., Maure, J. F., Partridge, J. F., Genier, S., Javerzat, J. P., and Allshire, R. C. (2001). Requirement of heterochromatin for cohesion at centromeres. Science *294*, 2539-2542.

Biggins, S., and Murray, A. W. (2001). The budding yeast protein kinase Ipl1/Aurora allows the absence of tension to activate the spindle checkpoint. Genes Dev *15*, 3118-3129.

Biggins, S., Severin, F. F., Bhalla, N., Sassoon, I., Hyman, A. A., and Murray, A. W. (1999). The conserved protein kinase Ipl1 regulates microtubule binding to kinetochores in budding yeast. Genes Dev *13*, 532-544.

Blangy, A., Lane, H. A., d'Herin, P., Harper, M., Kress, M., and Nigg, E. A. (1995). Phosphorylation by p34cdc2 regulates spindle association of human Eg5, a kinesin-related motor essential for bipolar spindle formation in vivo. Cell *83*, 1159-1169.

Bohnert, K. A., Chen, J. S., Clifford, D. M., Vander Kooi, C. W., and Gould, K. L. (2009). A Link between aurora kinase and Clp1/Cdc14 regulation uncovered by the identification of a fission yeast borealin-like protein. Mol Biol Cell *20*, 3646-3659.

Bollen, M., Gerlich, D. W., and Lesage, B. (2009). Mitotic phosphatases: from entry guards to exit guides. Trends Cell Biol *19*, 531-541.

Brown, N. R., Noble, M. E., Endicott, J. A., and Johnson, L. N. (1999). The structural basis for specificity of substrate and recruitment peptides for cyclin-dependent kinases. Nat Cell Biol *1*, 438-443.

Buschhorn, B. A., and Peters, J. M. (2006). How APC/C orders destruction. Nat Cell Biol *8*, 209-211.

Chang, L., Morrell, J. L., Feoktistova, A., and Gould, K. L. (2001). Study of cyclin proteolysis in anaphase-promoting complex (APC) mutant cells reveals the requirement for APC function in the final steps of the fission yeast septation initiation network. Mol Cell Biol *21*, 6681-6694.

Cheeseman, I. M., Anderson, S., Jwa, M., Green, E. M., Kang, J., Yates, J. R., 3rd, Chan, C. S., Drubin, D. G., and Barnes, G. (2002). Phospho-regulation of kinetochore-microtubule attachments by the Aurora kinase Ipl1p. Cell *111*, 163-172.

Cheeseman, I. M., Chappie, J. S., Wilson-Kubalek, E. M., and Desai, A. (2006). The conserved KMN network constitutes the core microtubule-binding site of the kinetochore. Cell *127*, 983-997.

Cheeseman, I. M., and Desai, A. (2008). Molecular architecture of the kinetochore-microtubule interface. Nat Rev Mol Cell Biol *9*, 33-46.

Chen, C. T., Peli-Gulli, M. P., Simanis, V., and McCollum, D. (2006). S. pombe FEAR protein orthologs are not required for release of Clp1/Flp1 phosphatase from the nucleolus during mitosis. J Cell Sci *119*, 4462-4466.

Choi, S. H., Peli-Gulli, M. P., McLeod, I., Sarkeshik, A., Yates, J. R., 3rd, Simanis, V., and McCollum, D. (2009). Phosphorylation state defines discrete roles for monopolin in chromosome attachment and spindle elongation. Curr Biol *19*, 985-995.

Ciferri, C., Pasqualato, S., Screpanti, E., Varetti, G., Santaguida, S., Dos Reis, G., Maiolica, A., Polka, J., De Luca, J. G., De Wulf, P., *et al.* (2008). Implications for kinetochore-

microtubule attachment from the structure of an engineered Ndc80 complex. Cell *133*, 427-439.

Cimini, D. (2007). Detection and correction of merotelic kinetochore orientation by Aurora B and its partners. Cell Cycle *6*, 1558-1564.

Cimini, D., Cameron, L. A., and Salmon, E. D. (2004). Anaphase spindle mechanics prevent mis-segregation of merotelically oriented chromosomes. Curr Biol *14*, 2149-2155.

Cimini, D., and Degrassi, F. (2005). Aneuploidy: a matter of bad connections. Trends Cell Biol *15*, 442-451.

Cimini, D., Fioravanti, D., Salmon, E. D., and Degrassi, F. (2002). Merotelic kinetochore orientation versus chromosome mono-orientation in the origin of lagging chromosomes in human primary cells. J Cell Sci *115*, 507-515.

Cimini, D., Howell, B., Maddox, P., Khodjakov, A., Degrassi, F., and Salmon, E. D. (2001). Merotelic kinetochore orientation is a major mechanism of aneuploidy in mitotic mammalian tissue cells. J Cell Biol *153*, 517-527.

Cimini, D., Moree, B., Canman, J. C., and Salmon, E. D. (2003). Merotelic kinetochore orientation occurs frequently during early mitosis in mammalian tissue cells and error correction is achieved by two different mechanisms. J Cell Sci *116*, 4213-4225.

Cimini, D., Wan, X., Hirel, C. B., and Salmon, E. D. (2006). Aurora kinase promotes turnover of kinetochore microtubules to reduce chromosome segregation errors. Curr Biol *16*, 1711-1718.

Cleveland, D. W., Mao, Y., and Sullivan, K. F. (2003). Centromeres and kinetochores: from epigenetics to mitotic checkpoint signaling. Cell *112*, 407-421.

Clifford, D. M., Wolfe, B. A., Roberts-Galbraith, R. H., McDonald, W. H., Yates, J. R., 3rd, and Gould, K. L. (2008). The Clp1/Cdc14 phosphatase contributes to the robustness of cytokinesis by association with anillin-related Mid1. J Cell Biol *181*, 79-88.

Corbett, K. D., Yip, C. K., Walz, T., and Harrison, S. C. (2009). Structure of the Fungal Monopolin Complex: A Bivalent Chromosome Cross-linker, Paper presented at: 49th ASCB annual meeting (San Diego, CA).

Courtheoux, T., Gay, G., Gachet, Y., and Tournier, S. (2009). Ase1/Prc1-dependent spindle elongation corrects merotely during anaphase in fission yeast. J Cell Biol *187*, 399-412.

Crasta, K., Lim, H. H., Zhang, T., Nirantar, S., and Surana, U. (2008). Consorting kinases, end of destruction and birth of a spindle. Cell Cycle *7*, 2960-2966.

Cueille, N., Salimova, E., Esteban, V., Blanco, M., Moreno, S., Bueno, A., and Simanis, V. (2001). Flp1, a fission yeast orthologue of the s. cerevisiae CDC14 gene, is not required for cyclin degradation or rum1p stabilisation at the end of mitosis. J Cell Sci *114*, 2649-2664.

D'Amours, D., Stegmeier, F., and Amon, A. (2004). Cdc14 and condensin control the dissolution of cohesin-independent chromosome linkages at repeated DNA. Cell *117*, 455-469.

DeLuca, J. G., Gall, W. E., Ciferri, C., Cimini, D., Musacchio, A., and Salmon, E. D. (2006). Kinetochore microtubule dynamics and attachment stability are regulated by Hec1. Cell *127*, 969-982.

Dephoure, N., Zhou, C., Villen, J., Beausoleil, S. A., Bakalarski, C. E., Elledge, S. J., and Gygi, S. P. (2008). A quantitative atlas of mitotic phosphorylation. Proc Natl Acad Sci U S A *105*, 10762-10767.

Desai, A., Rybina, S., Muller-Reichert, T., Shevchenko, A., Shevchenko, A., Hyman, A., and Oegema, K. (2003). KNL-1 directs assembly of the microtubule-binding interface of the kinetochore in C. elegans. Genes Dev *17*, 2421-2435.

Desai, A., Verma, S., Mitchison, T. J., and Walczak, C. E. (1999). Kin I kinesins are microtubule-destabilizing enzymes. Cell *96*, 69-78.

Ding, R., McDonald, K. L., and McIntosh, J. R. (1993). Three-dimensional reconstruction and analysis of mitotic spindles from the yeast, Schizosaccharomyces pombe. J Cell Biol *120*, 141-151.

Draviam, V. M., Xie, S., and Sorger, P. K. (2004). Chromosome segregation and genomic stability. Curr Opin Genet Dev *14*, 120-125.

Drummond, D. R., and Hagan, I. M. (1998). Mutations in the bimC box of Cut7 indicate divergence of regulation within the bimC family of kinesin related proteins. J Cell Sci *111 (Pt 7)*, 853-865.

Fu, C., Ward, J. J., Loiodice, I., Velve-Casquillas, G., Nedelec, F. J., and Tran, P. T. (2009). Phospho-regulated interaction between kinesin-6 Klp9p and microtubule bundler Ase1p promotes spindle elongation. Dev Cell *17*, 257-267.

Glotzer, M. (2009). The 3Ms of central spindle assembly: microtubules, motors and MAPs. Nat Rev Mol Cell Biol *10*, 9-20.

Gomez, R., Valdeolmillos, A., Parra, M. T., Viera, A., Carreiro, C., Roncal, F., Rufas, J. S., Barbero, J. L., and Suja, J. A. (2007). Mammalian SGO2 appears at the inner centromere domain and redistributes depending on tension across centromeres during meiosis II and mitosis. EMBO Rep *8*, 173-180.

Goshima, G., Saitoh, S., and Yanagida, M. (1999). Proper metaphase spindle length is determined by centromere proteins Mis12 and Mis6 required for faithful chromosome segregation. Genes Dev *13*, 1664-1677.

Goshima, G., and Vale, R. D. (2003). The roles of microtubule-based motor proteins in mitosis: comprehensive RNAi analysis in the Drosophila S2 cell line. J Cell Biol *162*, 1003-1016.

Goshima, G., Wollman, R., Stuurman, N., Scholey, J. M., and Vale, R. D. (2005). Length control of the metaphase spindle. Curr Biol *15*, 1979-1988.

Gould, K. L., Ren, L., Feoktistova, A. S., Jennings, J. L., and Link, A. J. (2004). Tandem affinity purification and identification of protein complex components. Methods *33*, 239-244.

Gregan, J., Riedel, C. G., Pidoux, A. L., Katou, Y., Rumpf, C., Schleiffer, A., Kearsey, S. E., Shirahige, K., Allshire, R. C., and Nasmyth, K. (2007). The kinetochore proteins Pcs1 and Mde4 and heterochromatin are required to prevent merotelic orientation. Curr Biol *17*, 1190-1200.

Gruneberg, U., Glotzer, M., Gartner, A., and Nigg, E. A. (2002). The CeCDC-14 phosphatase is required for cytokinesis in the Caenorhabditis elegans embryo. J Cell Biol *158*, 901-914.

Hagan, I., and Yanagida, M. (1992). Kinesin-related cut7 protein associates with mitotic and meiotic spindles in fission yeast. Nature *356*, 74-76.

Hagan, I. M. (1998). The fission yeast microtubule cytoskeleton. J Cell Sci *111 (Pt 12)*, 1603-1612.

Hassold, T., and Hunt, P. (2001). To err (meiotically) is human: the genesis of human aneuploidy. Nat Rev Genet *2*, 280-291.

Hauf, S., Cole, R. W., LaTerra, S., Zimmer, C., Schnapp, G., Walter, R., Heckel, A., van Meel, J., Rieder, C. L., and Peters, J. M. (2003). The small molecule Hesperadin reveals a role for Aurora B in correcting kinetochore-microtubule attachment and in maintaining the spindle assembly checkpoint. J Cell Biol *161*, 281-294.

He, X., Patterson, T. E., and Sazer, S. (1997). The Schizosaccharomyces pombe spindle checkpoint protein mad2p blocks anaphase and genetically interacts with the anaphase-promoting complex. Proc Natl Acad Sci U S A *94*, 7965-7970.

Higuchi, T., and Uhlmann, F. (2005). Stabilization of microtubule dynamics at anaphase onset promotes chromosome segregation. Nature *433*, 171-176.

Holt, L. J., Tuch, B. B., Villen, J., Johnson, A. D., Gygi, S. P., and Morgan, D. O. (2009). Global analysis of Cdk1 substrate phosphorylation sites provides insights into evolution. Science *325*, 1682-1686.

Howell, B. J., Hoffman, D. B., Fang, G., Murray, A. W., and Salmon, E. D. (2000). Visualization of Mad2 dynamics at kinetochores, along spindle fibers, and at spindle poles in living cells. J Cell Biol *150*, 1233-1250.

Howell, B. J., Moree, B., Farrar, E. M., Stewart, S., Fang, G., and Salmon, E. D. (2004). Spindle checkpoint protein dynamics at kinetochores in living cells. Curr Biol *14*, 953-964.

Hoyt, M. A., Totis, L., and Roberts, B. T. (1991). S. cerevisiae genes required for cell cycle arrest in response to loss of microtubule function. Cell *66*, 507-517.

Huang, J., Brito, I. L., Villen, J., Gygi, S. P., Amon, A., and Moazed, D. (2006). Inhibition of homologous recombination by a cohesin-associated clamp complex recruited to the rDNA recombination enhancer. Genes Dev *20*, 2887-2901.

Hunter, A. W., Caplow, M., Coy, D. L., Hancock, W. O., Diez, S., Wordeman, L., and Howard, J. (2003). The kinesin-related protein MCAK is a microtubule depolymerase that forms an ATP-hydrolyzing complex at microtubule ends. Mol Cell *11*, 445-457.

Indjeian, V. B., Stern, B. M., and Murray, A. W. (2005). The centromeric protein Sgo1 is required to sense lack of tension on mitotic chromosomes. Science *307*, 130-133.

Jin, Q. W., Ray, S., Choi, S. H., and McCollum, D. (2007). The nucleolar Net1/Cfi1-related protein Dnt1 antagonizes the septation initiation network in fission yeast. Mol Biol Cell *18*, 2924-2934.

Kallio, M. J., Beardmore, V. A., Weinstein, J., and Gorbsky, G. J. (2002a). Rapid microtubule-independent dynamics of Cdc20 at kinetochores and centrosomes in mammalian cells. J Cell Biol *158*, 841-847.

Kallio, M. J., McCleland, M. L., Stukenberg, P. T., and Gorbsky, G. J. (2002b). Inhibition of aurora B kinase blocks chromosome segregation, overrides the spindle checkpoint, and perturbs microtubule dynamics in mitosis. Curr Biol *12*, 900-905.

Kawashima, S. A., Tsukahara, T., Langegger, M., Hauf, S., Kitajima, T. S., and Watanabe, Y. (2007). Shugoshin enables tension-generating attachment of kinetochores by loading Aurora to centromeres. Genes Dev *21*, 420-435.

Kerres, A., Jakopec, V., and Fleig, U. (2007). The conserved Spc7 protein is required for spindle integrity and links kinetochore complexes in fission yeast. Mol Biol Cell *18*, 2441-2454.

Khmelinskii, A., Lawrence, C., Roostalu, J., and Schiebel, E. (2007). Cdc14-regulated midzone assembly controls anaphase B. J Cell Biol *177*, 981-993.

Khmelinskii, A., and Schiebel, E. (2009). Chromosome segregation: monopolin goes spindle. Curr Biol *19*, R482-484.

Khodjakov, A., La Terra, S., and Chang, F. (2004a). Laser microsurgery in fission yeast; role of the mitotic spindle midzone in anaphase B. Curr Biol *14*, 1330-1340.

Khodjakov, A., Rieder, C., Mannella, C. A., and Kinnally, K. W. (2004b). Laser micro-irradiation of mitochondria: is there an amplified mitochondrial death signal in neural cells? Mitochondrion *3*, 217-227.

Kline-Smith, S. L., Khodjakov, A., Hergert, P., and Walczak, C. E. (2004). Depletion of centromeric MCAK leads to chromosome congression and segregation defects due to improper kinetochore attachments. Mol Biol Cell *15*, 1146-1159.

Knowlton, A. L., Lan, W., and Stukenberg, P. T. (2006). Aurora B is enriched at merotelic attachment sites, where it regulates MCAK. Curr Biol *16*, 1705-1710.

Lachner, M., O'Carroll, D., Rea, S., Mechtler, K., and Jenuwein, T. (2001). Methylation of histone H3 lysine 9 creates a binding site for HP1 proteins. Nature *410*, 116-120.

Lampson, M. A., Renduchitala, K., Khodjakov, A., and Kapoor, T. M. (2004). Correcting improper chromosome-spindle attachments during cell division. Nat Cell Biol *6*, 232-237.

Lan, W., Zhang, X., Kline-Smith, S. L., Rosasco, S. E., Barrett-Wilt, G. A., Shabanowitz, J., Hunt, D. F., Walczak, C. E., and Stukenberg, P. T. (2004). Aurora B phosphorylates centromeric MCAK and regulates its localization and microtubule depolymerization activity. Curr Biol *14*, 273-286.

Leverson, J. D., Huang, H. K., Forsburg, S. L., and Hunter, T. (2002). The Schizosaccharomyces pombe aurora-related kinase Ark1 interacts with the inner centromere protein Pic1 and mediates chromosome segregation and cytokinesis. Mol Biol Cell *13*, 1132-1143.

Li, F., Ambrosini, G., Chu, E. Y., Plescia, J., Tognin, S., Marchisio, P. C., and Altieri, D. C. (1998). Control of apoptosis and mitotic spindle checkpoint by survivin. Nature *396*, 580-584.

Li, R., and Murray, A. W. (1991). Feedback control of mitosis in budding yeast. Cell *66*, 519-531.

Li, X., and Dawe, R. K. (2009). Fused sister kinetochores initiate the reductional division in meiosis I. Nat Cell Biol *11*, 1103-1108.

Lindqvist, A., Rodriguez-Bravo, V., and Medema, R. H. (2009). The decision to enter mitosis: feedback and redundancy in the mitotic entry network. J Cell Biol *185*, 193-202.

Liu, D., Vader, G., Vromans, M. J., Lampson, M. A., and Lens, S. M. (2009). Sensing chromosome bi-orientation by spatial separation of aurora B kinase from kinetochore substrates. Science *323*, 1350-1353.

Loiodice, I., Staub, J., Setty, T. G., Nguyen, N. P., Paoletti, A., and Tran, P. T. (2005). Ase1p organizes antiparallel microtubule arrays during interphase and mitosis in fission yeast. Mol Biol Cell *16*, 1756-1768.

Loog, M., and Morgan, D. O. (2005). Cyclin specificity in the phosphorylation of cyclin-dependent kinase substrates. Nature *434*, 104-108.

Mackay, A. M., Eckley, D. M., Chue, C., and Earnshaw, W. C. (1993). Molecular analysis of the INCENPs (inner centromere proteins): separate domains are required for association with microtubules during interphase and with the central spindle during anaphase. J Cell Biol *123*, 373-385.

Masui, Y., and Markert, C. L. (1971). Cytoplasmic control of nuclear behavior during meiotic maturation of frog oocytes. J Exp Zool *177*, 129-145.

Mekhail, K., Seebacher, J., Gygi, S. P., and Moazed, D. (2008). Role for perinuclear chromosome tethering in maintenance of genome stability. Nature *456*, 667-670.

Mishima, M., Pavicic, V., Gruneberg, U., Nigg, E. A., and Glotzer, M. (2004). Cell cycle regulation of central spindle assembly. Nature *430*, 908-913.

Mollinari, C., Kleman, J. P., Jiang, W., Schoehn, G., Hunter, T., and Margolis, R. L. (2002). PRC1 is a microtubule binding and bundling protein essential to maintain the mitotic spindle midzone. J Cell Biol *157*, 1175-1186.

Monje-Casas, F., Prabhu, V. R., Lee, B. H., Boselli, M., and Amon, A. (2007). Kinetochore orientation during meiosis is controlled by Aurora B and the monopolin complex. Cell *128*, 477-490.

Moreno, S., Klar, A., and Nurse, P. (1991). Molecular genetic analysis of fission yeast Schizosaccharomyces pombe. Methods Enzymol *194*, 795-823.

Moser, B. A., and Russell, P. (2000). Cell cycle regulation in Schizosaccharomyces pombe. Curr Opin Microbiol *3*, 631-636.

Murata-Hori, M., Tatsuka, M., and Wang, Y. L. (2002). Probing the dynamics and functions of aurora B kinase in living cells during mitosis and cytokinesis. Mol Biol Cell *13*, 1099-1108.

Musacchio, A., and Salmon, E. D. (2007). The spindle-assembly checkpoint in space and time. Nat Rev Mol Cell Biol *8*, 379-393.

Nabeshima, K., Nakagawa, T., Straight, A. F., Murray, A., Chikashige, Y., Yamashita, Y. M., Hiraoka, Y., and Yanagida, M. (1998). Dynamics of centromeres during metaphase-

anaphase transition in fission yeast: Dis1 is implicated in force balance in metaphase bipolar spindle. Mol Biol Cell *9*, 3211-3225.

Nakajima, Y., Tyers, R. G., Wong, C. C., Yates, J. R., 3rd, Drubin, D. G., and Barnes, G. (2009). Nbl1p: a Borealin/Dasra/CSC-1-like protein essential for Aurora/Ipl1 complex function and integrity in Saccharomyces cerevisiae. Mol Biol Cell *20*, 1772-1784.

Nicklas, R. B., Ward, S. C., and Gorbsky, G. J. (1995). Kinetochore chemistry is sensitive to tension and may link mitotic forces to a cell cycle checkpoint. J Cell Biol *130*, 929-939.

Nicklas, R. B., Waters, J. C., Salmon, E. D., and Ward, S. C. (2001). Checkpoint signals in grasshopper meiosis are sensitive to microtubule attachment, but tension is still essential. J Cell Sci *114*, 4173-4183.

Nousiainen, M., Sillje, H. H., Sauer, G., Nigg, E. A., and Korner, R. (2006). Phosphoproteome analysis of the human mitotic spindle. Proc Natl Acad Sci U S A *103*, 5391-5396.

O'Farrell, P. H. (2001). Triggering the all-or-nothing switch into mitosis. Trends Cell Biol *11*, 512-519.

Pangilinan, F., and Spencer, F. (1996). Abnormal kinetochore structure activates the spindle assembly checkpoint in budding yeast. Mol Biol Cell *7*, 1195-1208.

Peeper, D. S., Parker, L. L., Ewen, M. E., Toebes, M., Hall, F. L., Xu, M., Zantema, A., van der Eb, A. J., and Piwnica-Worms, H. (1993). A- and B-type cyclins differentially modulate substrate specificity of cyclin-cdk complexes. Embo J *12*, 1947-1954.

Pereira, G., and Schiebel, E. (2003). Separase regulates INCENP-Aurora B anaphase spindle function through Cdc14. Science *302*, 2120-2124.

Pesin, J. A., and Orr-Weaver, T. L. (2008). Regulation of APC/C activators in mitosis and meiosis. Annu Rev Cell Dev Biol *24*, 475-499.

Petersen, J., and Hagan, I. M. (2003). S. pombe aurora kinase/survivin is required for chromosome condensation and the spindle checkpoint attachment response. Curr Biol *13*, 590-597.

Petronczki, M., Matos, J., Mori, S., Gregan, J., Bogdanova, A., Schwickart, M., Mechtler, K., Shirahige, K., Zachariae, W., and Nasmyth, K. (2006). Monopolar attachment of sister kinetochores at meiosis I requires casein kinase 1. Cell *126*, 1049-1064.

Pidoux, A. L., and Allshire, R. C. (2004). Kinetochore and heterochromatin domains of the fission yeast centromere. Chromosome Res *12*, 521-534.

Pidoux, A. L., LeDizet, M., and Cande, W. Z. (1996). Fission yeast pkl1 is a kinesin-related protein involved in mitotic spindle function. Mol Biol Cell *7*, 1639-1655.

Pidoux, A. L., Uzawa, S., Perry, P. E., Cande, W. Z., and Allshire, R. C. (2000). Live analysis of lagging chromosomes during anaphase and their effect on spindle elongation rate in fission yeast. J Cell Sci *113 Pt 23*, 4177-4191.

Pinsky, B. A., and Biggins, S. (2005). The spindle checkpoint: tension versus attachment. Trends Cell Biol *15*, 486-493.

Przewloka, M. R., and Glover, D. M. (2009). The kinetochore and the centromere: a working long distance relationship. Annu Rev Genet *43*, 439-465.

Queralt, E., and Uhlmann, F. (2008). Cdk-counteracting phosphatases unlock mitotic exit. Curr Opin Cell Biol *20*, 661-668.

Rabitsch, K. P., Petronczki, M., Javerzat, J. P., Genier, S., Chwalla, B., Schleiffer, A., Tanaka, T. U., and Nasmyth, K. (2003). Kinetochore recruitment of two nucleolar proteins is required for homolog segregation in meiosis I. Dev Cell *4*, 535-548.

Radcliffe, P., Hirata, D., Childs, D., Vardy, L., and Toda, T. (1998). Identification of novel temperature-sensitive lethal alleles in essential beta-tubulin and nonessential alpha 2-tubulin genes as fission yeast polarity mutants. Mol Biol Cell *9*, 1757-1771.

Rieder, C. L., and Maiato, H. (2004). Stuck in division or passing through: what happens when cells cannot satisfy the spindle assembly checkpoint. Dev Cell *7*, 637-651.

Ruchaud, S., Carmena, M., and Earnshaw, W. C. (2007). Chromosomal passengers: conducting cell division. Nat Rev Mol Cell Biol *8*, 798-812.

Saito, R. M., Perreault, A., Peach, B., Satterlee, J. S., and van den Heuvel, S. (2004). The CDC-14 phosphatase controls developmental cell-cycle arrest in C. elegans. Nat Cell Biol *6*, 777-783.

Salic, A., Waters, J. C., and Mitchison, T. J. (2004). Vertebrate shugoshin links sister centromere cohesion and kinetochore microtubule stability in mitosis. Cell *118*, 567-578.

Sandall, S., Severin, F., McLeod, I. X., Yates, J. R., 3rd, Oegema, K., Hyman, A., and Desai, A. (2006). A Bir1-Sli15 complex connects centromeres to microtubules and is required to sense kinetochore tension. Cell *127*, 1179-1191.

Sawin, K. E., and Mitchison, T. J. (1995). Mutations in the kinesin-like protein Eg5 disrupting localization to the mitotic spindle. Proc Natl Acad Sci U S A *92*, 4289-4293.

Schuyler, S. C., Liu, J. Y., and Pellman, D. (2003). The molecular function of Ase1p: evidence for a MAP-dependent midzone-specific spindle matrix. Microtubule-associated proteins. J Cell Biol *160*, 517-528.

Sparks, C. A., Morphew, M., and McCollum, D. (1999). Sid2p, a spindle pole body kinase that regulates the onset of cytokinesis. J Cell Biol *146*, 777-790.

Spencer, F., and Hieter, P. (1992). Centromere DNA mutations induce a mitotic delay in Saccharomyces cerevisiae. Proc Natl Acad Sci U S A *89*, 8908-8912.

Stegmeier, F., and Amon, A. (2004). Closing mitosis: the functions of the Cdc14 phosphatase and its regulation. Annu Rev Genet *38*, 203-232.

Stoler, S., Keith, K. C., Curnick, K. E., and Fitzgerald-Hayes, M. (1995). A mutation in CSE4, an essential gene encoding a novel chromatin-associated protein in yeast, causes chromosome nondisjunction and cell cycle arrest at mitosis. Genes Dev *9*, 573-586.

Sullivan, M., and Morgan, D. O. (2007). Finishing mitosis, one step at a time. Nat Rev Mol Cell Biol *8*, 894-903.

Takahashi, K., Chen, E. S., and Yanagida, M. (2000). Requirement of Mis6 centromere connector for localizing a CENP-A-like protein in fission yeast. Science *288*, 2215-2219.

Tanaka, K., Chang, H. L., Kagami, A., and Watanabe, Y. (2009). CENP-C functions as a scaffold for effectors with essential kinetochore functions in mitosis and meiosis. Dev Cell *17*, 334-343.

Tanaka, T. U., Rachidi, N., Janke, C., Pereira, G., Galova, M., Schiebel, E., Stark, M. J., and Nasmyth, K. (2002). Evidence that the Ipl1-Sli15 (Aurora kinase-INCENP) complex

promotes chromosome bi-orientation by altering kinetochore-spindle pole connections. Cell *108*, 317-329.

Tasto, J. J., Carnahan, R. H., McDonald, W. H., and Gould, K. L. (2001). Vectors and gene targeting modules for tandem affinity purification in Schizosaccharomyces pombe. Yeast *18*, 657-662.

Tolic-Norrelykke, I. M., Sacconi, L., Thon, G., and Pavone, F. S. (2004). Positioning and elongation of the fission yeast spindle by microtubule-based pushing. Curr Biol *14*, 1181-1186.

Toth, A., Rabitsch, K. P., Galova, M., Schleiffer, A., Buonomo, S. B., and Nasmyth, K. (2000). Functional genomics identifies monopolin: a kinetochore protein required for segregation of homologs during meiosis i. Cell *103*, 1155-1168.

Toyoda, Y., Furuya, K., Goshima, G., Nagao, K., Takahashi, K., and Yanagida, M. (2002). Requirement of chromatid cohesion proteins rad21/scc1 and mis4/scc2 for normal spindle-kinetochore interaction in fission yeast. Curr Biol *12*, 347-358.

Trautmann, S., Rajagopalan, S., and McCollum, D. (2004). The S. pombe Cdc14-like phosphatase Clp1p regulates chromosome biorientation and interacts with Aurora kinase. Dev Cell *7*, 755-762.

Trautmann, S., Wolfe, B. A., Jorgensen, P., Tyers, M., Gould, K. L., and McCollum, D. (2001). Fission yeast Clp1p phosphatase regulates G2/M transition and coordination of cytokinesis with cell cycle progression. Curr Biol *11*, 931-940.

Troxell, C. L., Sweezy, M. A., West, R. R., Reed, K. D., Carson, B. D., Pidoux, A. L., Cande, W. Z., and McIntosh, J. R. (2001). pkl1(+)and klp2(+): Two kinesins of the Kar3 subfamily in fission yeast perform different functions in both mitosis and meiosis. Mol Biol Cell *12*, 3476-3488.

Ubersax, J. A., Woodbury, E. L., Quang, P. N., Paraz, M., Blethrow, J. D., Shah, K., Shokat, K. M., and Morgan, D. O. (2003). Targets of the cyclin-dependent kinase Cdk1. Nature *425*, 859-864.

Vader, G., Medema, R. H., and Lens, S. M. (2006). The chromosomal passenger complex: guiding Aurora-B through mitosis. J Cell Biol *173*, 833-837.

Vafa, O., and Sullivan, K. F. (1997). Chromatin containing CENP-A and alpha-satellite DNA is a major component of the inner kinetochore plate. Curr Biol *7*, 897-900.

Vanoosthuyse, V., and Hardwick, K. G. (2009). A novel protein phosphatase 1-dependent spindle checkpoint silencing mechanism. Curr Biol *19*, 1176-1181.

Vanoosthuyse, V., Prykhozhij, S., and Hardwick, K. G. (2007). Shugoshin 2 regulates localization of the chromosomal passenger proteins in fission yeast mitosis. Mol Biol Cell *18*, 1657-1669.

Wheatley, S. P., Carvalho, A., Vagnarelli, P., and Earnshaw, W. C. (2001). INCENP is required for proper targeting of Survivin to the centromeres and the anaphase spindle during mitosis. Curr Biol *11*, 886-890.

Wilson-Grady, J. T., Villen, J., and Gygi, S. P. (2008). Phosphoproteome analysis of fission yeast. J Proteome Res *7*, 1088-1097.

Winey, M., Mamay, C. L., O'Toole, E. T., Mastronarde, D. N., Giddings, T. H., Jr., McDonald, K. L., and McIntosh, J. R. (1995). Three-dimensional ultrastructural analysis of the Saccharomyces cerevisiae mitotic spindle. J Cell Biol *129*, 1601-1615.

Wolfe, B. A., and Gould, K. L. (2004). Fission yeast Clp1p phosphatase affects G2/M transition and mitotic exit through Cdc25p inactivation. Embo J *23*, 919-929.

Wolfe, B. A., McDonald, W. H., Yates, J. R., 3rd, and Gould, K. L. (2006). Phospho-regulation of the Cdc14/Clp1 phosphatase delays late mitotic events in S. pombe. Dev Cell *11*, 423-430.

Woodbury, E. L., and Morgan, D. O. (2007). Cdk and APC activities limit the spindle-stabilizing function of Fin1 to anaphase. Nat Cell Biol *9*, 106-112.

Yamano, H., Gannon, J., and Hunt, T. (1996). The role of proteolysis in cell cycle progression in Schizosaccharomyces pombe. Embo J *15*, 5268-5279.

Yokobayashi, S., and Watanabe, Y. (2005). The kinetochore protein Moa1 enables cohesion-mediated monopolar attachment at meiosis I. Cell *123*, 803-817.

Yu, H. (2002). Regulation of APC-Cdc20 by the spindle checkpoint. Curr Opin Cell Biol *14*, 706-714.

Zhu, C., Lau, E., Schwarzenbacher, R., Bossy-Wetzel, E., and Jiang, W. (2006). Spatiotemporal control of spindle midzone formation by PRC1 in human cells. Proc Natl Acad Sci U S A *103*, 6196-6201.